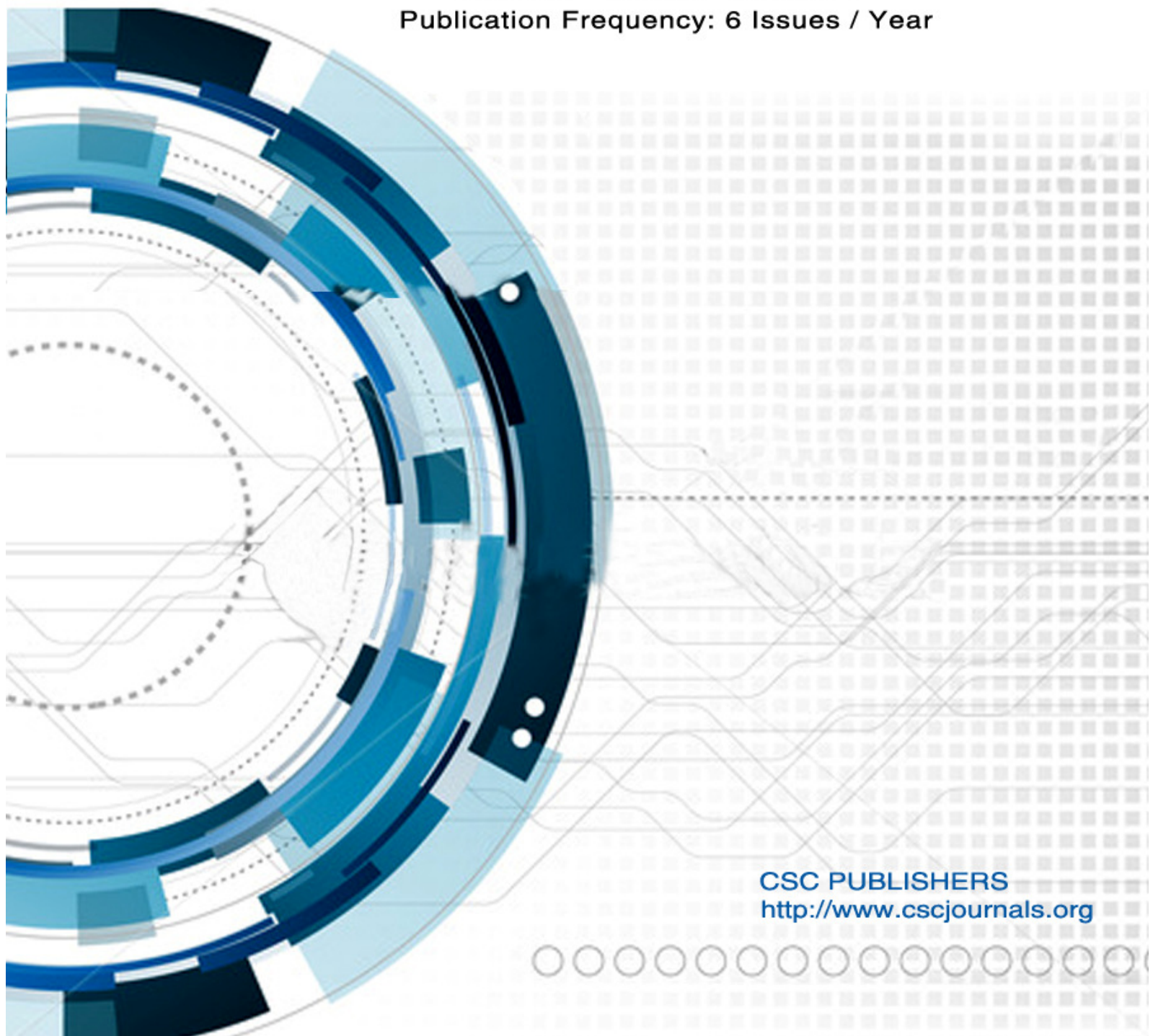


Editor-in-Chief  
Dr. Kouroush Jenab

INTERNATIONAL JOURNAL OF  
**ENGINEERING (IJE)**

ISSN : 1985-2312

Volume 5 ▪ Issue 2 ▪ May 2011  
Publication Frequency: 6 Issues / Year



CSC PUBLISHERS  
<http://www.cscjournals.org>



# **INTERNATIONAL JOURNAL OF ENGINEERING (IJE)**

**VOLUME 5, ISSUE 2, 2011**

**EDITED BY  
DR. NABEEL TAHIR**

ISSN (Online): 1985-2312

International Journal of Engineering is published both in traditional paper form and in Internet. This journal is published at the website <http://www.cscjournals.org>, maintained by Computer Science Journals (CSC Journals), Malaysia.

IJE Journal is a part of CSC Publishers

Computer Science Journals

<http://www.cscjournals.org>

## **INTERNATIONAL JOURNAL OF ENGINEERING (IJE)**

Book: Volume 5, Issue 2, May 2011

Publishing Date: 31-05-2011

ISSN (Online): 1985-2312

This work is subjected to copyright. All rights are reserved whether the whole or part of the material is concerned, specifically the rights of translation, reprinting, re-use of illustrations, recitation, broadcasting, reproduction on microfilms or in any other way, and storage in data banks. Duplication of this publication of parts thereof is permitted only under the provision of the copyright law 1965, in its current version, and permission of use must always be obtained from CSC Publishers.

IJE Journal is a part of CSC Publishers

<http://www.cscjournals.org>

© IJE Journal

Published in Malaysia

Typesetting: Camera-ready by author, data conversion by CSC Publishing Services – CSC Journals, Malaysia

**CSC Publishers, 2011**

## **EDITORIAL PREFACE**

This is the second issue of volume five of International Journal of Engineering (IJE). The Journal is published bi-monthly, with papers being peer reviewed to high international standards. The International Journal of Engineering is not limited to a specific aspect of engineering but it is devoted to the publication of high quality papers on all division of engineering in general. IJE intends to disseminate knowledge in the various disciplines of the engineering field from theoretical, practical and analytical research to physical implications and theoretical or quantitative discussion intended for academic and industrial progress. In order to position IJE as one of the good journal on engineering sciences, a group of highly valuable scholars are serving on the editorial board. The International Editorial Board ensures that significant developments in engineering from around the world are reflected in the Journal. Some important topics covers by journal are nuclear engineering, mechanical engineering, computer engineering, electrical engineering, civil & structural engineering etc.

The initial efforts helped to shape the editorial policy and to sharpen the focus of the journal. Starting with volume 5, 2011, IJE appears in more focused issues. Besides normal publications, IJE intend to organized special issues on more focused topics. Each special issue will have a designated editor (editors) – either member of the editorial board or another recognized specialist in the respective field.

The coverage of the journal includes all new theoretical and experimental findings in the fields of engineering which enhance the knowledge of scientist, industrials, researchers and all those persons who are coupled with engineering field. IJE objective is to publish articles that are not only technically proficient but also contains information and ideas of fresh interest for International readership. IJE aims to handle submissions courteously and promptly. IJE objectives are to promote and extend the use of all methods in the principal disciplines of Engineering.

IJE editors understand that how much it is important for authors and researchers to have their work published with a minimum delay after submission of their papers. They also strongly believe that the direct communication between the editors and authors are important for the welfare, quality and wellbeing of the Journal and its readers. Therefore, all activities from paper submission to paper publication are controlled through electronic systems that include electronic submission, editorial panel and review system that ensures rapid decision with least delays in the publication processes.

To build its international reputation, we are disseminating the publication information through Google Books, Google Scholar, Directory of Open Access Journals (DOAJ), Open J Gate, ScientificCommons, Docstoc and many more. Our International Editors are working on establishing ISI listing and a good impact factor for IJE. We would like to remind you that the success of our journal depends directly on the number of quality articles submitted for review. Accordingly, we would like to request your participation by submitting quality manuscripts for review and encouraging your colleagues to submit quality manuscripts for review. One of the great benefits we can provide to our prospective authors is the mentoring nature of our review process. IJE provides authors with high quality, helpful reviews that are shaped to assist authors in improving their manuscripts.

### **Editorial Board Members**

International Journal of Engineering (IJE)

## EDITORIAL BOARD

**Editor-in-Chief (EiC)**

**Dr. Kouroush Jenab**  
Ryerson University (Canada)

### ASSOCIATE EDITORS (AEiCs)

---

**Professor. Ernest Baafi**  
University of Wollongong  
Australia

**Dr. Tarek M. Sobh**  
University of Bridgeport  
United States of America

**Professor. Ziad Saghir**  
Ryerson University  
Canada

**Professor. Ridha Gharbi**  
Kuwait University  
Kuwait

**Professor. Mojtaba Azhari**  
Isfahan University of Technology  
Iran

**Dr. Cheng-Xian (Charlie) Lin**  
University of Tennessee  
United States of America

### EDITORIAL BOARD MEMBERS (EBMs)

---

**Dr. Dhanapal Durai Dominic P**  
Universiti Teknologi Petronas  
Malaysia

**Professor. Jing Zhang**  
University of Alaska Fairbanks  
United States of America

**Dr. Tao Chen**  
Nanyang Technological University  
Singapore

**Dr. Oscar Hui**

University of Hong Kong  
Hong Kong

**Professor. Sasikumaran Sreedharan**

King Khalid University  
Saudi Arabia

**Assistant Professor. Javad Nematian**

University of Tabriz Iran

**Dr. Bonny Banerjee**

Senior Scientist at Audigence  
United States of America

**AssociateProfessor. Khalifa Saif Al-Jabri**

Sultan Qaboos University  
Oman

**Dr. Alireza Bahadori**

Curtin University  
Australia

## TABLE OF CONTENTS

Volume 5, Issue 2, May 2011

### Pages

- 176 - 184      Effect of Temperature on Sliding Wear Mechanism under Lubrication Conditions  
*Nofal Al-Araji , Hussein Sarhan Sarhan*
- 185 - 193      Finite Element Analysis of Cold-formed Steel Connections  
*Bayan Anwer Ali, Sariffuddin Saad, Mohd Hanim Osman, Yusof Ahmad*
- 194 - 207      Reduction of Ultimate Strength due to Corrosion - A Finite Element Computational Method  
*J.M. Ruwan S. Appuhamy, Mitao Ohga, Tatsumasa Kaita, Ranjith Dissanayake*
- 208 - 216      Performance Evaluation of Adaptive Filters Structures for Acoustic Echo Cancellation  
*Sanjeev Kumar Dhull, Sandeep Arya, O.P Sahu*
- 217 – 241      A Distributed Optimized Approach based on the Multi Agent Concept for the Implementation  
of a Real Time Carpooling Service with an Optimization Aspect on Siblings  
*Manel Sghaier, Hayfa Zgaya, Slim Hammadi, Christian Tahon*

## Effect of Temperature on Sliding Wear Mechanism under Lubrication Conditions

**Nofal Al-Araji**

*Faculty of Engineering, Department of Materials and Metallurgical Engineering, Al-Balqa' Applied University, Al-Salt, Jordan*

*nofalaraji@yahoo.uk.com*

**Hussein Sarhan**

*Faculty of Engineering Technology, Department of Mechatronics Engineering, Al-Balqa' Applied University, Amman, PO Box: 15008, Jordan*

*sarhan\_52@hotmail.com*

---

### Abstract

Experimental program using ball-on-cylinder tester has been conducted to investigate the effects of temperature, normal load, sliding speed and type of lubricating oil on sliding wear mechanism. The worn surfaces and debris have been examined. Surface examination of the tested samples using scanning electron microscope SEM was used to study the wear particles and the wear surfaces. The results show that the temperature of the oils affects the probability of adhesion, oxidation, wear rates, and friction coefficient. At room temperature (40°C) and under lubrication conditions, friction and wear decreases with the increase of the running time. The increase in applied normal load tends to reduce the friction in all types of oils. The phosphorated oil SAE 90 was superior in minimizing friction and wear as compared with other oils. The results have shown that the lubricant temperature has a significant role in wear mechanism.

**Keywords:** Dry Sliding Wear, Surface Film, Friction Coefficient, Wear Particles, Oil Type.

---

### 1. INTRODUCTION

Wear, in modern lubricated mechanical systems, is characterized by ultra low wear rates. This statement applies to systems, like engines, as well as simple journal bearing. However, the majority of tribological publications deal with systems with wear rates of many micrometers per hour [1]. The regime of lubrication is defined as that in which the sliding surfaces are separated by lubricant films. The chemical and physical nature of the surfaces and the lubricant are of major importance [2]. The main function of the lubricant film is to reduce the amount of initial metallic contact between the sliding surfaces by interposing a layer, that is not easily penetrated, which possesses relatively low shear strength [3]. At the asperity level, the mechanical interaction can be characterized as plastic flow accompanied by mechanical intermixing followed by quenching. At common sliding velocities in the range of the asperities lasts only a few microseconds; thus in case of plastic flow, the material becomes quenched frequently [3]. It has been found through experimental investigations that liquid fatty oil is much more effective as boundary lubrication mode than other organic molecules of comparable chain length, such as alcohols. It has been observed that the organic boundary lubricants are effective at temperatures up to about 200°C. They can be made more effective at higher temperatures.

Temperature has a significant influence on the wear rate of lubricated rubbing pairs either with or without contaminants existing in the lubricant. All these contaminants will unavoidably affect the wear behavior. However, most of existing studies focus on the effects of contaminants at ambient temperature. It is essential and important to study the effects of lubricant temperature on wear process at elevated temperature.

This importance has been recognized by some researchers, and there are some studies on the temperature effects on boundary lubrication [4, 5]. The effect of oil types has been studied under lubrication boundary condition [6]. The results have shown that prior roughness of the sliding surfaces is not pronounced; friction and wear decreased with increased running time at room temperature. Under sever conditions of loading and lubrication, the type of oil film between surfaces plays an important role in reducing friction and wear, such as in the case of hydrodynamic lubrication [7]. This has been attributed to the exponential increase in viscosity of oil with pressure and the elastic deformation of contact surfaces, giving rise to the hydrodynamic effect, which is called elastohydrodynamic lubrication. However, there is a limited study on the effect of the mentioned parameters, especially in practical applications, such as steel industry, mining machinery, and some bearing or gears [8]. Based on the above reasons, the aim of this paper is to study the effect of lubricant temperature, oil type, and wear parameters on sliding wear process.

## 2. EXPERIMENTAL WORK

In this work, a ball-on-cylinder machine, shown in Figure 1, was used to conduct sliding wear tests under lubricating conditions. A cylindrical shape steel of outer diameter of 5.0cm, inner diameter of 2.5cm, height of 2.0cm, and surface roughness of  $0.32 \mu\text{m}$  has been used. The cylinder was specially designed to be transversely loaded under rotating conditions. The chemical composition of the cylinder is given in Table 1. A steel ball of 5mm in diameter was used as a rider to slide on that cylinder. The chemical composition of the ball is given in Table 2. The testing machine used in this work can provide rotational speed ranging from 0-3000 rpm and applied load ranging from 0-500N. The friction coefficient and oil temperature were recorder on line by a system, connected to the tester. Four types of oils were used in this work. The oils specifications are given in Table 3. Three groups of tests were provided for four types of oils. The first group of tests was conducted at temperature of  $40^\circ\text{C}$ , while the second and the third groups of tests were carried out after the oils have been heated and maintained at a temperature of  $90^\circ\text{C}$  and  $120^\circ\text{C}$ .

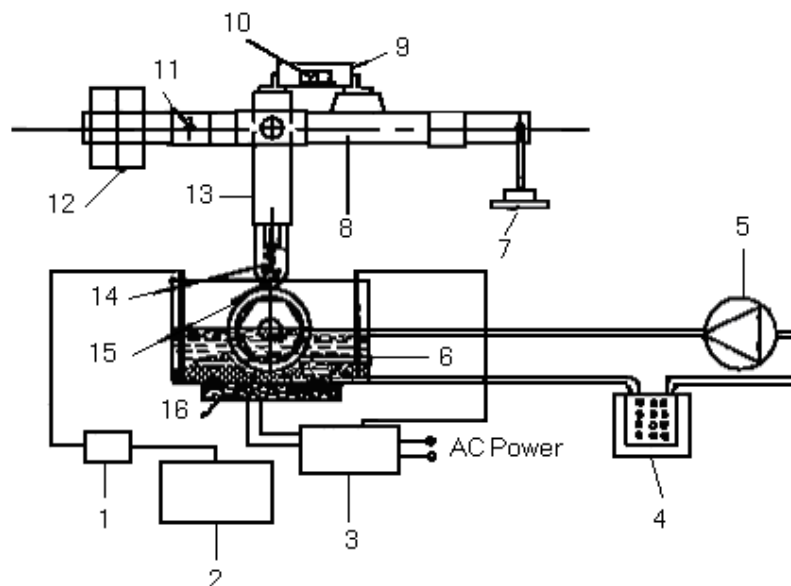


**FIGURE 1:** Schematic Diagram of the Continuous Wear Measurement Technique.

(1- Analog-to-digital converter; 2- Computer; 3- Temperature control unit; 4- Oil filter; 5- Pump; 6- Cylindrical specimen; 7- Loading weight; 8- Loading level; 9- Steel ring; 10-Strain gauge; 11- Fulcrum; 12- Balance weight; 13- Ball holder; 14- Steel spring; 15- Steel boll; 16- Heater)

%C	%Mn	%Si	%Cr	HRC
0.36-0.45	0.50-0.70	0.20-0.50	0.80-1.15	53 (heat treated)

TABLE 1: Chemical Composition of Rotating Cylinder Sample.

%C	%Mn	%Si	%Cr	HRC
0.95-1.02	0.20-0.30	0.15-0.30	1.20-1.60	51

TABLE 2: Chemical Composition of Ball (Rider) Sample.

Oil type	SAE grade	Specific gravity at 5-6°C	Flash point, °C	Viscosity at	
				40°C	100°C
Straight mineral	40	0.904	259	130	10.0
Phosphated	90	0.920	204	150	15.0
Supper cutting (Sulphrated)	30	0.888	260	102	6.6
Water soluble	50	0.930	220	98	4.8

TABLE 3: Specifications of Lubricating Oils.

### 3. RESULTS AND DISCUSSIONS

Analysis was conducted on the basis of obtained friction coefficients, wear particles generated from the sliding tests, and the surfaces of the tested samples. The examination of the friction coefficients and their changes provides information to assess the wear rates of the tests. The investigation of the characteristics of wear particles and wear surfaces of the tested samples offers information for assessing the wear mechanism and wear rates. The measured friction coefficients under different wear conditions are listed in Table 4. Several investigators have reported the effects of lubrication conditions on the wear mechanism. According to their experimental results [5, 8, 9], it has been confirmed that the increases in the oil temperature and its quality significantly affect the wear process. In this research, the influences of the oil temperature, sliding speed, sliding time, and applied load on friction coefficient and wear rate will be discussed.

#### 3.1 Effect of oil Temperature on Friction Coefficient

According to the results shown in Table 4, it is clear that there is a significant effect of oil temperature on the average friction coefficient at constant load and constant sliding speed in all types of oils. Also, it is clear that the SAE90 oil is superior in minimizing friction as compared with other oils under the same conditions, which are in agreement with other tribological results [10, 11]. The results in Table 4 indicate that boundary lubrication conduction occurred, which means that a normal sliding wear process exists. Also, the results show that as the oil's temperature increases, the friction coefficient decreases. This is due to the change in the oil properties, such as viscosity and the chains for oxidation, and formation of oxide film at the rubbing surfaces. This claim is in accordance with assertions in [12]. In all tests the thickness of oil film is smaller than the surface roughness of the rubbing pair surfaces, and a boundary lubrication condition predominant [13].

#### 3.2 Effect of Sliding Speed on Friction Coefficient

The results listed in Table 4 show that at constant load and constant temperature, the average friction coefficient increases as the sliding speed increased. This means that at high sliding speed, the temperature of rubbing pair surfaces rises and the thickness of the lubricating oil film

is not enough to make a good separator between the asperities of coating surfaces and to lower their temperatures [14].

### 3.3 Effect of Sliding Time on Friction Coefficient

During the running-in, at 40°C temperature and constant sliding speed and constant applied load, the friction coefficient gradually decreases as the sliding time increases in all types of oils, as shown in Figures (2-4). This means that more stable oil film exists at contact surfaces during the running-in, and the thickness of this film is sufficient to separate the contact surfaces and reduce the wear rate and friction coefficient. In this case, the wear mechanism is controlled by the type and stability of the oil film.

### 3.4 Effect of Surface Roughness of Rubbing Surfaces on Friction Coefficient

Surface average roughness  $R_a$  was used to describe the surface roughness of the worn surfaces. Table 5 shows the results of surface roughness  $R_a$ . It is clear that the value of  $R_a$  at constant load and constant sliding speed increases with the increase in the oil temperature. This is due to the change in the oil properties when the temperature rises [15].

Group	Test No.	Oil type	Oil temperature, °C	Sliding speed, m/min	Load, N	Friction coefficient, $\mu$
A	1	Soluble	40	785	30	0.140
	2	Sulphrated	40	785	30	0.085
	3	Straight mineral	40	785	30	0.067
	4	Phosphated	40	785	30	0.057
B	1	Soluble	90	785	30	0.158
	2	Sulphrated	90	785	30	0.104
	3	Straight mineral	90	785	30	0.072
	4	Phosphated	90	785	30	0.063
C	1	Soluble	120	785	30	0.186
	2	Sulphrated	120	785	30	0.121
	3	Straight mineral	120	785	30	0.090
	4	Phosphated	120	785	30	0.073
D	1	Soluble	40	1370	30	0.192
	2	Sulphrated	40	1370	30	0.162
	3	Straight mineral	40	1370	30	0.121
	4	Phosphated	40	1370	30	0.084
E	1	Soluble	40	2355	30	0.213
	2	Sulphrated	40	2355	30	0.175
	3	Straight mineral	40	2355	30	0.156
	4	Phosphated	40	2355	30	0.117

**TABLE 4:** Measured Average Friction Coefficients.

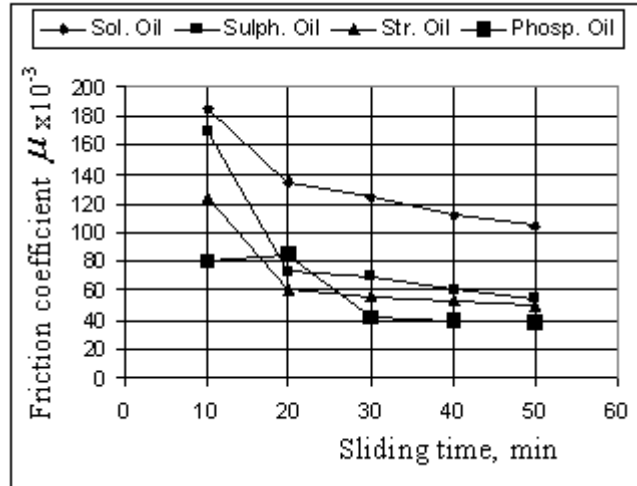


**FIGURE 2:** Friction Coefficient  $\mu$  Versus Sliding Time Under Lubricated Sliding. (Oil Temperature = 40°C, Load = 30N, Sliding Speed = 397 m/min)

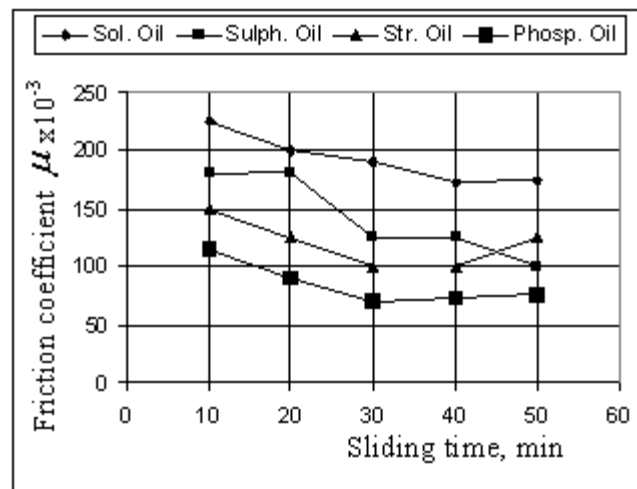


**FIGURE 3:** Friction Coefficient  $\mu$  Versus Sliding Time Under Lubricated Sliding. (Oil Temperature = 90°C, Load = 30N, Sliding Speed = 397 m/min)

### 3.5 Effect of Applied Load on Friction Coefficient

Figure 5 illustrates the effect of applied load on friction coefficient. It is clear that the friction coefficient decreases as the applied load increases, and the value of friction coefficient is higher during the initial transitory severe wear stage at low applied loads. The increase in applied load rises the temperature of the contact area of the rubbing surfaces, which leads to an increase in oil's temperature and gives more chances to the formation of oxide film, which reduces friction coefficient as the wear rate reduces [16].

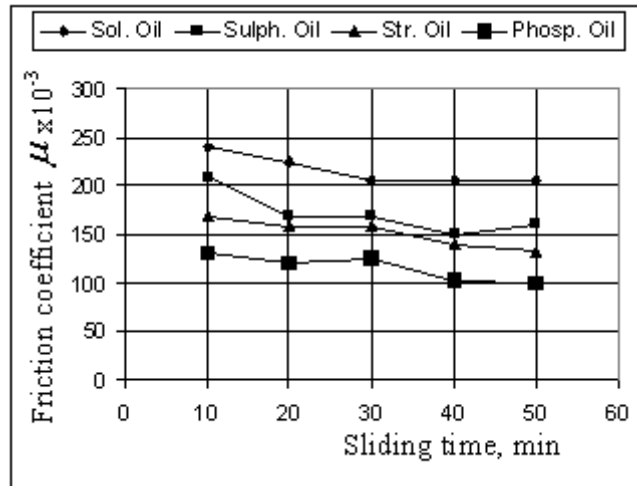


**FIGURE 4:** Friction Coefficient  $\mu$  Versus Sliding Time Under Lubricated Sliding. (Oil temperature = 120°C, Load = 30N, Sliding Speed = 397 m/min)

Group	Test No.	Surface roughness $R_a$ , $\mu m$		Oil's Temperature, °C
		Cylinder	Ball	
A	1	0.46	0.32	40
	2	0.34	0.27	40
	3	0.30	0.22	40
	4	0.28	0.18	40
B	1	0.48	0.35	90
	2	0.39	0.29	90
	3	0.35	0.24	90
	4	0.31	0.21	90
C	1	0.51	0.37	120
	2	0.40	0.34	120
	3	0.38	0.27	120
	4	0.33	0.25	120

**TABLE 5:** Surface Roughness  $R_a$  of the Worn Samples. (Sliding Speed = 785m/min = Constant and Applied Load = 30N = Constant)

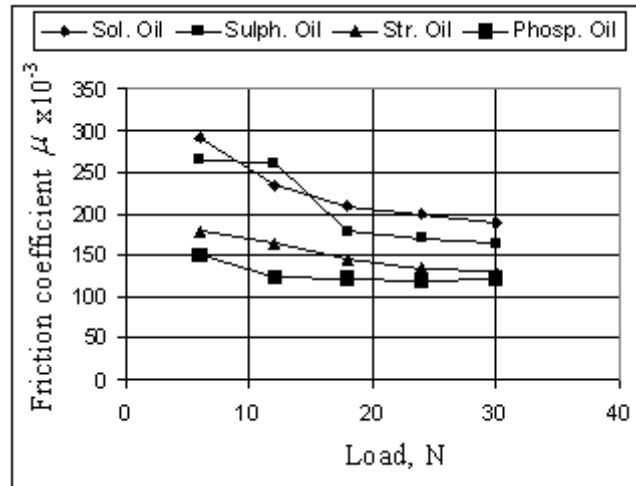


**FIGURE 5:** Friction Coefficient  $\mu$  Versus Applied Load. (Oil Temperature = 40°C, Sliding Speed = 788 m/min)

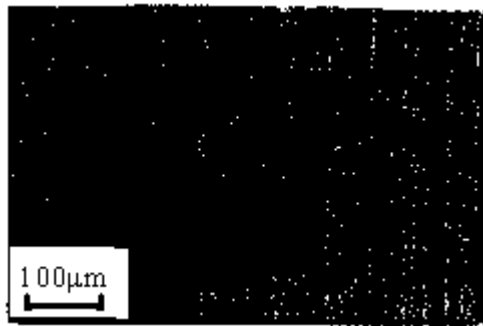
### 3.6 Effect of Surface Damages on Friction Coefficient

The surface topography of the ball and cylinder samples were examined at the end of each test using scanning electronic microscope SEM, as shown in Figure 6. The images can lead to more information about the wear mechanism that took place in this research. A commonly observed feature of the tracks may be termed as a "peeling" effect. This effect has been shown in Figure 6-a, group G, tests 1-4. In Figure 6-b, the surfaces appear as if the layers of materials have been removed progressively with the formation of a number of pitting and scoring in the wear scar. This can be explained in terms of the wear mechanism, which includes adhesion and oxidation according to the types of lubricating oils. Wear particles in the collected oil samples were analyzed for the tests at 120° C temperature for group C, table 4. The results show two major types of wear particles: long flat and oxidation particles. It is noticed that the amount of collected wear particles depended on the test conditions. The increase in surface deformation, coupled with fragmentation at high load levels, accounts  $\leq 7$  for the large increase in the amount of wear particles collected in the oil samples. From Figure 6-a, it can be seen that there are only normal sliding scratches on the wear scar of the ball sample. Generally, it is smooth in the contact area of cylinder sample, as shown in Figure 6-b.

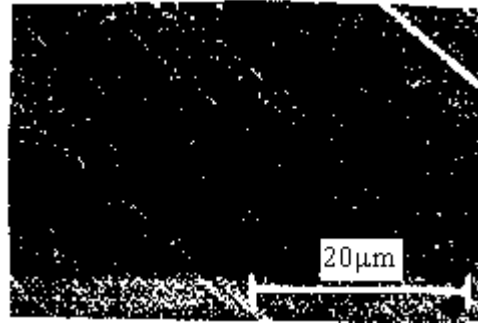
## 4. CONCLUSION

Based on the results of this study, the following conclusions can be made:

1. The temperature of the lubricating oils has significant influence on the wear mechanism.
2. In all tests, the phosphated oil is superior in minimizing friction coefficient and wear rate due to the formation of more stable oil film.
3. At constant sliding speed and load, the increase of sliding time has the same effect on the friction coefficient as the increase of applied load.
4. The decrease in the friction coefficient and wear rate with increasing in sliding time and applied load can be attributed to the improvement in hydrodynamic action.
5. Elastic deformation of contact surfaces under loading conditions gives rise to the elastohydrodynamic lubrication.
6. The amount of wear particles increases with increase in the oils temperature and the applied load.
7. As oil temperature increases, wear particles formed. These wear particles act as abrasives, which lead to increase in friction coefficient and wear rates.



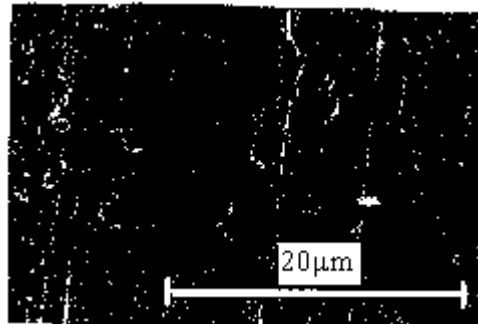
1-a. Water soluble oil



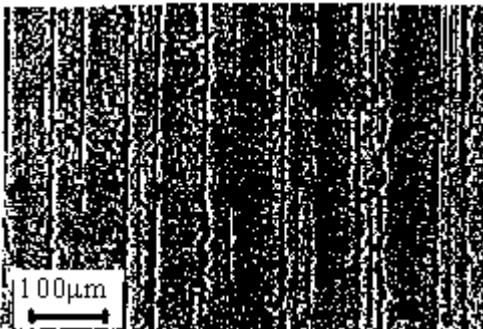
1-b. Water soluble oil



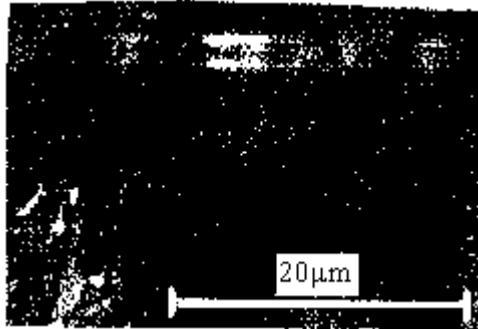
2-a. Sulphrated oil



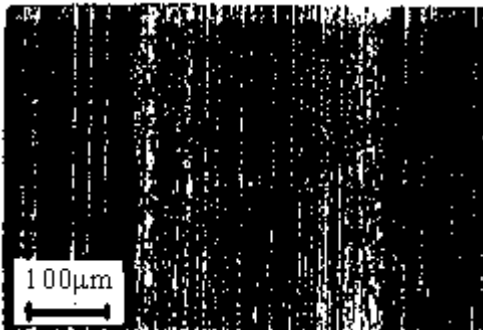
2-b. Sulphrated oil



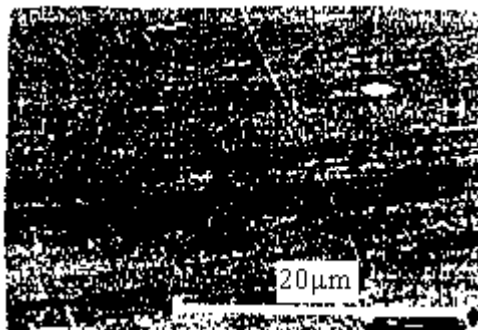
3-a. Phosphated oil



3-b. Phosphated oil



4-a. Straight mineral oil



4-b. Straight mineral oil

**a. Ball samples.**

**b. Cylinder samples.**

**FIGURE 6:** The SEM Surface Topography of the Tested Samples in Test Group G.

## 5. REFERENCES

- [1] D. Shakhvorostof, K. Pohlmann, M. Scherge. "An energetic approach to friction, wear and temperature", *Wear*, vol. 257, pp. 124-130, 2004.
- [2] M. Anderson and F.E. Schmidt. "Wear and lubricant testing", ASTM manual, 2002, chap. 25.
- [3] R.G. Bayer. "Wear analysis for engineers", HNB publishing, New York, 2002, pp. 220-230.
- [4] B. Cavdar. "Effect of temperature, substrate type, additive and humidity on the boundary lubrication in a linear perfluoropoly-alkyl ether fluid". *Wear*, vol.206, pp. 15-23, 1997.
- [5]. M. Masuko, S. Hirose, H. Okabe. "Boundary lubrication characteristics of polyolester class synthetic lubricant applied to silicon nitride at high temperature", *Lubr-Eng.*, vol. 52, pp. 641-647, 1996.
- [6] Ghazi Al-Marahleh. "Mechanism of sliding wear under lubrication condition", *Journal of Applied Sciences*, vol. 5, pp. 862-867, 2005.
- [7] P. J. Blau. "Glossary of terms, friction lubrication and wear technology", *ASTM Intl.*, vol. 18: pp. 180-210, 1992.
- [8] M. J. Neale. "The tribology handbook, second ed.". Butterworth-Heinemann, Oxford, 1995, pp. 280-360.
- [9] Z. Peng, T.B. Kirk, Z. L. X. Xu. "The development of three dimensioned imaging techniques of wear particle analysis", *Wear*, vol. 203/204, pp. 418-424, 1997.
- [10] P.A. Willerment, R. O. Carter, P. J. Schmitz, M. Everson, D. J. Scholl, W. H. Weber. "Structure and properties of lubricant-derived anti-wear films". *Lub. Sci.*, vol. 9, pp. 325-348, 1997.
- [11] M. L. S. Fuller, M. Kasrai, G. M. Bancroft, K. Fyfe, K.H. Tan. "Solution decomposition of ZDDP and its effect on anti-wear and thermal film formation studied by X-ray absorption spectroscopy", *Tribology International*, vol. 31, no. 10, pp. 627-644, 1998.
- [12] C. Q. Yuan et al. *Wear*, vol. 257 pp. 812-822, 2004.
- [13] B. Bhushan, B. K. Gupta. "Handbook of Tribology", MC Graw-Hill inco, 1991.
- [14] H. G. horn. "ASTM Handbook", 18, 1992, p. 399.
- [15] Oil-Owei, B. J. Roylance. "The effect of solid contamination on the wear and critical failure load in a sliding lubricated contact", *Wear*, vol. 112, pp. :255-259,1986.
- [16] S. W. E. Earles, D. Povfil. "5<sup>th</sup> Conf. Lubrication Wear", Plymouth, Inst. Mech. Engrs., Preprints, p. 171, 1967.
- [17] B.J Roylance. "Industrial wear particle atlas", 1997

## Finite Element Analysis of Cold-formed Steel Connections

**Bayan Anwer Ali**

*Faculty of Civil Engineering,  
Universiti Teknologi Malaysia, 81310 Skudai, Johor,  
Malaysia*

*engbayan@gmail.com*

**Sariffuddin Saad**

*Steel Technology Centre, Faculty of Civil Engineering,  
Universiti Teknologi Malaysia, 81310 Skudai, Johor,  
Malaysia*

*sariffuddin@utm.my*

**Mohd Hanim Osman**

*Steel Technology Centre, Faculty of Civil Engineering,  
Universiti Teknologi Malaysia, 81310 Skudai, Johor,  
Malaysia*

*mhanim@utm.my*

**Yusof Ahmad**

*Faculty of Civil Engineering,  
Universiti Teknologi Malaysia, 81310 Skudai, Johor,  
Malaysia*

*a-yusof@utm.my*

---

### Abstract

This paper presents a study on the structural performance of column-base and beam-column connections of cold-formed steel with the use of single-lipped C-sections with bolted moment connections. Experiments were done on two specimens; a column-base connection and a beam-column connection and the results showed that section failure caused by flexural buckling was always critical. Managing to attain moment resistances which are close to the results of connected sections, it was proven that the proposed connections were structurally efficient. Finite element models were established with the use of shell elements to model the sections while bar elements were used to model the bolted fastenings for the purpose of examining the structural behaviour of both the column-base and the beam-column connections. Incorporation of material non-linearity and comparison between the experimental and numerical results were presented. The proposed analysis method for predicting structural behaviour of column-base and beam-column connections with similar connection configuration proved to be adequate.

**Key Words:** Column Bases, Beam Column, Bolted Moment Connections, Finite Element Modeling.

---

### 1. INTRODUCTION

Being lightweight and able to provide high performance structurally, cold-formed steel sections are suitable for building construction. With thickness ranging between 1.2mm to 3.2mm and yielding strength of from 250 to 450 N/mm<sup>2</sup>, the most commonly available steel sections are lipped C and Z-sections. Connected onto primary structural members through web cleats as pinned or moment connections, cold-formed steel sections usually depend on the connection configurations as they act as secondary members. There are many design recommendations of cold-formed steel sections available for application in building construction such as AISI [1], BS5950 [2] and Euro code 3: Part 1.3 [3]. Moreover, there are also many design guides and commentaries available to assist structural engineers to design cold-formed steel structures [4, 5, 6, 7].

Since the last decade, there has been a widely growing trend in the construction of low to medium rise houses and modest span of portal frames where cold-formed steel sections are used as primary structural members. Therefore, in order to ensure practicality and efficiency in terms of the framing, it is important to develop simple and effective moment connections between cold-formed steel members. Despite being commonly used throughout the years, little research has been done on the use of cold-formed steel members especially among single cold-formed steel sections. Various studies by Chung and Lau [8] and Wong and Chung [9] presented the experimental results for the use of bolted moment connections between cold-formed steel members which were typically applied in building construction where the bolted moment connections between the cold-formed steel members showed high structural efficiency. Furthermore, another study by Ho and Chung [10] provided extended experimental investigation on the use of bolted moment connections between lapped Z-sections.

## **2. SCOPE OF STUDY**

This paper presents a study on the structural performance of column-base and beam-column connections of cold-formed steel with the use of single-lipped C-sections with bolted moment connections. Connection tests were done of two specimens; column base and beam column connections in order to study their structural behaviour as well as the moment resistances. Moreover, this paper shows the establishment of a finite element model through the modelling of the sections and the bolted fastenings with the use of shell and bar elements. Incorporation of material non-linearity and comparison between the experimental and numerical results will be presented more detailed in the following sections.

## **3. EXPERIMENTAL TESTS ON CONNECTIONS**

Tests on a column base and a beam column using single cold-formed lipped channel sections with bolted moment connections were carried out, and Figure 1 illustrates the details of the connection configurations.

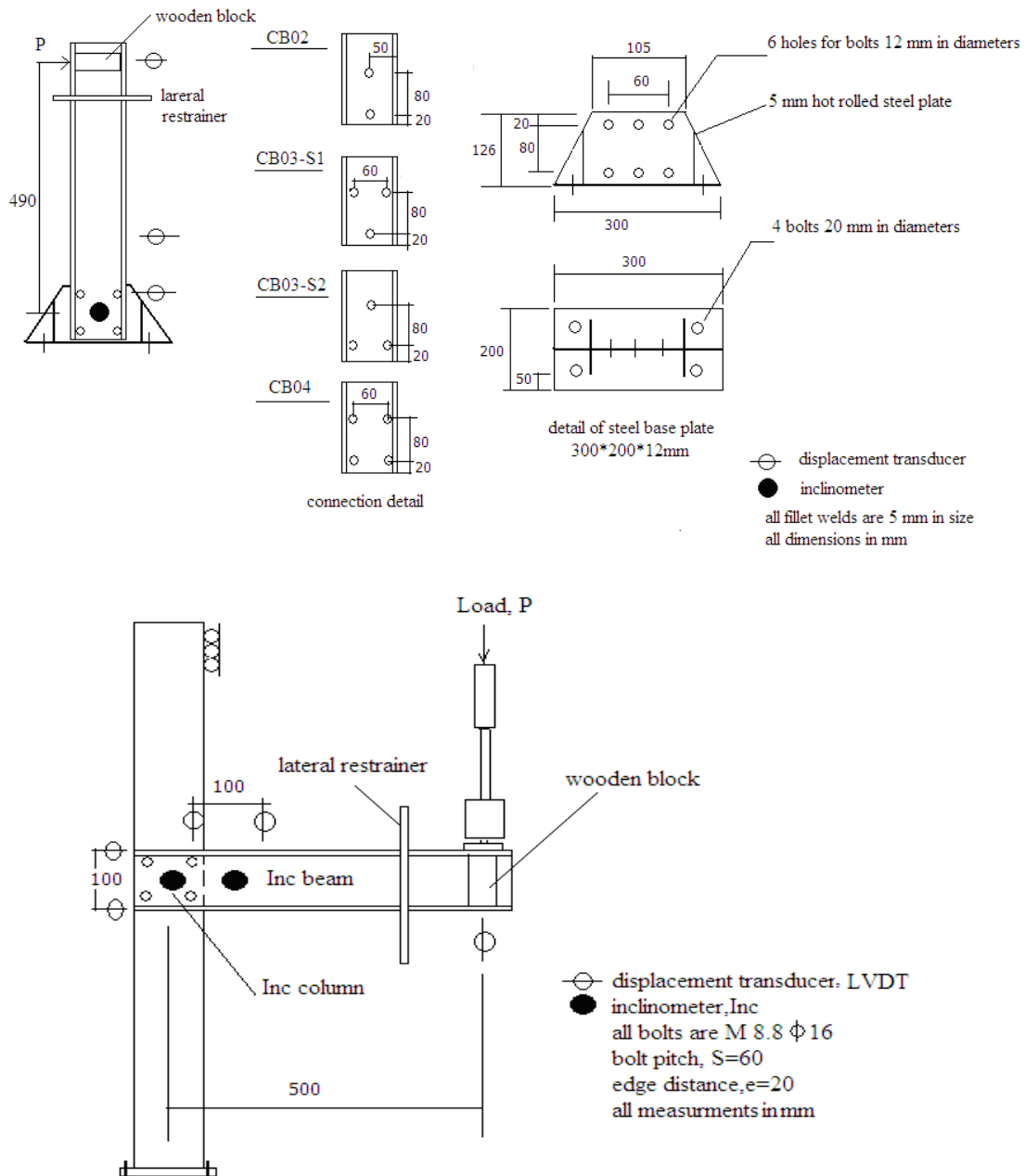


**FIGURE 1:** Detail of cold-formed steel column base and beam column connections

The beam and column members are formed from single cold-formed lipped channel sections. The flange width, web and lip depth of the cold-formed section are 50,100 and 14 mm respectively, with 1.6 mm thick section. The test specimens were designated as CB and BC for column base and beam column connections respectively as shown in Table 1. The measured yield strength was found to be 490 N/mm<sup>2</sup> and 572N/mm<sup>2</sup> for 1.6 mm thick section and bolt grade 8.8 of 12 mm diameter respectively. In all tests, loads were applied near the top of the test specimens and the applied load increased gradually until unloading occurred where continuous measurements were

taken for the applied loads, the deflections of the loaded points including the rotation of the members throughout the test. The failure of both test specimens occurred due to flexural buckling of section web near connections, as shown in Figure 2. The load-deflection and moment rotation curves of the tests for both the column base and beam column connections were plotted in Figure 3 and Figure 4 respectively. The results from both the experiment as well as the analysis of the finite element were plotted in same graph for easy comparison. It was shown that all the connections rotated linearly under low applied loads, and then exhibited non-linear deformation characteristics when the applied loads increased. The restriction of the moment resistances of the connections to be the applied moment is at the connection rotation of 0.05 rad [8]. The results of all the tests are as summarized in Table 1.

**TABLE 1:** Summarization of the test program and test results

$M_{r_{EXP}}$ : calculated resistance	Test	Bolt pitch (mm)	Eccentricity (mm)	$M_{r_{EXP}}$ @0.05rad (kNm)	Failure mode	denotes moment from
	CB	80	490	3.6	FF <sub>cs</sub>	
	BC	60	500	2.1	FF <sub>cs</sub>	

experimental; FF<sub>cs</sub>: denotes Flexural failure of connected section.

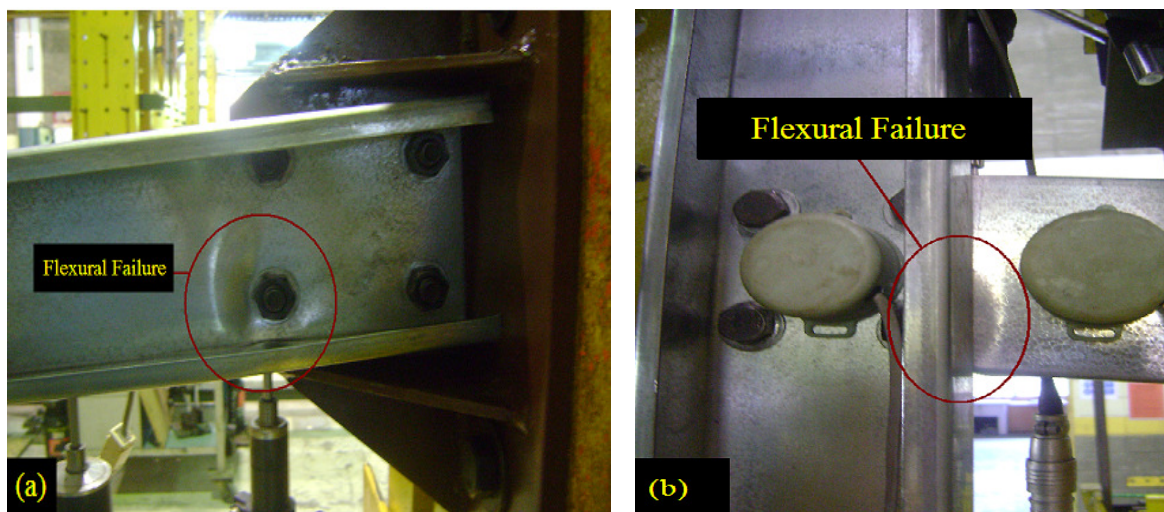
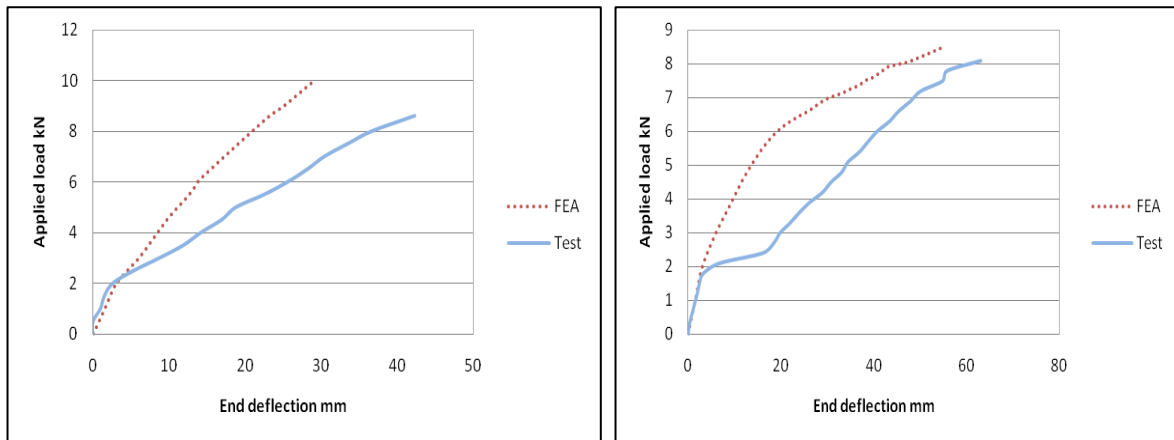


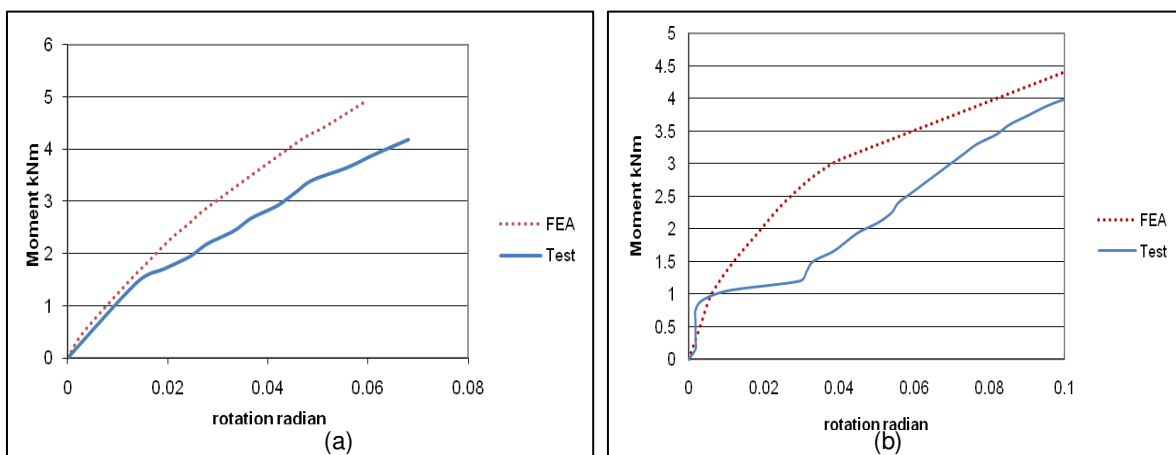
**FIGURE 2:** Flexural failure of connected section (a) column base connection (b) beam column connection.



(a)

(b)

**FIGURE 3:** Load-deflection curves of cold-formed steel connections (a) column base (b) beam column



(a)

(b)

**FIGURE 4:** Moment-rotation curves of cold-formed steel connections (a) column base (b) beam column

#### 4. NUMERICAL INVESTGATION

Compared to the typical hot-rolled steel sections, cold-formed steel sections are usually much more slender and can be notably deformed. Experiments on the connections between cold-formed steel sections and non-linear finite element modelling are considered to be particularly useful in tackling such problems. Moreover, finite element modeling can also provide important information of the structural responses of the cold-formed steel structures, such as the deformation of the shapes, initial stiffness, moment resistance and stress distributions. Numerical investigations [11] using commercial finite element packages were reported to study and assess the structural behaviour of bolted moment connections in which one of the most significant was a study by Chung et al. [12] which examined the load deformation characteristics of bolted fastenings under combined bending and shear through the application of advanced finite element modelling and with the use of three-dimensional solid elements with material and geometrical non-linearities.

#### 4.1. Finite Element Model

In this study, the purpose finite element package LUSAS, Version 13.5 [13] was adopted for the numerical simulation of the cold-formed steel column base and beam column connections, as shown in Figure 5. To increase the accuracy of the research, the LUSAS modeling process used the connection dimensions, boundary conditions and material properties as similar as possible to that of the experimental set-up model. However, to obtain better and accurate results, many models need to be generated before the most suitable element discretisation can be found. The finite element models were incorporated with the following features:

- Four-node three dimensional shell elements, QTS4, were used to model the C sections.
- Two-node three dimensional elements, BRS2, were used to model the bolt fasteners.
- The measured stress-strain curves obtained from the coupon tests were used for the material models of the C sections with the von Mises yielding criteria as an addition.

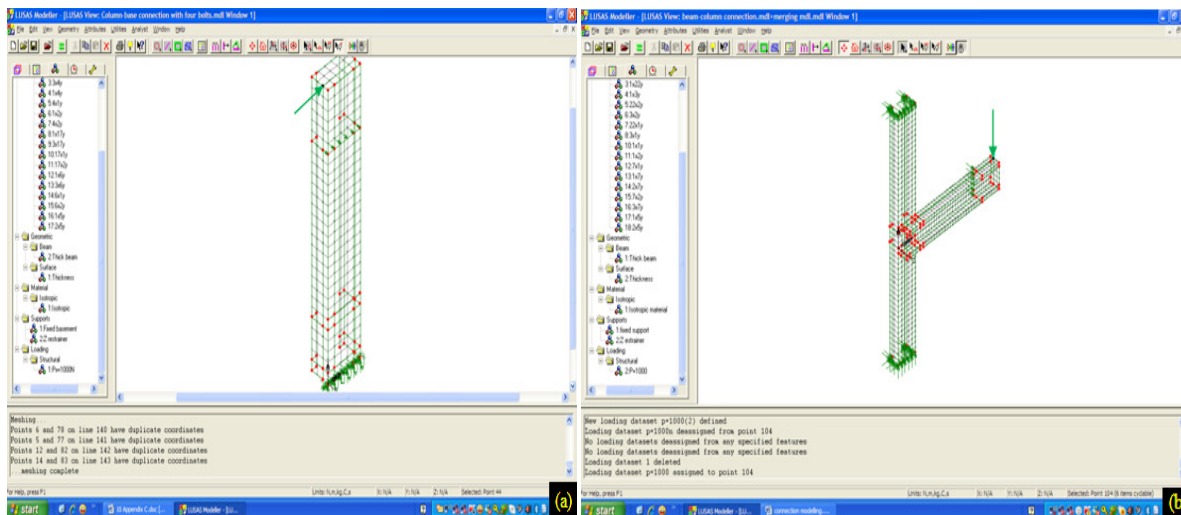


FIGURE 5: Finite element models of connections (a) column base (b) beam column

#### 4.2. Numerical Results

The load-deflection and moment-rotation curves of the connections provided by the established finite element models were plotted onto the same graphs of the measured curves in Figure 3 and Figure 4 respectively for direct comparison. Load-deflection curve can be obtained directly from the model result file while calculations are needed to be done by extracting the data from loadings and nodal displacements for the moment-rotation curve. Both the numerical and the curves which were measured in the experiment agreed very well over the linear stage while accuracy of the analysis decreased for the rest deformation ranges. Figure 6 illustrates the deformed shapes of the column base and beam column connections. According to the applied point load, larger deflection was expected and the prediction was proven true. Comparison of the moment resistances obtained with the use of the finite element models with the measured value are summarized in Table 2 to allow comparison. Establishing a model factor,  $\Psi_{FEM}$ , the finite element models were assessed structurally to ensure their adequacy. The model factor is defined as:

$$\Psi_{FEM} = \frac{\text{Predicted moment resistance obtained from finite element analysis, } M_{r FEM}}{\text{Measured moment resistance, } M_{r Test}} \quad (1)$$

The model factor for the finite element model of the column base connection was 1.2 while the factor for the beam column connection was 1.5 which shows the accuracy of the finite element models in the prediction of the moment resistance of the proposed connections. However, the

values of the model factors and the output results can be improved to be more accurate, by doing further advanced finite element analysis investigation that incorporate affect of material, geometrical and boundary non-linearities.

**TABLE 2:** Summary of moment resistances

$Mr_{EXP}$ : denotes calculated moment resistance from experimental;  $Mr_{FEM}$ : denotes moment resistance from finite element models;  $\Psi_{FEM}$  : is defined as  $Mr_{FEM} / Mr_{EXP}$

Test	$Mr_{EXP}$ (kNm)	$Mr_{FEM}$ (kNm)	Model factor $\Psi_{FEM}$
CB	3.6	4.4	1.2
BC	2.1	3.2	1.5

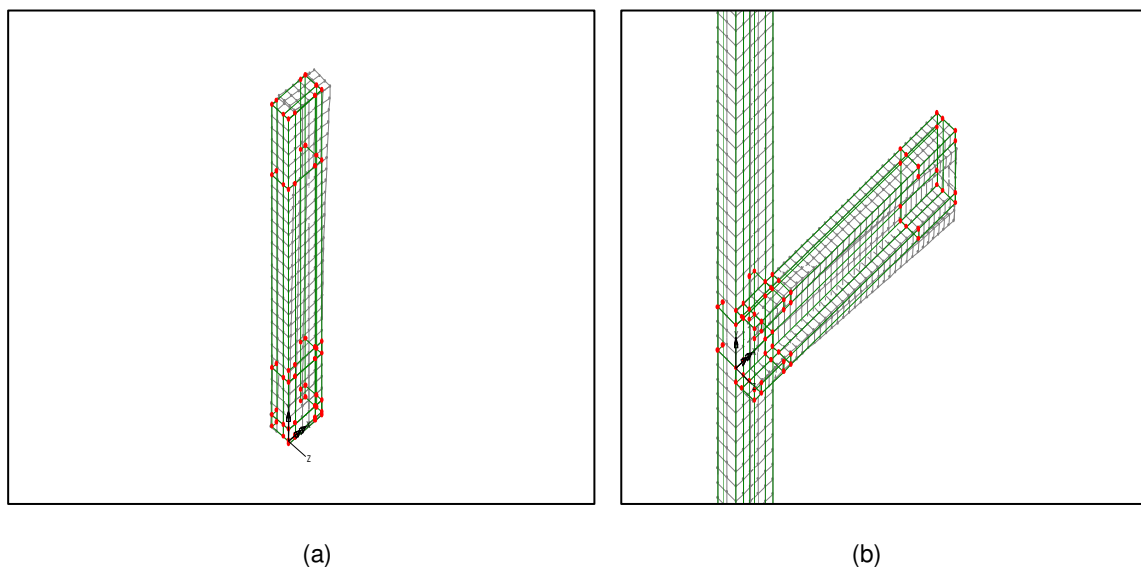


**FIGURE 6:** Deformed mesh for the connections (a) column base (b) beam column

## 5. CONCLUSIONS

Tests were done on a column base and a beam column connection with bolted moment connections where lateral loads were placed and the results of the experiment showed the structural behaviour of the connections. In the tests, the flexural failure of the connected C-sections proved to be always critical and through establishing finite element models, the structural behaviour of the connections were able to be predicted. Comparison on the moment resistances obtained from both the tests as well as the models showed that the results were satisfactory.

The established finite element models proved to be effective in assessing the moment resistances of typical column base connection and beam column connection and can be readily offered to be used by engineers in designing moment connections of cold-formed steel sections. The proposed method however, can be used only in bolted connections that have similar configurations to the ones investigated in the study.

## 6. REFERENCES

- [1] American Iron and Steel Institute. "AISI Specification for the design of cold-formed steel structural members", Washington (DC), 1996.
- [2] British Standards Institution. BS5950. "Structural use of steelwork in buildings: Part 5: Code of practice for the design of cold-formed sections", London, 1998.
- [3] Eurocode 3. "Design of steel structures". Part 1.3: General rules – Supplementary rules for cold-formed thin gauge members and sheeting, ENV 1993-1-3. Brussels: European Committee for Standardization, 1996.
- [4] Chung, K.F. "Building design using cold-formed steel sections". Worked examples to BS5950: Part 5: 1987. The Steel Construction Institute, 1993.
- [5] Hancock, G.J. "Design of Cold-Formed Steel Structures". 3rd ed. Australian Institute of Steel Construction, 1998.

- [6] Lawson, R.M., Chung, K.F. and Popo-Ola, S.O. "*Building Design using Cold-formed Steel Sections*". Structural Design to BS5950-5:1998 - Section properties and load tables, The Steel Construction Institute, SCI-P276, 1-234, 2002.
- [7] Yu, W.W. "*Cold-Formed Steel Design*". 3rd ed. New York: John Wiley and Sons Inc, 2000.
- [8] Chung, K.F. and Lau, L. "*Experimental investigation on bolted moment connections among cold-formed steel members*". Engineering Structure, 21(10), 898-911, 1999.
- [9] Wong, M.F. and Chung, K.F. "*Structural behaviour of bolted moment connections in beam-column sub-frames*". Journal of Constructional Steel Research, 58(2), 253-274, 2002.
- [10] Ho, H.C. and Chung, K.F. "*Experimental investigation into the structural behaviour of lapped connections between cold-formed steel Z sections*". Thin-Walled Structures, 42(7), 1013-1033, 2004.
- [11] Lim, J.B.P. and Nethercot, D.A. "*Ultimate strength of bolted moment-connections between cold-formed steel members*". Thin-Walled Structures, 41(11), 1019-1039, 2003.
- [12] Chung, K.F., Yu, W.K. and Wang a.J. "*Structural performance of cold-formed steel column bases with bolted moment connections*". Steel and Composite Structures. 5(4):289-304, 2005.
- [13] LUSAS. "*Modeler User's Manual*". Version 13.5, United Kindom.

## Reduction of Ultimate Strength due to Corrosion - A Finite Element Computational Method

**J.M. Ruwan S. Appuhamy**

*Department of Civil and Environmental Engineering,  
Ehime University, Bunkyo-cho 3,  
Matsuyama 790-8577, Japan.*

ruwan@cee.ehime-u.ac.jp

**Mitao Ohga**

*Department of Civil and Environmental Engineering,  
Ehime University, Bunkyo-cho 3,  
Matsuyama 790-8577, Japan.*

ohga@cee.ehime-u.ac.jp

**Tatsumasa Kaita**

*Department of Civil Engineering & Architecture,  
Tokuyama College of Technology,  
Shunan 745-8585, Japan.*

kaita@tokuyama.ac.jp

**Ranjith Dissanayake**

*Department of Civil Engineering,  
University of Peradeniya, Peradeniya,  
20400, Sri Lanka.*

ranjith@civil.pdn.ac.lk

---

### Abstract

Bridge safety is of paramount importance in transportation engineering and maintenance management. Corrosion causes strength deterioration and weakening of aged steel structures. Therefore, it is a vital task to estimate the remaining strength of corroded steel structures in order to assure the public safety. Due to the economic constraints and increase of number of steel highway and railway bridge structures, it will be an exigent task to conduct tests for each and every aged bridge structure within their bridge budgets. Therefore, this paper proposes a method of evaluating the residual strength capacities by numerical approach and compares the non-linear FEM analyses results with their respective tensile coupon tests. Further, since it is not easy to measure several thousands of points, to accurately reproduce the corroded surface by numerical methods and to predict their yield and ultimate behaviors, a simple and reliable analytical model is proposed by measuring the maximum corroded depth ( $t_{c,max}$ ), in order to estimate the remaining strength capacities of actual corroded members more precisely.

**Keywords:** Bridges, Corrosion, Maximum Corroded Depth, FEM Analysis, Remaining Strength.

---

### 1. INTRODUCTION

Corrosion of the members of a steel structure leads to impairment of its operation and progressive weakening of that structure. The consequences of corrosion are many and varied and effects of these on safe, reliable and efficient operation of structures are often considered than simply losing of a volume of metal. Various kinds of failures and the need of expensive replacements may occur even though the amount of metal destroyed is quite small. One of the major harmful effects of corrosion is the reduction of metal thickness leading to loss of mechanical strength and structural failure, causing severe disastrous and hazardous injuries to the people. Therefore, understanding of the influence of damage due to corrosion on the remaining load-carrying capacities is a vital task for the maintenance management of steel highway and railway infrastructures.

Though it's a maintenance issue, it can be addressed appropriately by specification of a proper corrosion system in the design phase. It has been proved that the corrosion played a significant role in the catastrophic collapse of both the Silver Bridge (Point Pleasant, WV) in 1967 and the Mianus River Bridge (Connecticut) in 1983, USA [1]. Those collapses indicated the paramount importance of attention to the condition of older bridges, leading to intensified inspection protocols and numerous eventual retrofits or replacements [2,3]. Therefore corrosion is not an issue to be taken lightly either in design phase or in maintenance stage. Detailed regular inspections are necessary in order to assure adequate safety and determine maintenance requirements, in bridge infrastructure management. But the number of steel bridge infrastructures in the world is steadily increasing as a result of building new steel structures and extending the life of older structures. So, there is a need of more brisk and accurate assessment method which can be used to make reliable decisions affecting the cost and safety.

During the past few decades, several experimental studies and detailed investigations of corroded surfaces were done by some researchers in order to introduce methods of estimating the remaining strength capacities of corroded steel plates [4-7]. But, to develop a more reliable strength estimation technique, only experimental approach is not enough as actual corroded surfaces are different from each other. Further, due to economic constraints, it is not possible to conduct tests for each and every aged bridge structure within their bridge budgets. Therefore, bridge engineers are faced with lack of experimental and field data. Therefore, nowadays, use of numerical analysis method could be considered to have a reliable estimation in bridge maintenance industry [8].

Sidharth *et al.* [9] stated the importance and reviewed the abreast development in the FE analysis technique used to study the corrosion effect on the plates. Ahmmad *et al.* [10] investigated the deformability of corroded steel plates under quasi-static uniaxial tension through both experimental and numerical analyses. They proposed empirical formulae to estimate the reduction in deformability and energy absorption capacity due to pitting corrosion and general corrosion under uniaxial tension. Therefore it can be seen that the finite element analysis method has now become the most common, powerful and flexible tool in rational structural analysis and makes it possible to predict the strength of complex structures more accurately than existing classical theoretical methods.

Even though, it is an exigent task to conduct detail investigations of all existing steel structures as the number of steel structures are steadily increasing in the world, it is necessary to assess those structures in regular basis to ensure their safety and determine the necessary maintenance. Therefore, developing a rapid and accurate methodology to estimate the remaining strength capacities of steel infrastructures is a vital task in maintenance engineering. Therefore, this paper proposes a simple, accurate and brisk analytical method which can be used to make reliable decisions on the maintenance management of existing steel infrastructures.

## **2. CORRODED TEST SPECIMENS**

The test specimens were cut out from a steel girder of Ananai River in Kochi Prefecture on the shoreline of the Pacific Ocean, which had been used for about hundred years. This bridge had simply supported steel plate girders with six spans, with each of 13.5 m. All plate girders were constructed by rivet joints and were exposed to high airborne salt environment by strong sea wind for a long time. It was constructed as a railway bridge in 1900, and in 1975 changed to a pedestrian bridge, when the reinforced concrete slab was cast on main girders. The bridge was dismantled due to serious corrosion damage in year 2001. Many severe corrosion damages distributed all over the girder, especially, large corrosion pits or locally-corroded portions were observed on upper flanges and its cover plates. Then, 21 (F1-F21) and 5 (W1-W5) test specimens were cut out from the cover plate on upper flange and web plate respectively.

Before conducting the thickness measurements, all rusts over both surfaces were removed carefully by using the electric wire brushes and punches. Then, two new SM490A plates

( $t=16\text{mm}$ ) were jointed to both sides of specimen by the butt full penetration welding for grip parts to loading machine, as shown in Figure 1. Here, the flange and web specimens have the widths ranged from 70-80 mm and 170-180 mm respectively. The test specimen configuration is shown in Figure 1. In addition, 4 corrosion-free specimens (JIS5 type) were made of each two from flange and web, and the tensile tests were carried out in order to clarify the material properties of test specimens. The material properties obtained from these tests are shown in Table 1.

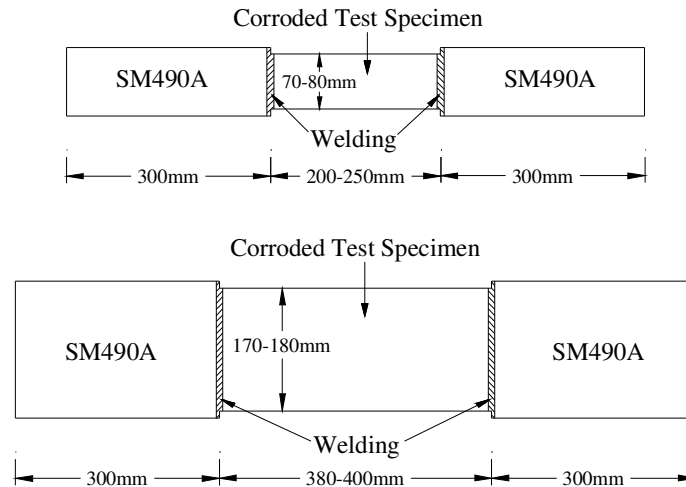


**FIGURE 1:** Dimensions of test specimens.

Specimen	Elastic modulus /(GPa)	Poisson's ratio	Yield stress /(MPa)	Tensile strength /(MPa)	Elongation at breaking /(%)
Corrosion-free plate (flange)	187.8	0.271	281.6	431.3	40.19
Corrosion-free plate (web)	195.4	0.281	307.8	463.5	32.87
SS400 JIS	200.0	0.300	245~	400~510	–

**TABLE 1:** Material properties

Accuracy, convenience, portability and lightness are highly demanded for choosing of a device for the on-site measurement of corroded surface irregularities. Therefore, the portable 3-dimensional scanning system, which can measure the 3-dimensional coordinate values at any arbitrary point on the corrosion surface directly and continuously, was used for the measurement of surface irregularities of the test specimens [11]. Here, the thickness of the corroded surface can be calculated easily from those measured coordinates. The measuring device has three arms and six rotational joints, and can measure the coordinates of a point on steel surface by using the non-contact scanning probe (laser line probe). The condition of thickness measurement is shown in Figure 2. Since this probe irradiates the steel surface with a laser beam, which has about 100mm width, the large number of 3-dimensional coordinate data can be obtained easily at a time. So, the thicknesses of all scratched specimens were measured by using this 3D laser scanning device and the coordinate data was obtained in a grid of 0.5mm intervals in both X and Y directions. Then, the remaining thicknesses of all grid points were calculated by using the difference of the coordinate values of both sides of those corroded specimens. Then, the statistical thickness parameters such as average thickness ( $t_{avg}$ ), minimum thickness ( $t_{min}$ ), standard deviation of thickness ( $\sigma_{st}$ ) and coefficient of variability (CV) were calculated from the measurement results.



**FIGURE 2:** Condition of thickness measurement.

Even though, various types of corrosion conditions in actual steel structures can be seen as the corrosion damage can take place in many shapes and forms, it is necessary to categorize those different corrosion conditions to few general types for better understanding of their remaining strength capacities. So, in this study, all specimens were categorized into 3 typical corrosion types concerning their visual distinctiveness, amount of corrosion, expected mechanical and ultimate behaviors and minimum thickness ratio,  $\mu$  (minimum thickness/ initial thickness) [7]. Here, the 3 different types of corrosion levels can be classified according to their severity of corrosion as follows:

- $\mu > 0.75$  ; Minor Corrosion
- $0.75 \geq \mu \geq 0.5$  ; Moderate Corrosion
- $\mu < 0.5$  ; Severe Corrosion

Three specimens F-14, F-13 and F-19 with minor, moderate and severe corrosion conditions respectively are shown in Figure 3.



**FIGURE 3:** Plates with (a) minor [F-14], (b) moderate [F-13] and (c) severe [F-19] corrosion.

### 3. EXPERIMENTAL ANALYSIS AND RESULTS

Tensile loading tests were carried out at constant velocity under loading control by using a hydraulic loading test machine (maximum load: 2940KN) for all 26 specimens with different corrosion conditions. The loading velocity was set to 200N/sec for minor corroded specimens and 150N/sec for moderate and severe corroded specimens.

Figure 4 shows the load-elongation curves for three different corroded specimens with 3 corrosion types. The specimens F-14 and F-13 have comparatively larger minimum thickness ratio ( $\mu = 0.783$  and  $0.512$  respectively) and the specimen F-19 in which the corrosion progression was more severe, the minimum thickness ratio is also diminutive ( $\mu = 0.061$ ). Herein, the specimen (F-14) with minor corrosion has almost same mechanical properties (such as apparent yield strength and load-elongation behavior etc.) as the corrosion-free specimen. On the other hand, the moderate corroded specimen (F-13) and the severe corroded specimen (F-19) show obscure yield strength and the elongation of the specimen F-19 decreases notably. The

reason for this is believed to be that the local section with a small cross-sectional area yields at an early load stage because of the stress concentration due to irregularity of corroded steel plate. And this will lead moderate and severe corroded members elongate locally and reach to the breaking point.

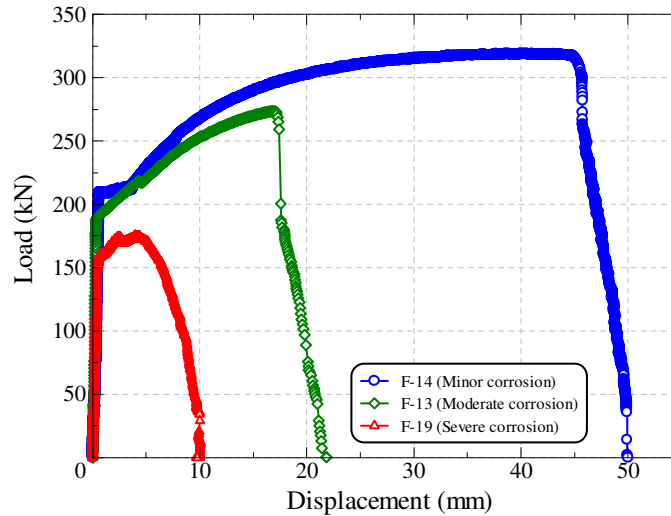


FIGURE 4: Load-displacement curves.

Even though the relation between the breaking section and the thickness distribution is not exactly clarified yet, it can be seen that most of minor corrosion members are failed in a section corresponds to a minimum thickness point ( $t_{min}$ ) or a minimum average thickness point ( $t_{sa}$ ) for the members with the thickness variation is very small. Also, it was noted that the breaking point of moderate and severe corrosion members are corresponds to a section of the minimum thickness point. Therefore, the local statistical parameters with the influence of stress concentration can be used for the yield and tensile strength estimations.

## 4. NUMERICAL INVESTIGATION

### 4.1 Analytical Model

The 3D isoparametric hexahedral solid element with eight nodal points (HX8M) and updated Lagrangian method based on incremental theory were adopted in these analyses. Non linear elastic-plastic material, Newton-Raphson flow rule and Von Mises yield criterion were assumed for material properties. Further, an automatic incremental-iterative solution procedure was performed until they reached to the pre-defined termination limit.

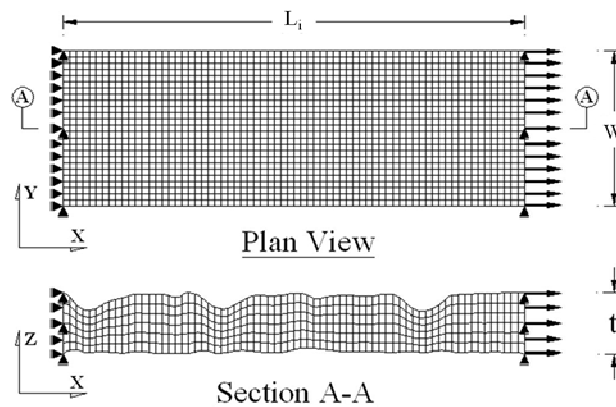


FIGURE 5: Analytical model of corroded member.

The analytical models with different length (L) and width (W) dimensions were modeled with their respective corrosion conditions as shown in Figure 5. One edge of the member's translation in X, Y and Z directions were fixed and only the Y and Z direction translations of the other edge (loading edge) were fixed to simulate with the actual experimental condition. Then the uniform incremental displacements were applied to the loading edge. Yield stress  $\sigma_y = 294.7$  [MPa], Elastic modulus  $E = 191.6$  [GPa], Poisson's ratio  $\nu = 0.276$  were applied to all analytical models, respectively.

#### 4.2 Ductile Fracture Criterion

Fracture is an important mode of failure in steel structures, and accurate assessment of fracture is necessary to understand the ultimate behaviors. The "Stress Modified Critical Strain Model (SMCS)" was proposed by Kavinde et al. (2006), to evaluate the initiation of ductile fracture as a function of multiaxial plastic strains and stresses [12]. This method was adopted in this analytical study. In SMCS criterion, the critical plastic strain ( $\epsilon_p^{Critical}$ ) is determined by the following expression:

$$\epsilon_p^{Critical} = \alpha \cdot \text{Exp}\left(-1.5 \frac{\sigma_m}{\sigma_e}\right) \quad (1)$$

Where,  $\alpha$  is toughness index and the stress traxiality  $T = (\sigma_m/\sigma_e)$ , a ratio of the mean or hydrostatic stress ( $\sigma_m$ ) and the effective or von Mises stress ( $\sigma_e$ ). The toughness index  $\alpha$  is a fundamental material property and hence obtained from the tensile test conducted for the non corroded specimen and obtained as follows:

$$\alpha = \frac{\epsilon_p^{Critical}}{\text{Exp}\left(-1.5 \frac{\sigma_m}{\sigma_e}\right)} \quad (2)$$

The ultimate strength of each corroded specimen was calculated accordingly by using the SMCS criterion and compared with their experimental ultimate capacities to understand the feasibility of the numerical modeling approach for remaining strength estimation of corroded steel plates with different corrosion conditions.

#### 4.3 Analytical Results and Discussion

The yield and ultimate strengths in analytical prediction were estimated and compared with that of the experimentally obtained values to evaluate the accuracy of the used analytical model. The percentage error in yield and tensile strength in analytical predictions are calculated as:

$$\% \text{ Error in } P_y = \left| \frac{P_{y[\text{Analytic al}]} - P_{y[\text{Experime ntal}]}}{P_{y[\text{Experime ntal}]}} \right| \cdot 100 \quad (3)$$

$$\% \text{ Error in } P_b = \left| \frac{P_{b[\text{Analytic al}]} - P_{b[\text{Experime ntal}]}}{P_{b[\text{Experime ntal}]}} \right| \cdot 100 \quad (4)$$

First, analytical modeling of the non-corroded specimen was done with above described modeling and analytical features to understand the accuracy of the adopted procedure. It was found that the analytical model results were almost same as the experimental results with having a negligible percentage error of 0.03% and 0.02% in yield and tensile strengths respectively. Then, all other experimentally successful specimens were modeled accordingly and their yield and ultimate strengths were compared with the experimentally obtained values.

##### (a) Minor Corrosion Members

The above described analytical procedure was used to model the members with minor corrosion to understand their yield and ultimate behaviors and to obtain their failure surfaces. Comparison of experimental and analytical load-displacement curves of specimen F-14 is shown in Figure 6. Here, the percentage errors in yield and tensile strength predictions of member F-14 are 0.53%

and 0.03% respectively. So, it is revealed that this numerical modeling technique can be used to predict the remaining strength capacities of minor corroded members accurately.

The failure surface was obtained from the most narrowed location of the deformed shape of the analytical model. Figure 7 shows that both experimental and analytical failure surfaces of the specimen F-14 are in good agreement.

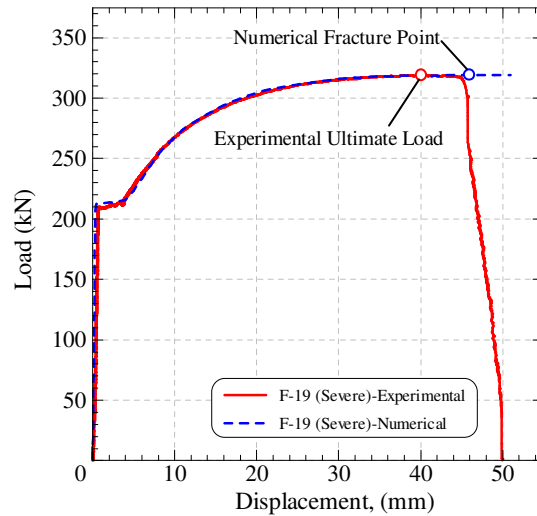


**FIGURE 6:** Comparison of load-displacement curves of minor corrosion member [F-14].

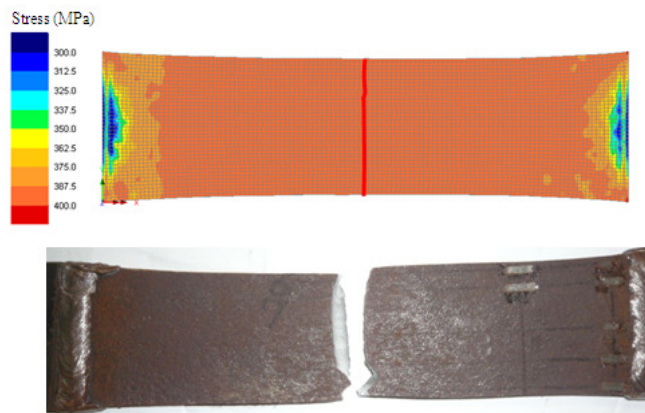


**FIGURE 7:** Stress distribution at ultimate load of minor corrosion member [F-14].

**(b) Moderate Corrosion Members**

Then, the members with moderate corrosion were also analyzed and compared with their respective experimental results. The Figure 8 shows the comparison of load-displacement behavior of moderately corroded member, F-13. It shows a very good comparison of experimental and analytical load-displacement behaviors in members with moderate corrosion as well and the percentage errors in yield and tensile strength predictions of member F-13 are 2.96% and 0.70% respectively.

Further, the Figure 9 shows that a similar failure surface could be obtained as in experimental analysis and this indicate the adaptability of this analytical modeling method and SMCS fracture criterion for moderately corroded members too, in order to predict their remaining strength capacities.

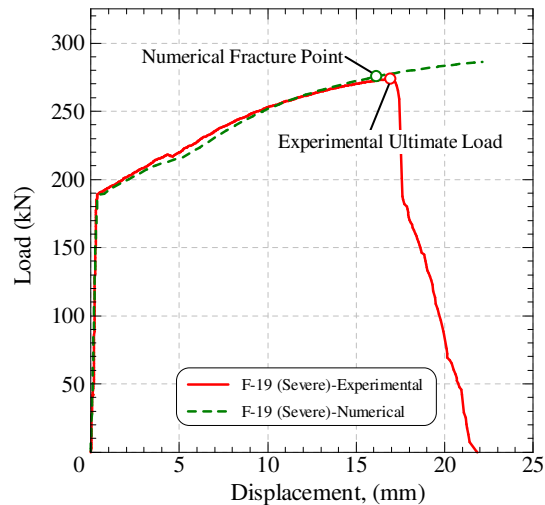


**FIGURE 8:** Comparison of load-displacement curves of moderate corrosion member [F-13].

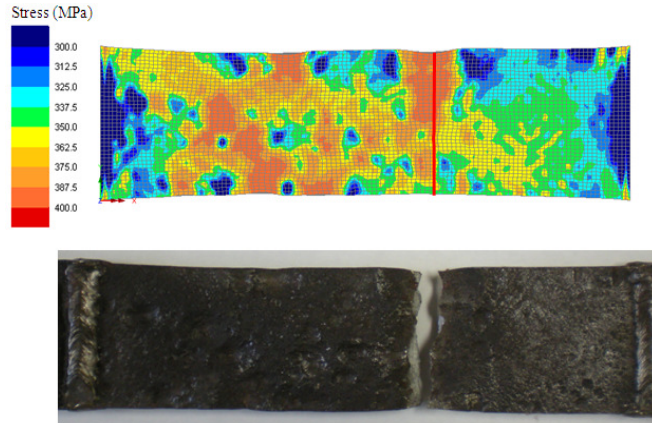


**FIGURE 9:** Stress distribution at ultimate load of moderate corrosion member [F-13].

### (c) Severe Corrosion Members

Finally, the severely corroded members too analyzed and observed their yield and ultimate behaviors and their failure surfaces. The Figure 10 shows the comparison of load-displacement behavior of severely corroded specimen F-19. It shows that an adequate comparison of experimental and analytical load-displacement behaviors can be obtained in members with severe corrosion as well.

The percentage errors in yield and tensile strength predictions of member F-19 shown in Figure 10 are 3.20% and 5.53% respectively. Though the ultimate behavior shows a slight difference, the failure surface shown in Figure 11 is almost same as in the experimental analysis.

Although the results of numerical predictions for yield and ultimate strengths of minor and moderate corroded members show a very good comparison with the experimental results, severe corrosion members show a little bit deviation in their ultimate strength predictions. The reason could be that, some microscopic cracks could also build-up with the development of corrosion which they could eventually results a loss of strength. Hence, there we can see a loss of tensile strength in experimental analyses than expected or predicted by analytical models in severely corroded specimens. So, careful microscopic observations for severe corroded surfaces and smoothing them neatly could reduce such errors with analytical prediction.

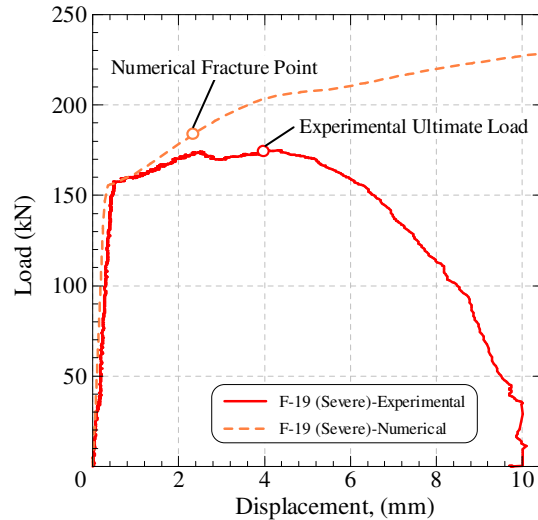


**FIGURE 10:** Comparison of load-displacement curves of severe corrosion member [F-19].

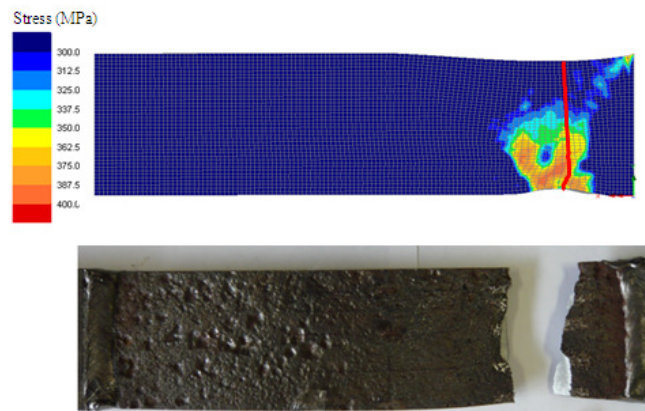


**FIGURE 11:** Stress distribution at ultimate load of severe corrosion member [F-19].

(d) Discussion

All experimentally successful flange and web specimens were modeled accordingly and their yield and ultimate strengths and failure surfaces were compared with the experimental behaviors. A good comparison of the experimental and analytical load-elongation behaviors for all three classified corrosion types was obtained. Figure 12 shows the comparison of ultimate load capacities of experimental and numerical analyses with 2mm models. Having a coefficient of correlation of  $R^2 = 0.994$  indicates the accuracy and the possibility of numerical investigation method to predict the tensile strength of actual corroded specimens.

Failure surfaces obtained from the analytical method and the experimental analysis indicated a very good comparison for all three corrosion categories and hence this fact too signifies the accuracy of the adopted numerical modeling method. Further, it can be seen that the elongation of members with minor corrosion have comparatively same elongation as corrosion free members, where as the moderately corroded members show lesser elongation than the minor corrosion members. Also the members with severe corrosion show significant reduction in elongation as well. The reason for this could be the local section with a small cross-sectional area yields at an early load stage because of the stress concentration due to irregularity of corroded steel plate which elongates locally and reach to the breaking point.

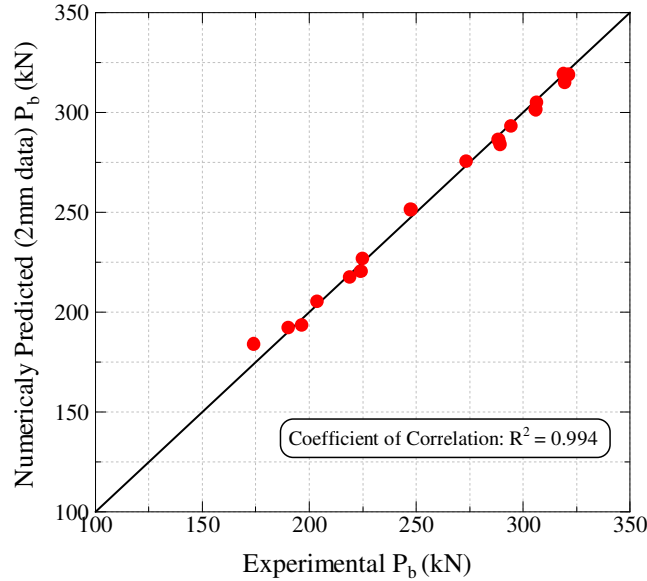


FIGURE 12: Comparison of experimental and analytical ultimate load capacities.

## 5. DEVELOPMENT OF BRISK ANALYTICAL METHOD

### 5.1 Corrosion Condition Modeling (CCM) Parameters

Since it is an exigent task to conduct detail corroded surface measurements for all aged steel infrastructures as the number of steel structures are steadily increasing in the world, a simple, accurate and brisk method is deemed necessary to model different corroded surfaces numerically and predict their yield and ultimate behaviors. Therefore two parameters were defined to model the corroded surface considering the stress concentration effect and to obtain the yield and ultimate behaviors more accurately. The following Figure 13(a) shows the variation of diameter of the maximum corroded pit vs. maximum corroded depth ( $t_{c,max}$ ) and Figure 13(b) shows the normalized average thickness ( $t_{avg}/t_0$ ) vs. normalized maximum corroded depth ( $t_{c,max}/t_0$ ). Both Figures show a very good linear relationship and hence these parameters were used to develop an analytical model which can be used to predict the yield and ultimate behaviors of corroded steel plates with different corrosion conditions.

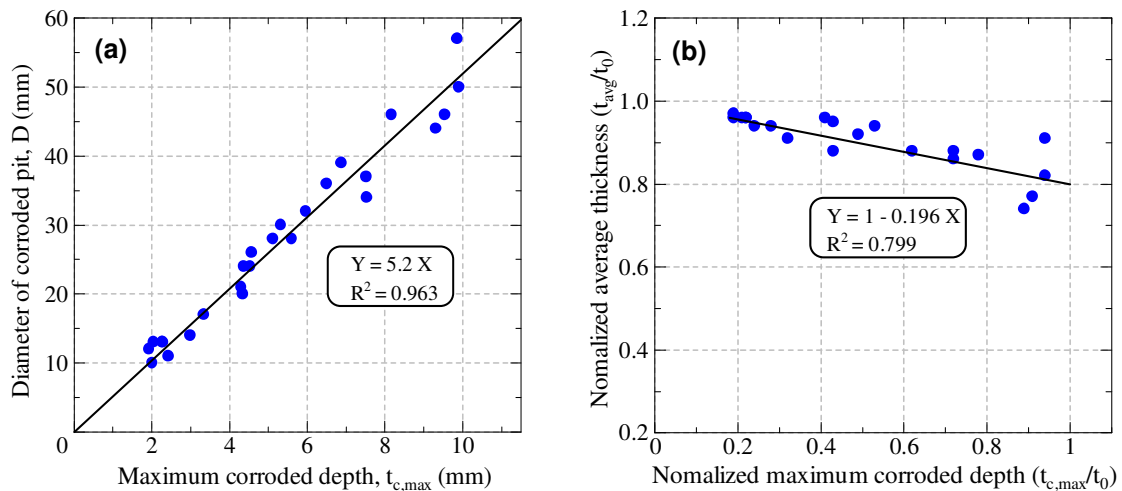


FIGURE 13: Relationship of (a) D vs.  $t_{c,max}$  and (b) normalized  $t_{avg}$  vs.  $t_{c,max}$ .

Therefore, by considering the Figures 13(a) and (b), the two equations for the corrosion condition modeling (CCM) parameters can be defined as:

$$D^* = 5.2 t_{c,max} \quad (5)$$

$$t^*_{avg} = t_0 - 0.2 t_{c,max} \quad (6)$$

where  $D^*$  and  $t^*_{avg}$  are the representative diameter of maximum corroded pit and representative average thickness respectively.

## 5.2 Analytical Model

An analytical model is developed with the above CCM parameters for each corroded specimen with different corrosion conditions as shown in Figure 14. Here, the maximum corroded pit was modeled by using the representative diameter ( $D^*$ ) which could account the stress concentration effect and the material loss due to corrosion was considered by using the representative average thickness parameter ( $t^*_{avg}$ ). The same modeling features and analytical procedure as described in section 4 were adopted for the analyses. Then the results of this model were compared with the experimental results to understand the effectiveness of the proposed model.

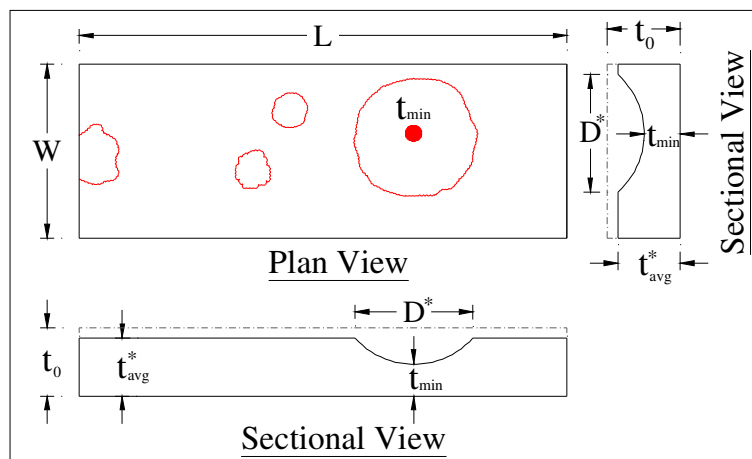
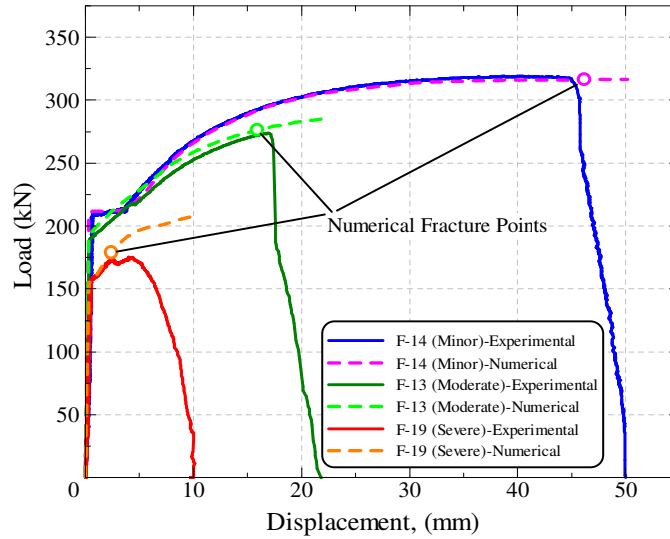


FIGURE 14: Analytical model with CCM parameters.

## 5.3 Analytical Results and Discussion

The load-elongation behavior of 3 members F-14, F-13 and F-19 with minor, moderate and severe corrosion conditions respectively are shown in Figure 15 below. It was revealed that a very good comparison of the load-elongation behavior can be seen for the all three classified corrosion types. Here, the percentage errors in yield and tensile strength predictions of the proposed analytical model for the three corrosion types are 0.13% and 0.83% in F-14, 0.38% and 1.01% in F-13 and 3.51% and 2.69% in F-19 respectively. Further it was noted that there is no significance in % errors even though they tend to increase with the severity of corrosion.

Then, all experimentally successful specimens were modeled accordingly with the proposed analytical model and their yield and ultimate strengths and failure surfaces were compared with the experimental results. The Figure 16 shows the comparison of ultimate load capacities of proposed model and experimental results. A very good comparison with a coefficient of correlation of  $R^2 = 0.992$  was attained. This fact divulges the accuracy of the proposed model and the possibility of the use of proposed analytical model instead of the model with detailed corroded surface measurements. Therefore it can be comprehended that the adopted method and the proposed analytical model can be used to predict the yield and ultimate behaviors precisely. Further it was noticed that a good agreement of the failure surfaces of experimental and proposed model can be obtained too.



**FIGURE 15:** Comparison of load-elongation curves of proposed analytical model.

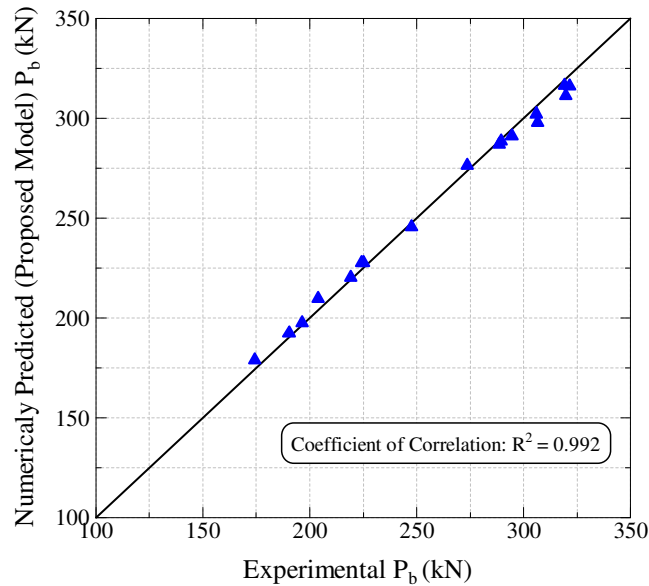


**FIGURE 16:** Comparison of experimental and proposed model's ultimate load capacities.

Further, it was noted that the available numerical methods and empirical equations developed by various authors require conducting detail corroded surface measurements and the measurement of average thickness and/or the minimum average thickness, in order to develop the analytical model and predict the yield and ultimate behaviors of that corroded members. But, the proposed model require only the measurement of maximum corroded depth ( $t_{c,max}$ ), which can be easily identified through a careful visual inspection of the corroded surface, in order to develop the analytical model considering the stress concentration effect and the material loss due to corrosion. Therefore, this method can be used as a simple, reliable and brisk analytical method for the maintenance management of steel infrastructures.

A further detailed study comprises with experimental and numerical analysis of more specimens with different corrosion conditions is deemed necessary to understand the significance of the proposed method and verify this for different corroded levels and environmental conditions.

## 6. CONCLUSIONS

The 26 specimens taken out of the scrapped plate girder which had been used for about 100 years with severe corrosion, was used to perform the tensile tests to estimate the mechanical properties of corroded plates and understand the relationship of strength reduction and their level of corrosion. A non-linear FEM analysis was carried out to understand the mechanical behavior, stress distribution, ultimate behavior etc. for members with different corroded conditions. The main conclusions are as follows:

1. The corrosion causes strength reduction of steel plates and minimum thickness ratio ( $\mu$ ) can be used as a measure of the level of corrosion and their strength degradation.
2. A very good agreement between the experimental and non linear FEM results can be seen for all three classified corrosion types. Further, failure surfaces of those specimens too showed a very good comparison with the experimental results. So, the adopted numerical modeling technique can be used to predict the remaining strength capacities of actual corroded members accurately.
3. Proposed analytical model with CCM parameters showed a very good agreement with the experimental results for all three classified corrosion types. Further, the proposed method is simple and gives more accurate remaining strength estimation of corroded steel plates. Therefore this analytical model, developed by the measurement of maximum corroded depth only, can be used as a reliable and brisk method for the maintenance management of corroded steel infrastructures.

## 7. ACKNOWLEDGEMENTS

The authors would like to thank the technical staffs of Mitutoyo Corporation (Japan) for their assistance in surface measurement of corroded specimens and Mr. Y. Tanabe, Mr. H. Ikeda and Mr. K. Itogawa for their support extended during the experimental work.

## 8. REFERENCES

- [1] NSBA. "Corrosion protection of steel bridges". Steel Bridge Design Handbook, Chapter 23, National Steel Bridge Alliance, 2006.
- [2] T. Natori, K. Nishikawa, J. Murakoshi and T. Ohno. "Study on Characteristics of Corrosion Damages in Steel Bridge Members". Journal of Structural Mechanics and Earthquake Engineering, Vol.668, No.54, pp. 299-311, 2001.
- [3] T. Kitada. "Considerations on recent trends in, and future prospects of, steel bridge construction in Japan". Journal of Constructional Steel Research, Vol.62, pp. 1192-1198, 2006.
- [4] M. Matsumoto, Y. Shirai, I. Nakamura and N. Shiraishi. "A Proposal of effective Thickness Estimation Method of Corroded Steel Member". Bridge Foundation Engineering, Vol. 23, No.12, pp. 19-25, 1989. (in Japanese)
- [5] A. Muranaka, O. Minata and K. Fujii. "Estimation of residual strength and surface irregularity of the corroded steel plates". Journal of Structural Engineering, Vol. 44A, pp. 1063-1071, 1998. (in Japanese)
- [6] A. Kariya, K. Tagaya, T. Kaita and K. Fujii. "Basic study on effective thickness of corroded steel plate and material property". Annual conference of JSCE, 2003, pp. 967-968. (in Japanese)
- [7] J.M.R.S. Appuhamy, M. Ohga, T. Kaita and K. Fujii. "Effect of Measuring Points on Remaining Strength Estimation of Corroded Steel Plates". Proc. of PSSC2010, China, 2010, pp. 1504-1516.

- [8] T. Kaita, Y. Kawasaki, H. Isami, M. Ohga and K. Fujii. "Analytical Study on Remaining Compressive Strength and Ultimate Behaviors for Locally-corroded Flanges". Proc. of EASEC-11, Taiwan, 2008.
- [9] A.A.P. Sidharth. "Effect of pitting corrosion on ultimate strength and buckling strength of plate- a review". Digest Journal of Nanomaterials and Biostructures, Vol.4, No.4, pp. 783-788, 2009.
- [10] M.M. Ahmmad and Y. Sumi. "Strength and deformability of corroded steel plates under quasi-static tensile load". Journal of Marine Science and Technology, Vol.15, pp. 1-15, 2010.
- [11] T. Kaita, K. Fuji, M. Miyashita, M. Uenoya, M. Okumura and H. Nakamura. "A simple estimation method of bending strength for corroded plate girder", Collaboration and Harmonization in Creative Systems, Vol. 1, pp. 89-97, 2005.
- [12] A.M. Kavinde and G.G. Deierlein. "Void Growth Model and Stress Modified Critical Strain Model to Predict Ductile Fracture in Structural Steels". Journal of Structural Engineering, Vol.132, No.12, pp. 1907-1918, 2006.

## Performance Evaluation of Adaptive Filters Structures for Acoustic Echo Cancellation

### Sanjeev Dhull

Asst.Professor/ECE G.J.U.S&T,Hisar  
Hisar, 125001 , India

*sanjeev\_dhull\_ap@yahoo.co.in*

### Dr.Sandeep Arya

Associate Professor/ECE G.J.U.S&T,Hisar  
Hisar,125001 , India

*arya1sandeep@rediffmail.com*

### Dr.O.P Sahu

Associate Professor/ECE N.I.T Kurukshetra  
Kurukshetra, 136118, India

*ops\_nitk@yahoo.co.in*

---

### Abstract

We have designed and simulated an acoustic echo cancellation system for conferencing. This system is based upon a least-mean-square (LMS) adaptive algorithm and uses multi filter technique. A comparative study of both structure has been carried out and it is found that this new multi-filter converge faster than similar single long adaptive filter.

**Keywords:** LMS,Multiple Sub Filter ,Echo Cancellation

---

## 1. INTRODUCTION

Acoustic echo cancellation (AEC) [1] is used in teleconferencing and its purpose is to provide high quality full-duplex communication. The main part of an AEC is an adaptive filter which estimates the impulse response of the loudspeaker-enclosure-microphone (LEM)[2] system. There are various adaptive algorithms for the AEC filter update, these are the least mean square, normalized least mean square (LMS, NLMS), affine projection (AP) and recursive least squares (RLS) algorithms. As the echo cancellation environment is not stationary therefore echo reduction in rooms with long reverberation time is necessary. Hence, the signal processing methods are in demand in industry. Several partial update methods for computational complexity reduction of various adaptive filtering algorithms have been proposed and analyzed, e.g. [25]-[31] for the LMS/NLMS/AP .The technique used in earlier stages was echo suppression [23][24].Due to some disadvantages of echo suppression echo cancellation came into picture and the process of Acoustic echo cancellation [24][27], [29] is achieved with the help of adaptive filter which models the LEM system. The purpose of an acoustic echo-canceller is to reduce the amount of sound which a far-end teleconference transmits from returning to them. Traditional approaches to acoustic echo cancellation have used filtering algorithms which try to estimate the impulse response of the acoustic path and filter the incoming signal from the far-end [23],[24]. In this paper, we are proposing a multi sub filter approach for echo reduction and comparing their results. This paper is organized in four sections. Section two describes the simulation model of AEC in mat lab using multifactor approach. Further, section three discusses the results. In the end section four concludes the paper.

## 2. MULTIFILTER APPROACH FOR AEC

First of all before considering the other issues of this multiple sub filter approach the first most desired thing is the modeling of acoustic path through which communication takes place. As shown in figure1 when signal travel it experience the echo's of the signal and some noise also

added in the signal. The multiple sub filters (MSF) structure is constituted by using the time delays and filter orders estimated as shown in fig.2.

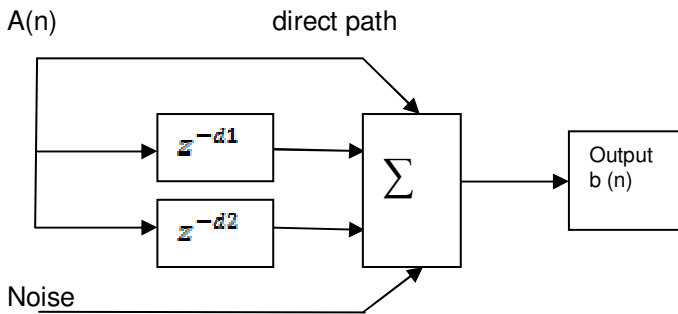


FIGURE 1: Modeling of Acoustic Path

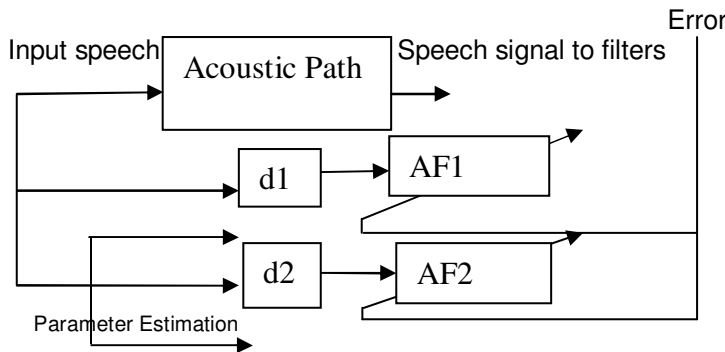


FIGURE 2: Model of Multiple Subfilter

Following equations described the behavior of multiple sub filter model used.  $e(n) = b(n) - \sum_{k=0}^M W_k^T(n) \hat{X}_k(n)$ ; Adaptation of each sub filter is given as

$W_k(n+1) = W_k(n) + \mu_k \hat{X}_k(n)e(n)$ ;  $k = 0,1,2,\dots, M$  The output of the multiple sub filter is given by  $b(n) = \sum_{k=0}^M W_k^T(n) \hat{X}_k(n)$ ;  $n = 0,1,2,\dots, N - 1$  Each individual filter is updated with the help

of a adaptive algorithm as shown in fig.2 and adaptation step size is separately chosen for each sub filter. the step size of the multiple sub filter structure[33][34] is same as for single long adaptive filter .Let us define the weight error vector  $V_j(n)=W_j(n)-H_j$ .The MSE is  $\zeta(n)=E(e^2(n))$ ,

$$\zeta(n) = \sigma_\eta^2 + \sum_{j=0}^M \sum_{k=0}^M E[V_j(n)]G_{kj}E[V_k(n)] + \sum_{j=0}^M \tau \{G_{j,j}E[V_j(n)V_j^T(n)]\} \quad \text{here } G_{j,j} = E[X_j(n)X_j^T(n)].$$

For the MSE to

converge, it is necessary that  $E[V_j(n)]$  and  $\tau \{G_{j,j}E[V_j(n)V_j^T(n)]\}$  coverage  $\forall j = 0,1,2,\dots, M$ .

Taking expectation both sides we have  $E(V_j(n+1)) = (I - \mu_j G_{j,j})E[V_j(n)] - \mu_j \sum_{\substack{k=0 \\ k \neq j}}^M G_{jk} E(V_k(n))$  The

mean of the  $j^{\text{th}}$  sub filter weight error vector converge, i.e.  $E(V_j(\infty))=0$  If  $0 < \mu_j \leq \frac{2}{(\lambda_{\max})_j} \forall j = 0,1,2,\dots, M$  this is adaptation step size expression[33][34]. Stability is improved if

the step size is chosen such that

$$0 < \mu_j \leq \frac{2}{3\tau(G_{j,j})} \quad \forall j = 0, 1, 2, \dots, M$$

The next work is to do simulations of conventional approach and multiple filter approach. For simulations comparisons we are taking far end and near end speech signals. Two basic performance criteria mean square error (MSE) and ERLE are the main comparison parameters for these approaches. The comparison results will show the path that which approach is better for AEC. Simulations is carried taking into account the time delay ,gain and stepsize.we are using step size 0.5,delay 351 and 254,gain .85 and .9.The order of low pass filter is 10.Length of adaptive filter chosen is 194 and leakage factor is 1.

### 3.SIMULATION RESULTS OF MULTIPLE SUB FILTER APPROACH AND SINGLE FILTER

Following are the results of two approaches compared. We are using lms and its different variants for updating the filter coefficients.Fig.3is representing the far end & near end speech signals, fig. 4& 5 are MSE results of multiple sub filter's and conventional approach. Fig. 6, 7,8are results of conventional approach of single long adaptive filter method for acoustic echo cancellation.fig.9, 10,11are ERLE graphs of MSF for LMS and NLMS.

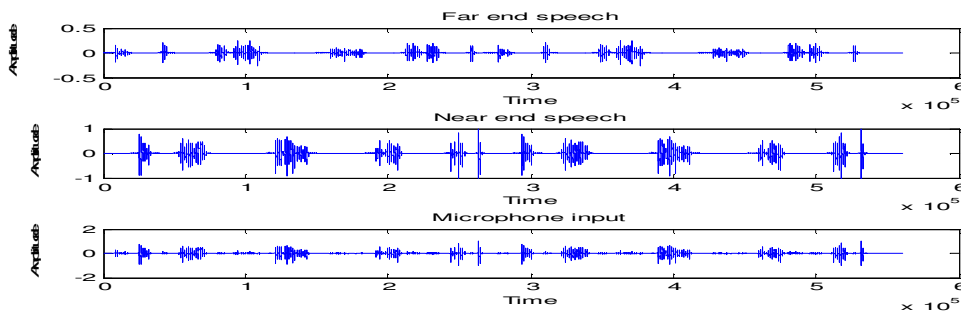


FIGURE 3: Far end and Near end speech signal

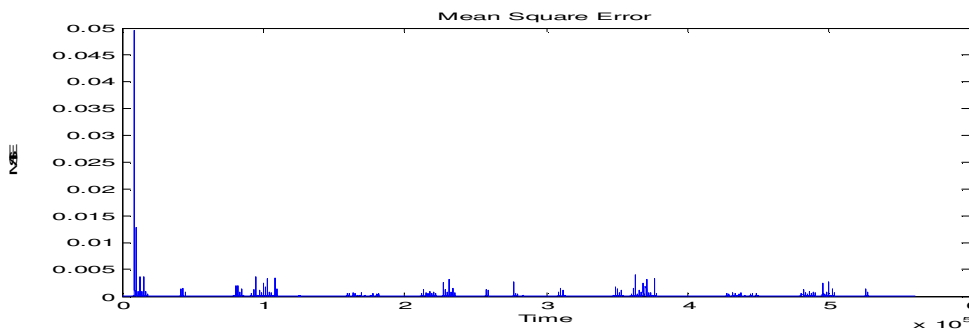
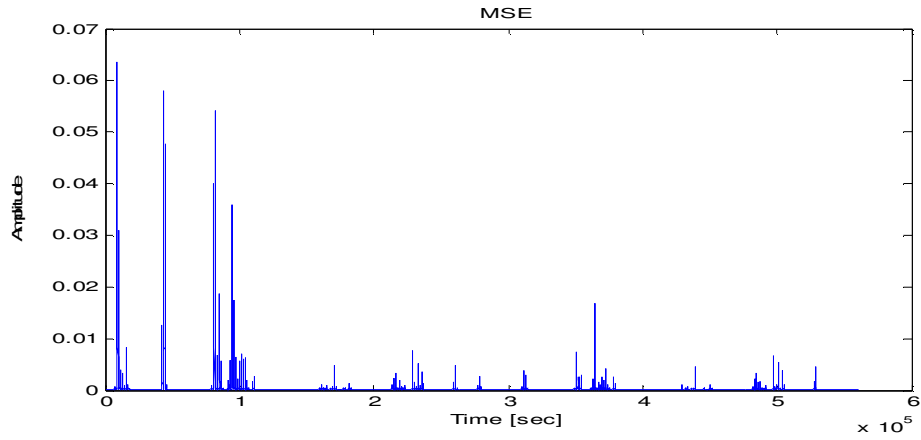
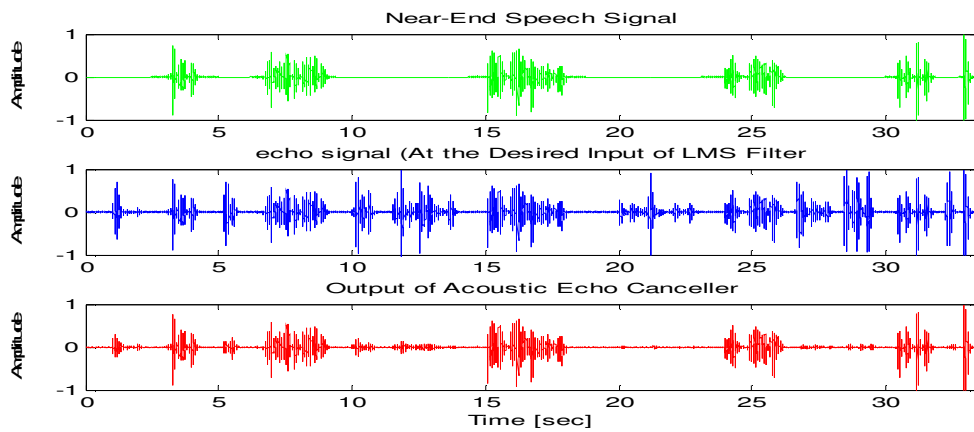


FIGURE 4: MSE of multiple filter approach (LMS)



**FIGURE 5:** MSE of single filter approach(LMS)



**FIGURE 6:** Single Adaptive Filter approach output

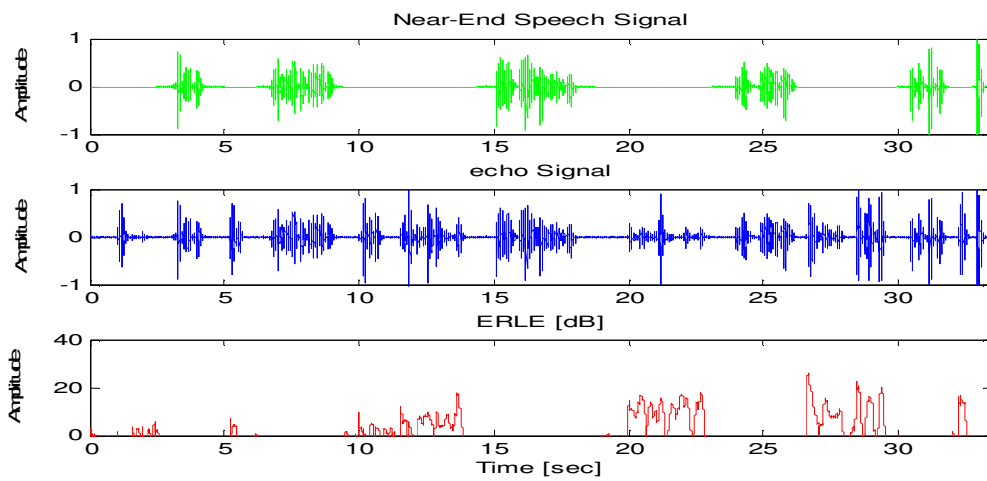


**FIGURE 7:** ERLE of Single long Adaptive Filter

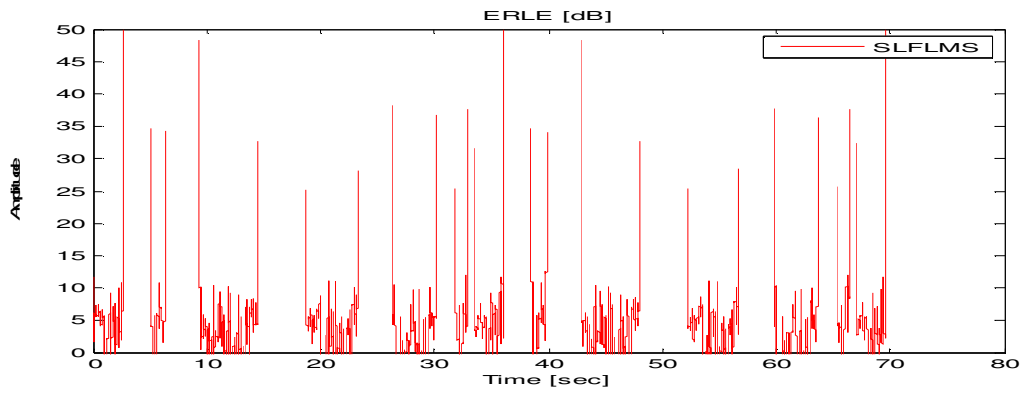


FIGURE 8: ERLE of single long Adaptive Filter(LMS)

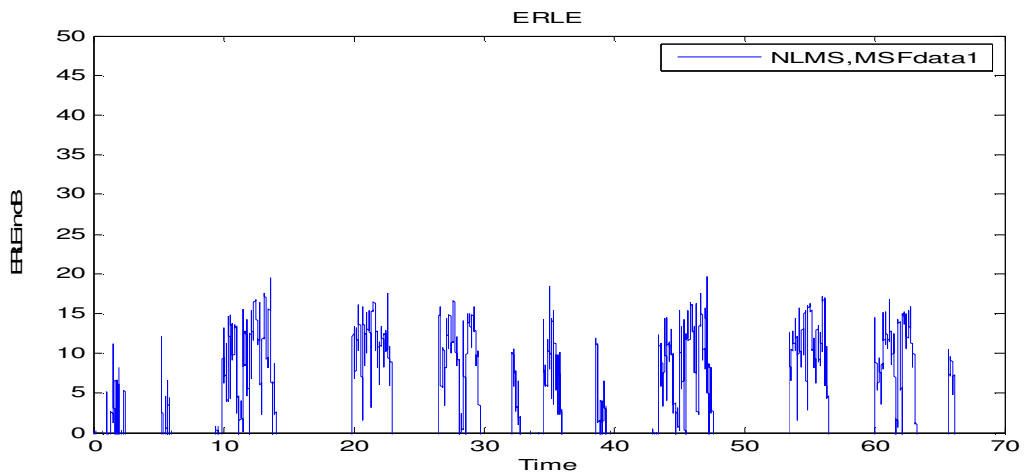


FIGURE 9: ERLE for MSF using NLMS

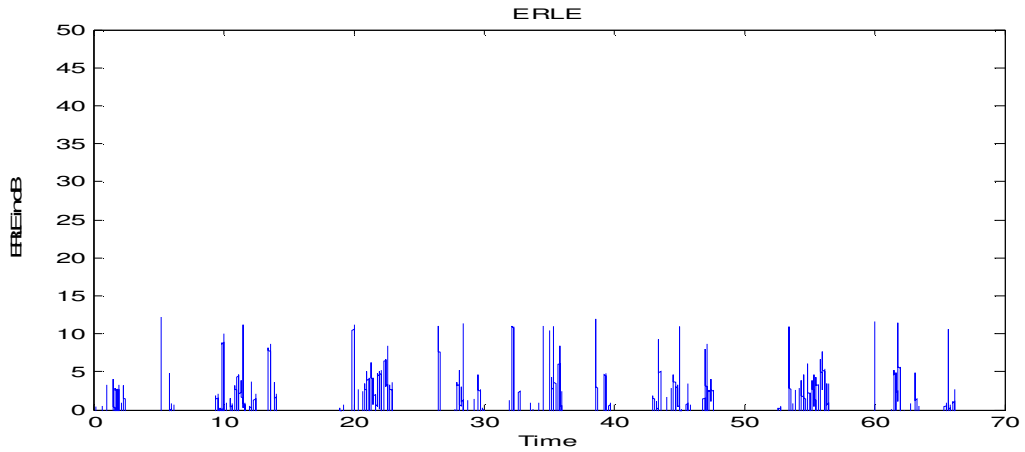


FIGURE 10: ERLE for MSF using SELMS

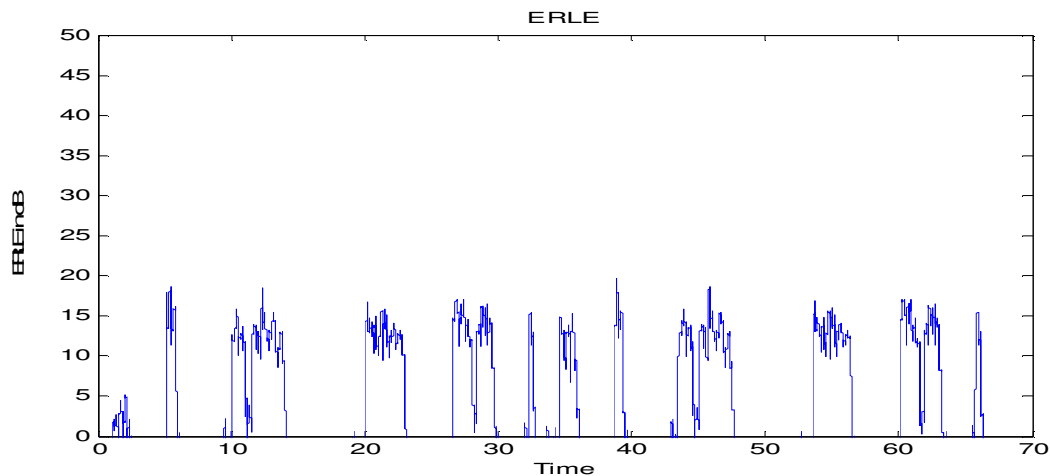


FIGURE 11: ERLE for MSF using LMS

#### 4.CONCLUSION

As seen from different figures we are comparing the performance behaviour of long and multiple sub filters. Fig.3 indicating the Far end , Near end speech signal and input to microphone signals in the case of multiple filter and conventional approach. Fig.4 and 5 representing the MSE of two different approaches ,MSE in case of multi subfilter approach is less as compared to conventional approach. ERLE (Fig.7,8) in case of conventional approach is more than 40 db where as in case of multiple sub filter (Fig.9,10,11) it is near to 15-20 db. Thus MSE results shows that single long adaptive filter shows poor performance as compared to multiple subfilter structure. Thus our results achieved confirms the idea of using multiple adaptive filters.

#### 5.REFERENCES

- [1]. Widrow, B., Stearns, S.D., "Adaptive Signal Processing," Englewood Cliffs, NJ: Prentice. Englewood Cliffs, NJ: Prentice. Hall, 2001
- [2]. Brennan, R., Schneider. , "A flexible filter bank Structure for extensive signal manipulation in digital Hearing aids," Proc. IEEE Int. Symp. Circuits and Systems, pp. 569-572, 1998
- [3]. Mounir Ghogho, Mohamed Ibnkahla, and Neil J. Bershad, "Analytic Behavior of the LMS adaptive Line Enhancer for Sinusoids Corrupted by Multiplicative and Additive Noise," IEEE transactions on signal processing, vol.46, no.9, sept.
- [4]. Jafar Ramadhan Mohammed, "A New Simple Adaptive Noise Cancellation Scheme Based On ALE and NLMS Filter," Fifth Annual Conference on Communication Networks and Services Research (CNSR'07) IEEE-2007.
- [5]. Naoto Sasaoka, Yoshio Itoh, Keiichi Wakizaka and Kensaku Fujii, " A study on less computational load of noise reduction method based on noise reduction method based on ALE and noise estimation filter," Proceedings of 2005 International Symposium on Intelligent Signal Processing and Communication Systems, December 13-16, 2005.
- [6]. Farhang-Boroujeny, B. 1999, Adaptive Filters, Theory and Applications. John Wiley and Sons, New York

- [7]. GUO Yemi and ZHAO Junwei, "Combined Kurtosis Driven Variable Step Size Adaptive Line Enhancer," 2004 8th International Conference on Control, Automation, Robotics and Vision Kunming. China, 6-9th December 2004.
- [8]. Toshihiro Miyawaki, Naoto Sasaoka, Yoshio Itoh, Kensaku Fujit and Sumio Tsuiki , "A Study on Pitch Detection of Sinusoidal Noise for Noise Reduction System," 2006 international Symposium on Intelligent Signal Processing and Communication Systems (ISPACS2006).
- [9]. Isao Nakanishi and Yuudai Nagata, Yoshio Itoh, Yutaka Fukui, "Single-Channel Speech Enhancement Based on Frequency Domain ALE" ISCAS 2006
- [10]. Michael Hutson, "Acoustic echo cancellation using DSP"Nov.2003
- [11]. P. M.Clarkson, Adaptive and optimal signal processing, CRC,1993
- [12]. Sophocles J. Orfanidis,Optimum Signal Processing ,Second Edition,2001
- [13]. Naoto Sasaoka, Koji Shimada, Shota Sonobe, Yoshio Itoh and Kensaku Fujii , "Speech enhancement based on adaptive filter with variable step size for wideband and periodic noise" 2009 ieee
- [14]. V.Umapathi Reddy,Bo Egardt, Thomas Kailath, "Optimized lattice-form Adaptive Line Enhance for a sinusoidal signal in Broad band noise"1981,iee
- [15]. F T.Aboulnasr, K. Mayyas, "A Robust Variable Step-size LMS Type Algorithm: Analysis and Simulations," IEEE Trans. on signal processing,vol.45, No.3, pp. 631-639, March 1997
- [16]. D. W. Tufts, L. J. Griffiths, B. Widrow, J. Glover, J. McCool, and J.Treichler , "Adaptive Line Enhancement and Spectrum Analysis," Proceedings of the IEEE, Letter, pp. 169, January 1977.
- [17]. J. Treichler, "Transient and convergent behavior of the adaptive line enhancer," ieee Trans. Acoust., Speech, Signal Processing, Vol. ASSP-27, No. 1, pp. 53-63, February 1979.
- [18]. Rickard and J. R. Zeidler, "Second-order output statistics of the adaptive line enhancer," IEEE Trans. Acoust., Speech, Signal Processing, Vol. ASSP-27, no. 1, pp. 31-39, February 1979.
- [19]. N. J. Bershad and O. Macchi, "Adaptive recovery of a chirped sinusoid in noise Performance of the LMS algorithm," IEEE Trans. Signal Processing, vol. 39, pp. 595-602, Mar. 1991.
- [20]. J. R. Treichler , "Transient and convergent behavior of the ALE," IEEE Trans. Acoust., Speech, Signal Processing, vol. ASSP-27, pp. 53-63, Feb. 1979.
- [21]. Zeidler., "Adaptive enhancement of multiple sinusoids in uncorrelated noise," IEEE Trans. Acoust., Speech, Signal Processing, vol. ASSP-26, pp. 240-254, June 1978.
- [22]. G. R. Elliott and S. D. Stearns, "The Adaptive Line Enhancer applied to chirp detection," IEEE International Symposium on Circuits and Systems, vol. 2, pp. 1319-1322, 1990.
- [23]. Haykin, S., Adaptive Filter Theory, Englewood Cliffs, N.J., Prentice-Hall, 1991.
- [24]. Sondhi, M. M., Berkley, D.A. "Silencing Echoes on the Telephone Network," Proc. IEEE, Vol. 68, NO. 8, August 1980, pp. 948-963.

- [25]. Sondhi, M. M., Mitra, D. ,“New Results on the Performance of a Well-Known Class of Adaptive filter”, IEEE, 1976, Vol. 64, No. 11, pp. 1583-1597
- [26]. Brehm, H., Stammer, W. “Description and generation of spherically invariant speech-model signals”, *Signal Processing* vol. 12, no. 2, pp. 119–141, March 1987.
- [27]. Moon, T. K., Stirling, W. C. ,*Mathematical Methods and Algorithms for Signal Processing*, New Jersey, Prentice Hall, 2000.
- [28]. Farhang-Boronjeny, B. ,*Adaptive Filters Theory and Application*, New York, Wiley, 2000.
- [29]. Mukund Padmanabhan, “ A Hyper-stable Adaptive Line Enhancer for Fast Tracking of Sinusoidal Inputs,” *ieee transactions on circuits and systems of analog and digital signal processing*, vol44-april 1996
- [30]. Mader.A. Puder, H., Schmidt, G.U, “Step-size control For acoustic cancellation filters”, *Signal Process.* vol. 80, pp. 1697–1719, 2000.
- [31]. Ben Jebara, S., Besbes, H. ,“A variable step size filtered sign algorithm for acoustic echo cancellation,” *IEEE*vol. 39, no. 12, pp. 936-938, June 2003.
- [32]. Douglas, S. “A family of normalized LMS algorithms”, *IEEE signals processing letters*, vol. 1, no. 3, pp. 49-51, March1994.
- [33]. R.N.Sharma, A.K.Chaturvedi and G.Sharma, “AEC using multiple subfilter,”*Tencon* 2003.
- [34]. A.M.Ali, “Multiple subfilter approach for AEC,” *Radio Science Conference* 2008, Tanta.

Author(s) Name

# A Distributed Optimized Approach based on the Multi Agent Concept for the Implementation of a Real Time Carpooling Service with an Optimization Aspect on Siblings

**Manel Sghaier**

LAGIS, EC-Lille  
Ecole Centrale de Lille, BP 48 - Cité Scientifique  
Villeneuve d'Ascq, 59650, France

*manel.sghaier@ec-lille.fr*

**Hayfa Zgaya**

ILIS  
42, Rue Ambroise Paré  
59120 - LOOS, France

*hayfa.zgaya@univ-lille2.fr*

**Slim Hammadi**

LAGIS, EC-Lille  
Ecole Centrale de Lille, BP 48 - Cité Scientifique  
Villeneuve d'Ascq, 59650, France

*slim.hammadi@ec-lille.fr*

**Christian Tahon**

UVHC - LAMIH CNRS  
Université de Valenciennes et du Hainaut-Cambrésis  
Valenciennes Cedex, France

*tahon@univ-valenciennes.fr*

---

## Abstract

Thanks to the important and increasing growth of the carpooling phenomenon throughout the world, many researchers have particularly focused their efforts on this concept. Most of the existent systems present multiple drawbacks regarding automation, functionalities, accessibility, etc. Besides, only few researchers focused on real time carpooling concept without producing promising results. To address these gaps, we introduce a novel approach called DOMARTiC: a Distributed Optimized approach based on the Multi-Agent concept for the implementation of a Real Time Carpooling service. We particularly focus on the distributed and dynamic aspect not only within the geographical network's representation but also regarding the used automatic tools and the implementing algorithms. Adequate modeling on the base of which a distributed architecture is set up has been adopted helping to perform decentralized parallel process. This helped to take into consideration different aspects we should be involved in, especially the optimization issue as users' requests must be performed in a reasonable runtime. Responses provided to users should also be efficient with regards to the fixed optimization criteria.

**Keywords:** Real Time Carpooling, Optimization, Network's Decomposition, Distributed Dynamic Graph Modeling, Multi-Agent System, Distributed Algorithm.

---

## 1. INTRODUCTION

With the emergence of organisms and events focusing on the emergency of addressing current environmental problems, researches have been developed to provide better conditions for survival. In particular, financial problems in addition to environmental ones caused by transport means evolution, made researchers consider this issue more in depth.

According to a study achieved in year 2000 [1], the total number of cars exceeded 740 million in the world. This car's invasion came to extend individual and collective problems (i.e. financial limitations, CO2 emission ...) [2] importantly influencing people behavior [3]. Although public transport means remedied to almost all of these problems, they unfortunately could not afford as

much moving liberty, flexibility and comfort. Thus, tackling those problems has become increasingly urgent. Efforts developed in this context to reach a compromise, led to innovative transport services. Among them, carpooling is a concept that brought a great interest since more than a couple of decades. Indeed, several researchers dealt with carpool problem and many systems are already operational in Europe and throughout the world [2]. Technologies used in such systems and results carried out up to now are rather promising and very rewarding [4]. The fact remains that existing works show some limits. This made us consider this issue and propose a novel approach called DOMARTiC with an optimization dilemma dealing with real time users' requests and trying to perform optimized responses. Thus, in this paper, we focus on the carpooling concept, basically, with an innovative view that tackles the problem of handling instantaneously received users' requests. Our first target is then to improve the quality of service so that subscribers could obtain real time generated responses, efficiently and promptly. For this purpose, we consider a new network's representation, a conceptual modeling and the automatic tools needed to implement necessary algorithms to generate optimized carpooling service. We mainly focus on the multi-agent concept since it provides, in combination with high technologies, the efficiency required to deal with real time users' queries.

The rest of this paper is then organized as follows: in section 2, a general background provides a non-exhaustive list of the existent carpooling systems. Section 3 describes the proposed approach DOMARTiC with a focus on the multi-agent concept and the distributed assignment algorithm performed to generate optimized matching. Details are also given about the formal specifications of our problem, the optimization aspect within it and the network's decomposing process is briefly described. Section 4 comes to sum up our work and present future prospects.

## 2. SCRUTINY OF THE RELATED WORKS

Also known as ride-sharing or lift-sharing, carpooling refers to the shared use of a car by the driver and one or more passengers, usually for commuting<sup>1</sup>. Carpoolers share journeys if their personal choices match<sup>2</sup> (i.e. Trip origin, destination, date and time or time slots, etc.), (Figure 1).

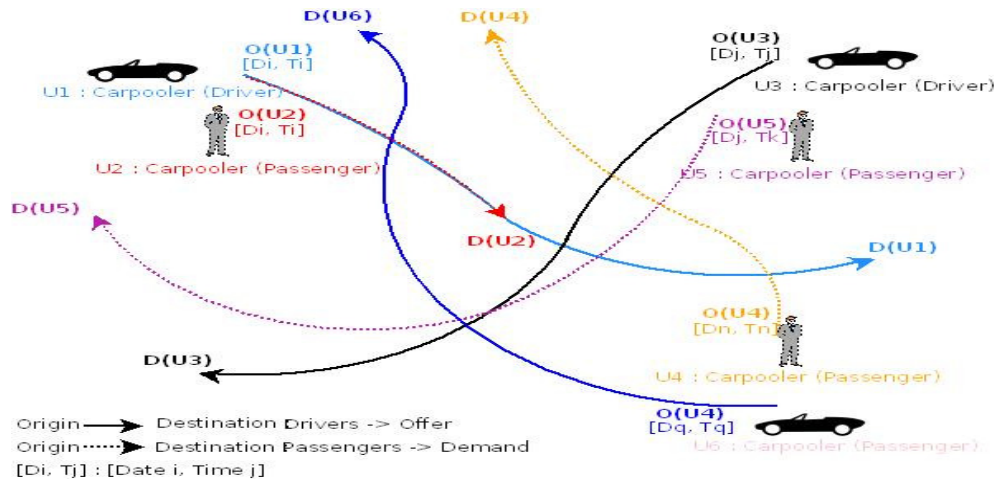


FIGURE 1: Carpooling : Offers and Demands.

Largely due to its multiple advantages [4], carpooling has become in recent years a remarkable phenomenon and individuals increasingly tend to appreciate it. In this context, urban carpooling is often promoted as an alternative to owning a car [5], [6]. Besides, carpooling combats rising traffic congestion [4], reduces energy consumption and moving costs.

<sup>1</sup> <http://www.answers.com/topic/carpool>

<sup>2</sup> <http://www.carpoolglobal.com>

Regarding its promising impact on people and environment, it was considered in many works [2] and formal carpool projects have been around in a structured form since the mid-1970s. They are rather shown as:

- Virtual supports for reservations' management such as 123envoiture<sup>3</sup> <sup>4</sup> or aide-covoiturage.com<sup>5</sup> that allow users to subscribe in order to access carpooling services and post specifications about their trips or consult planned trips and join each other if one of the available proposals meet their needs.
- Virtual social networks or forums (e.g. COMOVE<sup>6</sup>) that propose automatic tools allowing their subscribers to directly meet and agree on details about trips to share. Forums suit for the same principle as the one detailed above since they are presented as websites where, besides of consulting drivers' offers and passengers' requests, people can meet and directly discuss through chat-rooms.

Despite the important progress experimented on carpooling concept thanks to the existent works, it still remains in embryonic stage regarding automation and real time aspects. Indeed, existing systems only consider the standard deal with offers and requests storage. Almost all of these works only tackle the static ridesharing issue whereby users must plan their trips in advance (Figure 2) and so neglecting the dynamic aspect.

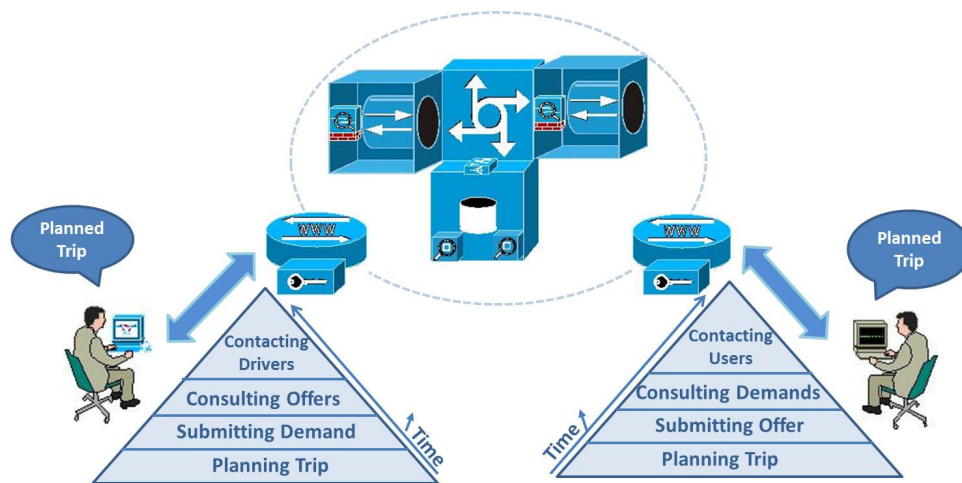


FIGURE 2: Carpooling: Existing Systems.

In order to make up this shortfall, we propose to consider the dynamic aspect. In fact, even if real time carpooling was considered in some approaches (e.g. GoLoco, Easy-Rider, T.écovoiturage...) [2, 7], most of them no longer exist. Furthermore, none of the existent systems evoked the security issue which is one of the main reasons hindering their success. Thus, we are especially involved in the concepts of traceability, communication and security services.

### 3. DOMARTIC: AN OPTIMIZED PROCESS TO PROVIDE A REAL TIME CARPOOLING SERVICE

Setting up a ridesharing service as satisfactory as possible is our main objective. Proceeding from this basic principle and in an attempt to remedy the problems outlined above, we consider the problem of processing real time users' requests. The proposed approach mainly aims at carrying out a system that allows its users to reach a vehicle anywhere, at any time and as rapidly

<sup>3</sup> <http://www.greencove.fr>

<sup>4</sup> <http://www.123envoiture.com/>

<sup>5</sup> <http://www.aide-covoiturage.com>

<sup>6</sup> <http://www.comove.com/forum-covoiturage/index.php>

as possible. For this purpose, adequate tools as well as an appropriate solving methodology are considered. Among them, a based GPS positioning tool as we need to be provided with real time information about drivers and passengers so that we can process their requests and perform vehicles' traceability and so ensure users' safety. To do this, system users must have already agreed on a number of terms of use. For example, they must accept to be located at any time of the trip. This is done first time they access the system so that they can subscribe.

As the technological development is at its peak (e.g. GPS geolocation, mobile devices connected via GPRS or Internet...), it is convenient to take advantage from the observed advancement especially in networks and communication to set up a highly interactive framework. The elaborated automated support enables users to communicate with each other and with the system itself. Figure 3 illustrates a real view of our system showing possible communications between its actors. In addition to users, vehicles and the GPS module, the assignment process constitutes a main and central actor and has a pivotal role ensuring communication with and between the other actors. As it is responsible for automatically processing dynamic and optimized allocation of vehicles to users, it is considered as the core of our work.

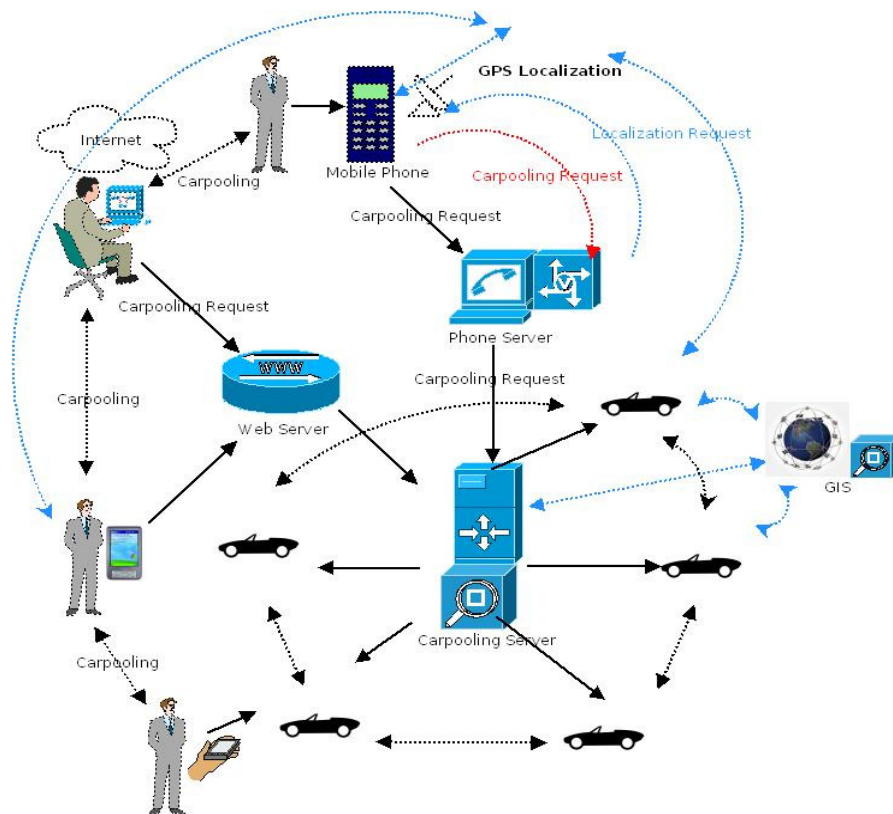


**FIGURE 3:** A based Communication Support within DOMARTiC.

In this context, our work is directly involved in setting up a complete carpooling framework that primarily establishes several functionalities (see Figure 4). Among the latter, parallel requests acquisition and their parallel decentralized process according to a distributed architecture set up through a subdivision process lately defined.

Optimization is the key word in the process developed and is considered on more than one sight: Firstly considering the optimized requests' process according to the chosen criteria, And secondly considering the real time constraints according to which responses must be provided within an acceptable time of processing (i.e. as minimum as possible). Consequently, we are mainly concerned with providing, within a reasonable response delay, the best solution or at least an optimized or an approximate one.

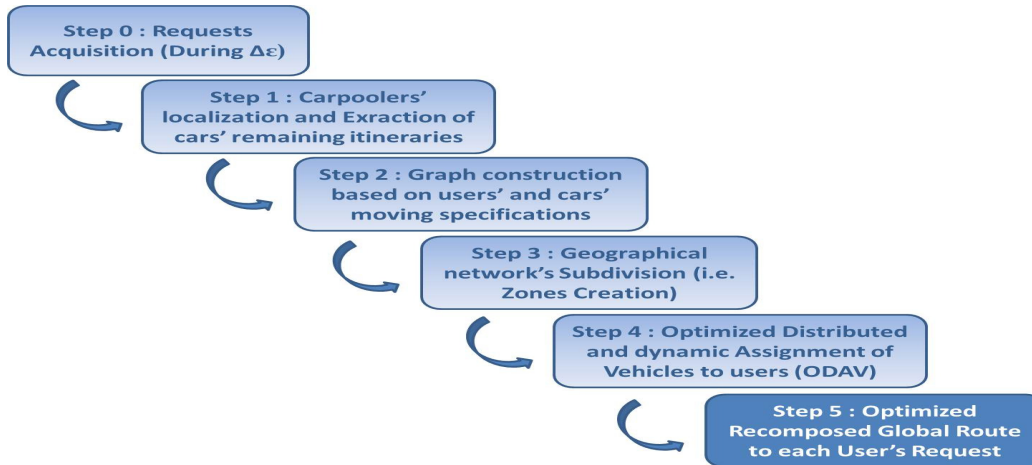


FIGURE 4: DOMARTiC's Main Functionalities to establish an Optimized Process.

### 3.1. Parallel Requests' Processing

Setting up a dynamic ridesharing system should instantly take into account users' requests for immediate trips. Thus, to guaranty users' satisfaction regarding required optimum response delay, we are involved in instantaneously process their requests. Moreover, users may probably issue queries approximately at the same time which should be processed in parallel. For this purpose, we introduce a parameter called  $\Delta\mathcal{E}$  [8] that indicates a negligible time lapse during which requests' acquisition should be performed (Figure 5).

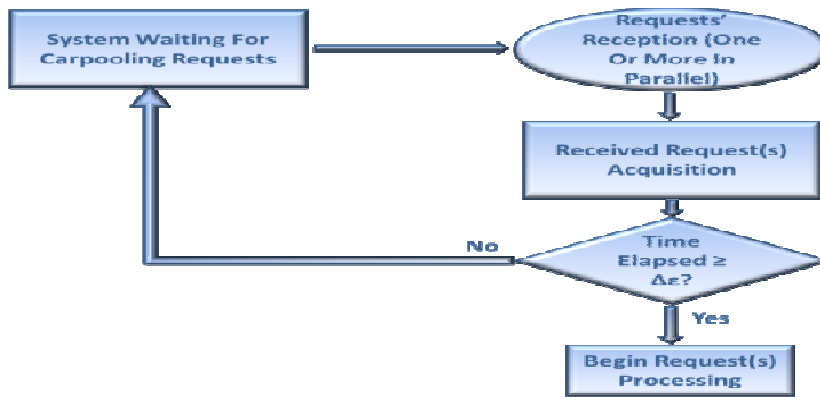


FIGURE 5: Parallel Requests Processing within an Optimized Real Time Carpooling System.

### 3.2. Optimization Within DOMARTiC: Towards a better Quality of Service

Considering the dynamic carpooling issue involves optimization with a driving idea that refers to users' satisfaction. As shown in figure 6, multiple criteria could be considered for this purpose.



**FIGURE 6:** Optimization Criteria to consider in Dynamic Carpooling Services.

Optimization mainly concerns vehicles' dynamic allocation to passengers, searching for the best offer meeting users requests' specifications, or at least an approximate proposal.

In this paper, optimization primarily lies in selecting solutions maximizing comfort (i.e. minimizing the number of transfers) trying by the way to ensure trips' continuity. In this context, vehicles serving a given route asked by a given user are considered if and only if they satisfy a set of feasibility constraints (lately formulated). These constraints mainly refer to the number of places available, times of departure and arrival, itineraries of the considered cars that must fit the asked route while matching the user's moving preferences (i.e. departure and arrival time, number of persons...) on this route.

Secondly, an optimal solution is chosen among the firstly selected ones considering another criterion. Indeed, the final selection focuses on the solution that minimizes the global Trip Duration. The latter involves both of the Waiting time ( $W_t$ ) and the Traveling time ( $T_t$ ). Thus, a Fitness function aggregating  $W_t$  and  $T_t$  is considered in a multiobjective optimization optical view.

**Complexity of the Optimized Real Time Carpooling Problem (ORTCP)**

Considering an optimized dynamic carpooling system implies to consider the problem of its combinatorial complexity. To prove ORTCP's high complexity, we consider a comparative study (Table 1) with the *Dynamic Pick-up and Delivery Problems (DPDPs)*, especially the *Swapping Problem (SP)* [9] or *Dial-a-Ride problem (DARP)*. *PDPs* are a class of vehicle routing problems in which objects or people have to be transported between an origin and a destination [10].

Problem	Parameters	Constraints	Objective Function
DPDPs: Dynamic Pick-up and Delivery Problems	Vertices with objects or persons (Dynamic Swapping Problem <i>SP</i> or Dial-a-Ride Problem <i>DARP</i> )	Vehicle with limited unit capacity, real time requests...	Search for the shortest path to accomplish the rearrangement of the objects (or persons)
Optimized Real Time Carpooling Problem ( <i>ORTCP</i> )	Users' Locations, Requests' Specifications (Origins and Destinations), Intersections with Cars' Routes	Cars with limited number of available places, cars' itineraries, real time requests...	Search For an Optimized itinerary regarding Trip Duration For Each User's Request

**TABLE 1:** Dynamic Carpooling Problem in comparison with *SP* and *DARP*.

*ORTCP* is obviously analogous to *DPDPs*. The *SP* as well as *DARP* are known to be of exponential complexity and belong to the NP-Hard problems category. So, this comes to confirm the high complexity of *ORTCP* and states it as a combinatorial optimization problem (i.e.  $O(ORTCP) \equiv O(SP) \equiv O(DARP)$ ). Moreover, many other aspects have not been considered in the previous study and are liable to heighten even more the complexity. Among those aspects:

- ORTCP should also take into account cars' moving specifications,
- There is more than one car that could respond to one or more request ...

Jointly solving those problems become even more complex as much as there is more users' requests and/or more available cars (i.e.  $O(ORTCP) > O(SP)$ ).

This study reveals many difficulties that would probably present a big handicap through the way to process optimization tasks. Thus, we propose to decompose the original problem into partial ones to promote distributed parallel process.

### 3.3. A Subdivision Principle to set up a Distributed Dynamic Architecture

In order to overcome ORTCP's high complexity, we propose a novel network representation mainly concerned with the way to elaborate a distributed architecture trying to divide the initial whole task into smaller parallel ones and so reduce the initial problem's complexity. Proceeding from this basic concept, we might be able to perform distributed parallel requests processing.

#### DOMARTiC's Formal Specification

Partially inspired by the PDPs and the Vehicle Routing Problem (VRP) formal modeling [11], we define the dynamic optimized carpooling problem, at a given time  $t$ , as the triplet  $T(t) = (G(t), D(t), O(t))$  where:

- $G(t) = (N(t), A(t))$  is a directed graph with :
  - $N(t)$ : The set of nodes set up on the base of geographical coordinates corresponding to origins, destinations or Intermediate Destinations of either asked or offered trips at time  $t$ .
  - $A(t)$ : A set of directed arcs that represent real time constructed paths relating origins to their destinations. They concern vehicles' remaining itineraries and users' asked routes in function of existent intermediate destinations.

$G(t)$  is real time constructed and has no fixed characteristics or shape since it mainly depends on users' requests (i.e.  $D(t)$ ) and cars' offers (i.e.  $O(t)$ ). Consequently,  $G(t)$  is a dynamic graph.

- $D(t) = \bigcup_{p=1}^n D_{U_p}(t)$  is the set of carpooling demands received at time  $t$ . It refers to

$U(t) = \bigcup_{p=1}^n (U_p(t))$ : the set of  $n$  users having issued requests. Each user  $U_p$ 's

request is defined as  $D_{U_p}(t) = (d_{U_p}^+, d_{U_p}^-, P_{U_p}, [De_{U_p}, A_{U_p}])$  where :

- $d_{U_p}^+$  is the origin of the required route. It may refer to his geographical localization whenever it is not specified by the user  $U_p$ .
- $d_{U_p}^-$  is the destination of this route. Moving origins and destinations are represented by a couple of nodes in the graph  $G(t)$ . Thus,  $N_D(t)$  is the set of nodes in  $G$  specific to users' demands:

$$N_D(t) = \bigcup_{p=1}^n (d_{U_p}^+, d_{U_p}^-) (t) \subset N(t)$$

- $P_{U_p}$  is the number of Persons including  $U_p$ , that must move from  $d_{U_p}^+$  to  $d_{U_p}^-$ .
- $[De_{U_p}, A_{U_p}]$  designates a limited time interval that defines the global trip duration.

$De_{U_p}$  is the Departure time at the earliest, and  $A_{U_p}$  is the time of Arrival at the latest. This interval, when specified, represents the preferred departure time and at worst the tolerated Arrival time for a given request. Otherwise, the concerned user may have no preferences and do not specify one of these parameters or both. In this case, default values of  $De_{U_p}$  and  $A_{U_p}$  are respectively the current time and an Estimated Arrival Time (EAT) calculated as follows:

$$EAT(d_{U_p}^+, d_{U_p}^-, t) = TT(d_{U_p}^+, d_{U_p}^-, t) + TDT(d_{U_p}^+, d_{U_p}^-)$$

Where the Traveling Time ( $TT(O, D, t)$ ) is the function weighting arcs of G and calculating the time needed to traverse a path from a given origin O to a determined destination D:

$$TT(O, D, t) = Distance(O, D) * TAT(O, D, t) / (O, D) \in A(t)$$

and  $TDT(O, D)$  is the Tolerable Delay Threshold apportioned to a fixed tolerable delay of 10 minutes per 50 kilometers. It represents the acceptable maximum delay on the distance between O and D:

$$TDT(O, D) = Distance(O, D) * \frac{10}{50}$$

Distance (O, D) is the formula calculating distance between two GPS coordinates:

$$Distance(O, D) = \sqrt{(Longitude_O - Longitude_D)^2 + (Latitude_O - Latitude_D)^2}$$

TAT is a given data on the Traveling Average Time that depends on roads' type, the period of traveling (e.g. rush hour, normal period...) and the weather. Then, arcs' weights could vary over time. Based on this and on its real time defined specifications (i.e. arcs and nodes), we can state that G(t) is a highly dynamic graph. A graph is dynamic if at least one of its parameters is function of time [12][13].

As two users or more could ask for a same route, the set of requests D (t) is then modeled as an Origin to Destination  $OD_{U_i}(t)$  matrix (k x k):

$$D(t) = \begin{matrix} & \begin{matrix} d_1^- & \dots & d_i^- & \dots & d_k^- \end{matrix} \\ \begin{matrix} d_1^+ \\ \vdots \\ d_i^+ \\ \vdots \\ d_k^+ \end{matrix} & \begin{pmatrix} D_{(d_1^+, d_1^-)} & \dots & \dots & \dots \\ \dots & \dots & \dots & \dots \\ \dots & \dots & D_{(d_i^+, d_i^-)} & \dots \\ \dots & \dots & \dots & \dots \\ \dots & \dots & \dots & D_{(d_k^+, d_k^-)} \end{pmatrix} \end{matrix}$$

Each element  $D_{(d_i^+, d_i^-)} / i \in \{1..k\}$  of the matrix refers to the set of users' demands on a given route i defined by its origin  $d_i^+$  and destination  $d_i^-$ . As

there could be more than one user asking for the same route  $(d_i^+, d_i^-)$ , matrix's element referring to the latter contains the set of users' demands on this route showing the different parameters (i.e. number of persons, time of departure at the earliest, and the arrival time required) specific to each one of them.

$$O(t) = \bigcup_{j=1}^m O_{V_j}(t) \text{ is the set of cars' offers. } V(t) = \bigcup_{j=1}^m (V_j(t)) \text{ is a fleet of } m \text{ vehicles}$$

offering journeys and already circulating through the geographical network at time t or not

yet. Each vehicle  $V_j$  has a limited capacity  $C_{V_j} \in C$  and its origin ( $O_{V_j}^+$ ) and destination ( $O_{V_j}^-$ ) are designated by a couple of nodes in  $G(t)$  :

$$N_o(t) = \bigcup_{j=1}^m (O_{V_j}^+, O_{V_j}^-)(t) \subset N(t)$$

$N_o(t)$  is the set of offered trips' specifications related to cars' origins and destinations.

$$O_{V_j}(t) = (O_{V_j}^+, O_{V_j}^-, PL_{V_j}, \begin{pmatrix} ID_1 \\ \dots \\ ID_z \end{pmatrix}, [De_{V_j}, A_{V_j}])$$

is  $V_j$ 's offer where besides of parameters ( $O_{V_j}^+, O_{V_j}^-, [De_{V_j}, A_{V_j}]$ ) similar to those defined in requests, the driver may specify:

- $PL_{V_j}$  : the number of places available in  $V_j$  at time  $t$  for a given route (i.e.  $[O_{V_j}^+, O_{V_j}^-]$ ).
- $ID_{V_j} = \begin{pmatrix} ID_1 \\ \vdots \\ ID_z \end{pmatrix}_{V_j} = \bigcup_{q=1}^z ID_{q,V_j}$  : The set of addresses  $V_j$  would pass by to reach

its final destination. These addresses are defined as Intermediate Destinations ( $ID$ ) that can be either specified by the driver or set by the system in previous process as pickup or deposit places and represent a set of specific vertices  $N_{ID}(t)$  of  $G(t)$  :

$$N_{ID}(t) = \bigcup_{j=1}^m \bigcup_{q=1}^z ID_{q,V_j}(t) \subset N(t)$$

Thus,

$$N(t) = N_D(t) \cup N_O(t) \cup N_{ID}(t)$$

The set of offers (i.e.  $O(t)$ ) is modeled as an Origin to Destination (i.e.  $OD_V(t)$ ) matrix that considers each single route  $[o, d] / (o, d) \in (\bigcup_{i=1}^f O_i = N_O(t) \cup N_{ID}(t))^2$ .

$$O(t) = \begin{matrix} & O_1^- & \dots & O_i^- & \dots & O_f^- \\ \begin{matrix} O_1^+ \\ \vdots \\ O_i^+ \\ \vdots \\ O_f^+ \end{matrix} & \begin{pmatrix} O_{(O_1^+, O_1^-)} \\ \dots \\ \vdots \\ * \\ X \end{pmatrix} & & \begin{pmatrix} \dots \\ \dots \\ O_{(O_i^+, O_i^-)} \\ \dots \end{pmatrix} & & \begin{pmatrix} \dots \\ * \\ \vdots \\ X \\ O_{(O_f^+, O_f^-)} \end{pmatrix} \end{matrix}$$

A given element  $O_{o,d}(t)$  of  $O(t)$  refers to an elementary or composed path ( $[o, d]$ ) from an origin  $o$  to a destination  $d$ .  $O_{o,d}(t)$  may take one of the following values:

$$O_{(o,d)}(t) = \begin{cases} X : \text{if according to the road law, } [o, d] \text{ could not be traversed in this} \\ \text{direction;} \\ * : \text{if there is no offer considering this route (i.e. no vehicle passing by } [o, d] \text{);} \\ \text{The set of parameters } (Pl_{o,d}^j, De_{o,d}^j, A_{o,d}^j) \text{ of each vehicle } V_j \text{ serving the} \\ \text{route } [o, d] \end{cases}$$

When at least one offer exists on a given route  $[o, d]$ , related matrix element  $O_{(o, d)}(t)$  contains several information on the concerned offer(s) for each vehicle  $V_j$  serving it:

- $Pl_{o,d}^j$  : The number of places available within  $V_j$  on  $[o, d]$ . This parameter could differ from a partial route to another with reference to passengers' deposit and / or pickup at intermediate destinations,
- $[De, A]_{o,d}^j(t)$  : indicates  $V_j$ 's Departure time at the earliest from  $o$  and its Arrival time at the latest on  $d$  that are calculated as in what follows:  
For each two successive route's segments  $[h,o]$  and  $[o,d]$  /  $[[h, o], [o, d]] \subseteq O_{V_j}(t)$  :

$$\begin{cases} De_{o,d}^j(t) = De_{h,o}^j(t) + TT(h, o, t) \\ A_{o,d}^j(t) = A_{h,o}^j(t) + TT(h, o, t) + TDT(h, o) \end{cases}$$

Cars' itineraries are composed of several sections and different vehicles may have in common some partial routes or simply intersection points. Each node of  $G(t)$  could then have one or more successors referring to potential intermediate or final destinations. This helps distinguish two main sets for each node  $x \in N(t)$  :

1. The set of successors denoted  $N_x^+(t)$  defined as:

$$N_x^+(t) = \{v \in N(t) / (x, v) \in A(t)\}$$

2. The set of predecessors denoted  $N_x^-(t)$  defined as:

$$N_x^-(t) = \{v \in N(t) / (v, x) \in A(t)\}$$

Cars' global itineraries are then modeled as n successors' chain,  $\forall j \in \{1..m\}$ :

$$IT_{V_j}(t) = (v_0, v_1, \dots, v_n) \text{ with } \begin{cases} v_k \in N(t), \forall k \in [0, n] \\ v_0 = O_{V_j}^+, v_n = O_{V_j}^-, \bigcup_{q=1}^{n-1} v_q = ID_{V_j}(t) \\ \forall v_k, v_{k+1} \in IT_{V_j}(t), (v_k, v_{k+1}) \in A(t) \end{cases}$$

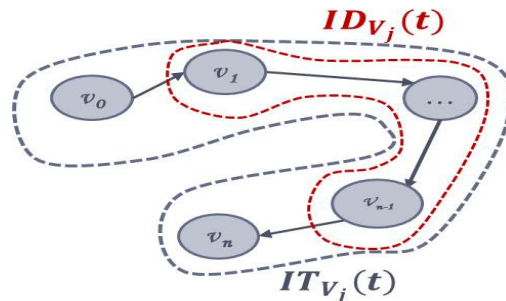


**FIGURE 7:** A global itinerary composed of several sections. and so as a composed route of a finite number of Partial Itineraries (PI):

$$IT_{V_j}(t) = \bigcup_{s=1}^{n-1} PI_s^j = \{[O_{V_j}^+, ID_1], [ID_1, ID_2], \dots, [ID_{q-1}, ID_q], \dots, [ID_z, O_{V_j}^-]\}$$

Where  $PI_s^j$  is the partial itinerary  $s$  of the vehicle  $V_j$ . Two cars could share itineraries intersection without having any common partial route but can also share Partial Itineraries as well. Shared PIs could be served by different vehicles at different times or (almost) simultaneously. As the system may process users' requests generating recomposed solutions (Figure 8) with limited number of transfers if no complete solution exists, responses provided to users in this case are then defined as:

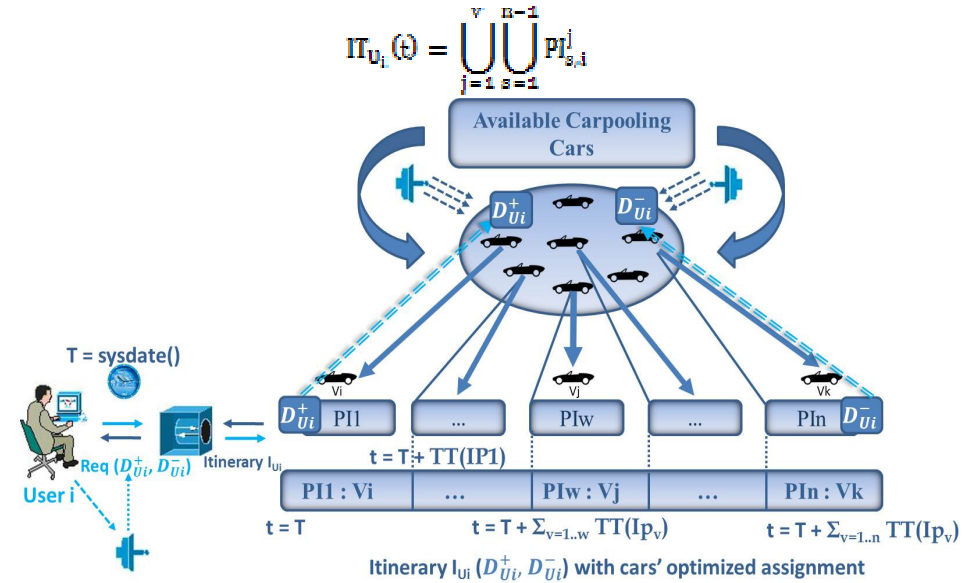


FIGURE 8: A composed optimized solution.

Here  $PI_{s,i}^j$  refers to the vehicle  $V_j$  that optimizes the Trip Duration on the Partial Itinerary  $s$  ( $PI_{s,i}$ ) composing the global solution provided to user  $i$ . To be considered as a potential feasible solution on ( $PI_{s,i}$ ),  $V_j$  must firstly satisfy some constraints:

- $PI_s^j \geq P_{U_i}$ :  $V_j$  must have enough available places  $PI_s^j$  on partial itinerary  $s$  according to the number of places asked by user  $i$ .
- $PI_{s,i} \in IT_{V_j}$ :  $V_j$  serves the section  $s$  ( $PI_{s,i}$ ) in the correct order from its origin ( $PI_{s,i}^+$ ) to its destination ( $PI_{s,i}^-$ ).
- $De_{PI_{s,i}^+} \geq De_{U_i}$ :  $V_j$  could be assigned to the first leg of the given solution to user  $U_i$  if and only if its departure time at the earliest from the concerned route's origin is greater or equal to the one specified by the user.
- $De_{PI_{s,i}^+} \geq A_{PI_{s-1,i}^+}$ ,  $\forall s \in (1..n-1)$ : for each two successive partial itineraries,  $V_j$  is considered as a solution on  $PI_{s,i}$  only if its departure time at the earliest at its origin ( $PI_{s,i}^+$ ) is later or equal to the arrival time of the vehicle  $V_v$  on the previous

leg destination ( $PI_{s-1,i}^- = PI_{s,i}^+$ ).

- $A_{PI_{n-1,i}^j} \leq A_{U_i}$ , the vehicle  $V_j$  serving the last route's section of  $IT_{U_i}(t)$  must reach the final destination ( $d_{U_i}^-$ ) at  $A_{U_i}$  at the latest.

Based on this and on the optimization criteria considered, the final decision considering the optimized solution for each partial route (s) is taken on the base of an aggregative fitness function optimizing the trip duration on the considered route:

$$TD_s^* = \text{Min}_{j \in V_s} (TD_{s,j} = w_{1,z} W_{t_{j,s}} + w_{2,z} T_{t_{j,s}})$$

Where  $V_s$  is the set of vehicles serving the route s while satisfying the whole set of constraints mentioned above.

The whole global solution corresponds to the one optimizing the global Trip Duration of  $IT_{U_i}(t)$ :

$$TD_{U_i}^* = \sum_{s=1}^{n-1} \text{Min}_{j \in V_s} (TD_{s,j}) = \sum_{s=1}^{n-1} \text{Min}_{j \in V_s} (w_{1,z} W_{t_{j,s}} + w_{2,z} T_{t_{j,s}})$$

$w_{1,z}$  and  $w_{2,z}$  computation details are given in what follows.

### A Subdivision Principle to Establish a Physical Distributed Architecture

To optimize execution properties and response delay, requests' acquisition is performed in parallel and then processed simultaneously. According to DOMARTiC's formal specifications, a dynamic graph is used to represent the set of requests and offers. Based on this graph, a distributed architecture is established through a subdivision process. This helped to convey the idea of setting up an optimized decentralized process performing dynamic vehicles' assignment. Hence, we are mainly involved in the way to decompose the whole process into a finite number of less complex tasks executed in parallel. Trying to translate that idea, the first step was to break the geographical served network into several areas of limited surfaces and having the same circular shape and dimensions, created areas have common characteristics:

- They refer to geographical zones with limited perimeters,
- Zones may intersect and have common parts with each other,
- Zones' shape is the same for all the established areas. They are presented as circles which centers are dynamically determined,
- Zones are real time constructed according to the instantly received demands and the available offers at the considered time t ...

The subdivision process adopted [14] determines sets of neighbors coordinates (i.e. nodes of  $G(t)$  that are close to each other with respect to the fixed zones' diameter) and establishes several areas. Each one of the created areas corresponds to a given set of neighbors and responds to the stated characteristics. In this decomposing process, two main steps are considered:

- Step 1: Whereby Primary Zones ( $PZ$ ) are established considering only passengers' requests specifications (i.e. asked origins and destinations) on the base of which groups of neighbors coordinates are determined. A  $PZ$  is created for each one of them.
- Step 2: Including drivers' moving specifications and their moving itineraries, the same principle is followed to set up Intermediate Zones ( $IZ$ ) taking into account the firstly established ones (i.e.  $PZ$ ).

This decomposing principle is the base of the decentralized process where optimized responses management is performed in a distributed way over the several created zones. Based on this and as we consider a fitness function aggregating  $W_t$  and  $T_t$ , their weights differ from one zone to another and are calculated properly to each zone z of the considered areas ( $z \in Z$ ).  $W_t$  and  $T_t$  weights (i.e.  $w_{1,z}$ ,  $w_{2,z}$ ) are calculated according to the Proportion of Positive Delay (PPD<sub>z</sub>):

$$PPD_z(t) = VPD_z [t - \theta, t] / TN [t - \theta, t]$$

This parameter reflects, more faithfully than any other, users' waiting and traveling time within each zone at a given time  $t$  and helps estimating trips' global duration based on prior knowledge observed on  $\Delta t = [t - \theta, t]$  (i.e. the number of cars that started their journeys in  $z$  later than firstly indicated ( $VPD_z$ : Vehicle having Positive Delay) compared with the Total Number of cars (TN).

In fact,  $PPD_z$  shows the impact of different factors (e.g. traffic congestion, disturbances ...) observed during an elapsed period of time  $\theta$  in a zone  $z$  and that might directly or not affect the traveling duration. Thus, based on this concept,  $\omega_1$  and  $\omega_2$  differ from one zone to another and may change over time. Their respective formulas are defined as:

$$\begin{aligned}\omega_{1,z}(t) &= PPD_z(t) \\ \omega_{2,z}(t) &= 1 - PPD_z(t)\end{aligned}$$

The established architecture is then presented as a distributed dynamic graph that is largely appropriate to parallel requests processing jointly considering the multi-agent concept [13].

### 3.4. Setting up a Distributed Software Architecture Based on the Multi-Agent Concept

Multi-Agent Systems (MAS) are composed of several entities that can be seen as interacting intelligent agents with parallel operations [15]. These agents act in a specific environment according to a certain organization and follow pre-established communication rules to ensure a coherent global process. MAS can be used to solve problems with high complexity. Thus, this concept is perfectly well adapted to represent carpool community where different agents must coexist and cooperate to provide a real time carpooling service as satisfactory as possible.

#### Review of Existent Multi-agent Systems

MAS have known a great success in the analysis and description of traffic systems increasing traffic components autonomy and facilitating the integration of several frameworks [16, 17]. In classical carpooling systems [18], users are represented by software agents. A special one called super-agent is responsible for managing users' requests searching for possible matchings, but the final choice is yet done by the concerned users and decision is always made by them.

Some mobile-based multiagent applications have been proposed such as MobiAgent [19]<sup>7</sup> that allows users to access various services (e.g. web search, remote applications control ...) using their mobile phones or PDAs. A Personal Agent (PA) is created in a centralized server for each user sending a request for a specific service. The latter get disconnected from the network and is then notified by the PA of the results it has found. Another System called Andiamo [16] suits for the same principle proposing an agent-based framework using the ToothAgent architecture [20].

Existent ride sharing systems mainly tackle the problem of accessing the system through mobile phones or PDA but remain limited since they are very restricted to the only task of searching for possible matching according to users' moving needs without allowing any flexibility. Thus, automated requests management performed by super-agents was their only important contribution to ameliorate the carpooling service overriding real time and optimization aspects.

#### The Multi-agent Concept Within DOMARTiC

As stated above, processing dynamic carpooling users' requests is of combinatorial complexity. Besides, the network's modeling previously proposed is suitable for a distributed architecture. This comes to confirm the choice of adopting the multi-agent concept to efficiently deal with dynamic carpooling service. Furthermore, the multi-agent concept is yet more useful as we consider an optimization issue.

Several entities referring, among others, to users' and cars' assistants evolve within our system and are able to communicate and exchange information. Users of our system are then provided with a communication support so that they can instantly interact and communicate with each other and with the carpooling server that is also made up of several entities.

<sup>7</sup> <http://www.docstoc.com/docs/58249789/Genghis---A-Multiagent-Carpooling-System>

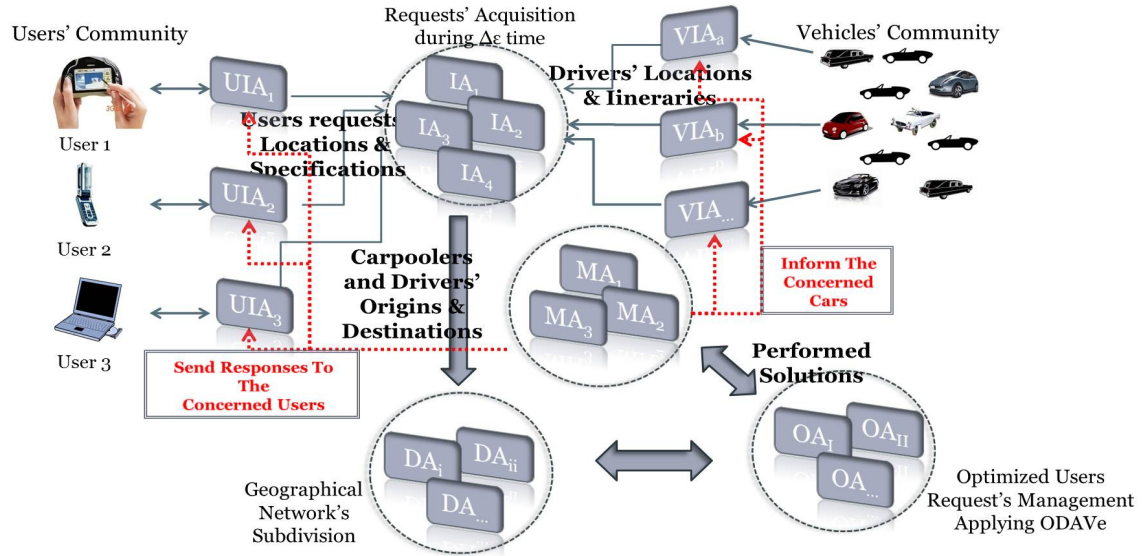
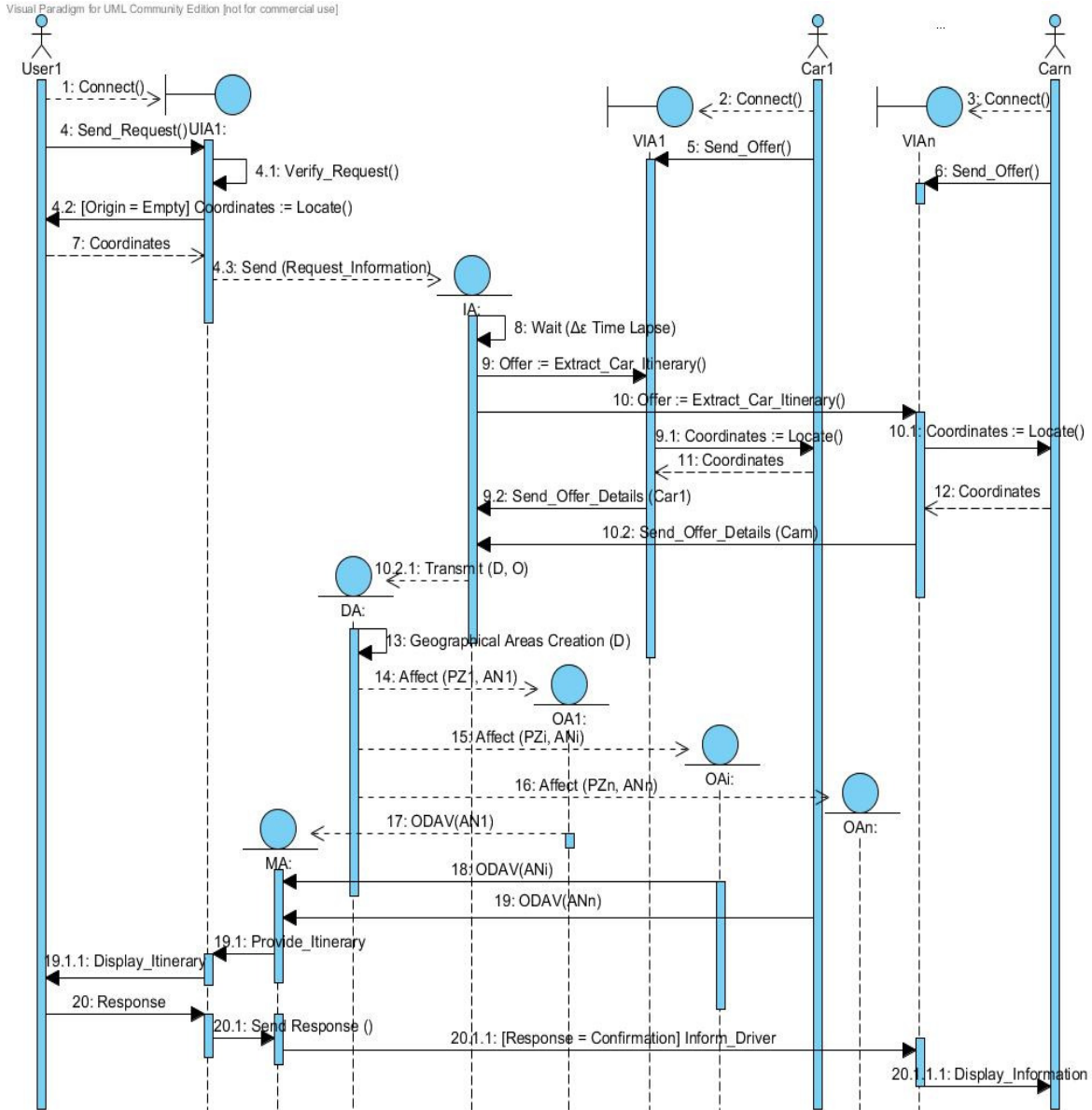


FIGURE 9: Agent modeling within DOMARTiC.

Thanks to this concept, DOMARTiC is provided with an interactive support, enabling the involved entities to exchange information and ensure a coherent process as it is show in Figure 10.



**FIGURE 10:** Messages exchange to perform DOMARTiC's process.

**Agents' functioning:**

In this section, entities involved in our system are described with the main features they are responsible for:

**User Interface Agent (UIA):** created for each user connected to the system and is responsible for receiving its demand and transmits it to the Information Agent (IA). After the optimized process is performed, it provides the user with the generated response,

**Vehicle Interface Agent (VIA):** ensures driver's exchange with the involved agents (i.e. IA respectively the MA) transmitting the offer it proposes or receiving notifications of pickup and deposit addresses.

**Information Agent (IA):** must provide the Decomposing Agent with the necessary information on

users' requests and the itineraries (i.e. drivers' offers) that might be suitable for those requests. For this purpose, it should firstly perform requests reception during  $\Delta t$  time, an example of received requests at time  $t = 9h10$  is given in table 2.

User's Identifier	Request's Origin	Request's Destination	Number of Persons	De	A
$U_1$	$U_1^+$	$V_1^-$	1	9h10	10h40
$U_2$	$U_2^+$	$V_2^-$	2	9h10	10h00
$U_3$	$U_3^+$	$V_3^-$	1	9h10	10h15
$U_4$	$U_4^+$	$V_4^-$	2	9h10	10h10
$U_5$	$U_5^+$	$V_5^-$	2	9h13	10h00
$U_6$	$U_6^+$	$V_6^-$	4	9h10	10h30

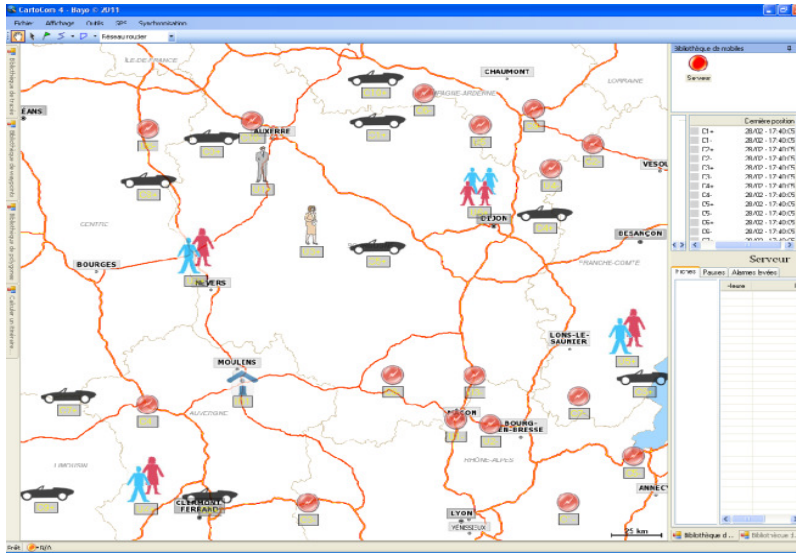
**TABLE 2:** Users' requests received at time  $t$  (D(t))

Secondly, the IA asks for available offers' specifications (table 3) sending a specific message (Request\_For\_Offer) to each operating VIA. This is based on the concept of agents' coalition to ensure coherence of the responses provided.

Vehicle's Identifier	Offer's Origin	Offer's Destination	Number of Places	ID	De	A
$C_1$	$C_1^+$	$C_1^-$	1	$ID_{C_1}$	–	10h15
$C_2$	$C_2^+$	$C_2^-$	3	$ID_{C_2}$	–	13h00
$C_3$	$C_3^+$	$C_3^-$	4	$ID_{C_3}$	–	11h00
$C_4$	$C_4^+$	$C_4^-$	3	$ID_{C_4}$	–	12h15
$C_5$	$C_5^+$	$C_5^-$	7	$ID_{C_5}$	–	11h15
$C_6$	$C_6^+$	$C_6^-$	8	$ID_{C_6}$	–	12h10
$C_7$	$C_7^+$	$C_7^-$	2	$ID_{C_7}$	–	12h00
$C_8$	$C_8^+$	$C_8^-$	1	$ID_{C_8}$	–	9h45
$C_9$	$C_9^+$	$C_9^-$	3	$ID_{C_9}$	–	13h15
$C_{10}$	$C_{10}^+$	$C_{10}^-$	4	$ID_{C_{10}}$	–	10h30

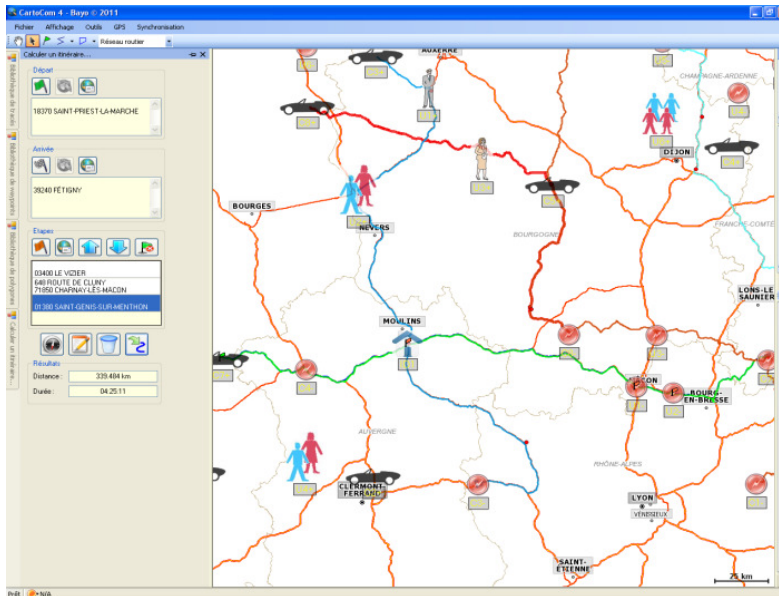
**TABLE 3:** Cars' offers available at time  $t$  (O(t))

Decomposing agent (DA): Having received the required information (i.e. Requests and Offers' specifications) from the IA, the DA is responsible for performing the previously described subdivision principle and according to which it should determine nodes close to each other and create a zone for each set of neighbors and an optimizing Agent for each established zone. Based on available information (table 2 and Table 3), Figure 11 illustrates a view of the served network on real map here limited to the only geographical area including the whole set of offers and demands. In this Figure, users' dispersion through the considered real map are represented according to their location (i.e. current coordinates) captured through GPS tools. Addresses to go to (i.e. final destinations of users and drivers) are also represented.



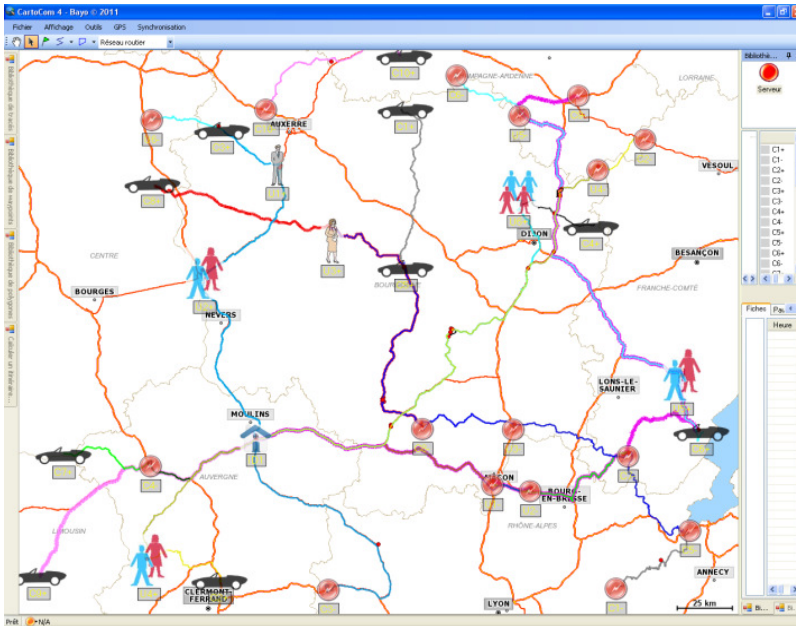
**FIGURE 11:** Offers and demands' specifications across the geographical network.

To establish such view, we have used automatic geolocation software called Cartocom. The latter integrates world real maps and is based on GPS tools to calculate itineraries based on the information inserted. An example of car itinerary's generation according to its origin, final and intermediate destinations is given by Figure 12.



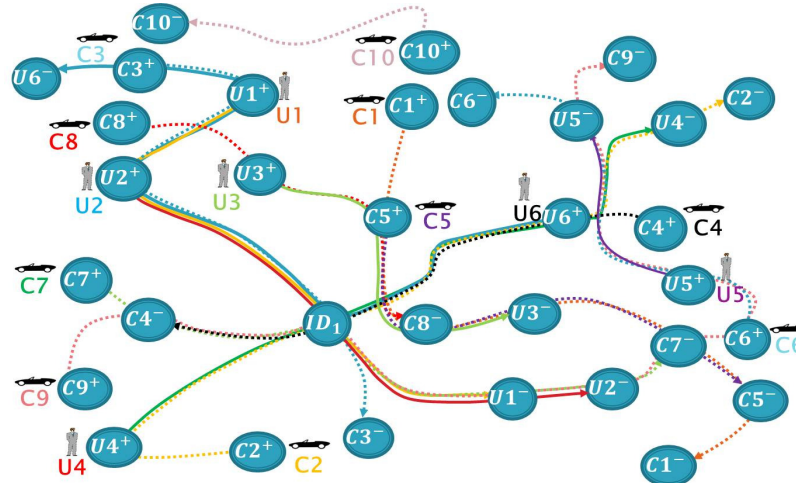
**FIGURE 12:** C<sub>7</sub>' itinerary's view on real maps.

Figure 13 shows how users and cars are spread with their respective itineraries over the considered area, here French regions, as the given example has been tested in France.



**FIGURE 13:** Vehicles' and users' scattering over the network.

Based on the established itineraries, a graph modeling is realized defining automated data structures that contain the available information according to the previously defined formalism. Figure 14 illustrates an automated translation of the real network's representation observed in Figure 13.



**FIGURE 14:** Graph modeling of users' requests and cars' offers.

The several steps involved within the decomposition process are then carried out on the established model. Consequently, several sets of neighbors are constructed leading to many distinct zones spread over the network as shown in Figure 15.

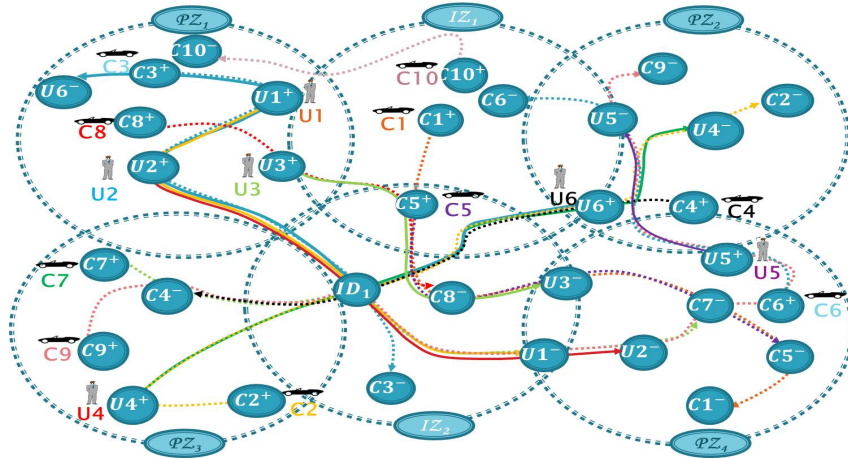


**FIGURE 15:** Zones established according to the decomposition process.

Optimizing Agent: locally processes optimized algorithms to search for convenient and optimized cars allocation. The optimized responses generation is performed in parallel, in a decentralized way, according to the distributed physical architecture set up through the subdivision process. In fact, an Optimizing Agent is created for each area established by the decomposition process and locally processes users' requests involved within its boundaries performing Algorithm 1. Each OA performs the implemented algorithm processing Optimized and Distributed Assignment of Vehicles to users (ODAVe) in order to find out the best cars' allocation regarding the global traveling duration while ensuring the continuity of the journey (i.e. providing final optimized and complete solution). Before optimization process begins, each zone  $OA_p$  determines the optimization's parameters  $w_{1,p}$  and  $w_{2,p}$ .

Algorithm 1 is performed by every Optimizing Agent  $OA_p$  responsible for locally processing optimized assignment of vehicles to users requests ( $D_{O,p}(t)$ ) which specifications (i.e. origins) are included within the zone  $Z_p$  it represents. Thus, in the beginning of the process, Optimizing Agents (OAs) representing Primary Zones that include users' requests' origins are firstly launched. In fact, these OAs represent the only zones including users' requests that could be performed at the process first iteration.

However, in later iterations, many Optimizing Agents, may them represent either Primary or Intermediate zones, could be involved within the running process since they could have received requests from other OAs. Indeed, as shown in Algorithm 1 which is performed by each OA receiving a request, the way to process requests is the same for each partial or global initial request:

At first,  $OA_p$  has to search for Optimized Global Itinerary (i.e. OGI) responding to the whole asked trip and fitting the previously established constraints (i.e. De, A, number of places ...) (Verify Constraints(...)).

As shown in Algorithm 2, each optimizing agent begins its process searching for possibilities (i.e. vehicles' offers) that may be assigned to a given request. A set of Potential Solutions (PS) is then filled with the extracted feasible solutions. Each potential solution is a data structure representing a given possibility related to a vehicle's offer on a given route. Thus, each single PS is characterized by trip's specifications (i.e. origin, destination, Vehicle Identifier, the number of available places within it, the Global Duration (GD), the departure time at the earliest (De) of the considered vehicle at the given origin, its arrival time (A) at the specified destination, and the related fitness value). Thereafter, the final solution is chosen as the optimal one ( $PS_o$ ) with regards to the previously stated objective function (i.e. Fitness value for each considered possibility of a specific vehicle).

**Data:**  $D_{OA_p}(t)$  : set of Demands included within the represented zone  $Z_p$  incumbent on  $OA_p$ ;  $O(t)$ : set of Offers; TDT: Tolerable Delay Threshold; TAT: Traveling Average Time; time system  $t$ ;  
**Results:** The set of Solutions  $S$  for the considered requests ( $D_{OA_p}(t)$ )

**Initialization:** Solution  $S \leftarrow \emptyset$ ;

1.  $\omega_{1p}, \omega_{2p} \leftarrow$  Calculate Optimization Parameters;
2. **For Each** Demand  $D_i$  **such that**  $D_i \in D_{OA_p}(t)$  **do**
3.  $S_i \leftarrow$  OGI ( $D_i$ );
4. **If** ( $S_i = \emptyset$ ) **then**
5. **For Each** Offer  $O_{V_j}$  **such that**  $O_{V_j} \in O(t)$  **do**
6.  $IN \leftarrow IN \cup$  Intersection ( $D_i, O_{V_j}$ )
7. **End for**
8. **Repeat**
9.  $NN \leftarrow$  Nearest\_Node ( $IN, D_i^-$ )
10.  $IN \leftarrow IN \setminus NN$
11. **Set** Request  $D_{i_1} \leftarrow (D_i^+, NN, P_{D_i}, D_{e_{D_i}}, EAT(D_i^+, NN, t))$
12.  $S_{i_1} \leftarrow$  OGI ( $D_{i_1}$ )
13.  $Z_c \leftarrow$  Containing\_Zone ( $NN$ ) { $NN \in Z_c$ }
14. **Set** Request  $D_{i_2} \leftarrow (NN, D_i^-, P_{D_i}, EAT(D_i^+, NN, t), A_{D_i})$
15. Send Request  $D_{i_2}$  to  $OA_c$  ( $OA_c$  is the Optimizing Agent responsible for performing requests which origins belong to  $Z_c$  perimeter)
16.  $S_{i_2} \leftarrow$  Receive Response From  $OA_c$  ( $OA_c$  performs ODAVe on  $D_{i_2}$  and sends partial solutions  $S_{i_2}$  to  $OA_p$ )
17. **If** ( $S_{i_2} = \emptyset$ ) **then**
18.  $S_i \leftarrow \emptyset$
19. **Else**
20.  $S_i \leftarrow S_{i_1} \oplus S_{i_2}$
21. **End if**
22. **Until**  $S_i \neq \emptyset$  Or  $IN \neq \emptyset$
23. **End If**
24.  $S \leftarrow S \cup S_i$
25. **End for**
26.  $MA \leftarrow$  Select a Merging Agent ()
27. Send  $S$  to  $MA$

**ALGORITHM 1:** ODAV : Optimized Distributed and dynamic Assignment of Vehicles to users.

Secondly, if no car serves the whole considered route or could not fulfill the considered user's expectations in terms of time of departure or/and time of arrival or/and number of places available, etc.  $OA_p$  searches for possible itineraries combinations... For this purpose, it must: Determine a set of Intersection Nodes (IN). Each element of this set corresponds to the closest node served by a given vehicle to the asked final destination. For this purpose, the whole set of existing drivers' offers is considered. IN is then established based on a comparison of the itineraries of each available car with the asked itinerary determining their intersection. Extract the most approximate served node (i.e. NN : the Nearest Node to the final destination  $D_i^-$ ),

Decompose the initial request into two distinct demands. The first one is performed by the considered operating OA (i.e.  $OA_p$ ),

Calculate the necessary parameters (i.e. De, A, ...) characterizing the second partial request,

Determine the zone  $Z_c$  containing NN and the corresponding Optimizing Agent ( $OA_c$ ) over which the whole process (i.e. Algorithm 1) is relaunched dealing with the second partial demand, Wait for the corresponding solution. The latter must be valid (i.e. not empty) so that the first agent can recompose a whole global itinerary, Otherwise, step 2 is performed until the received solution is valid as there remain possibilities to test.

According to the previously established distributed architecture and on the base of the given example, 5 OAs have been created to ensure the optimized requests processing. The whole set of solutions provided by the end of the process is illustrated in Figure 16.

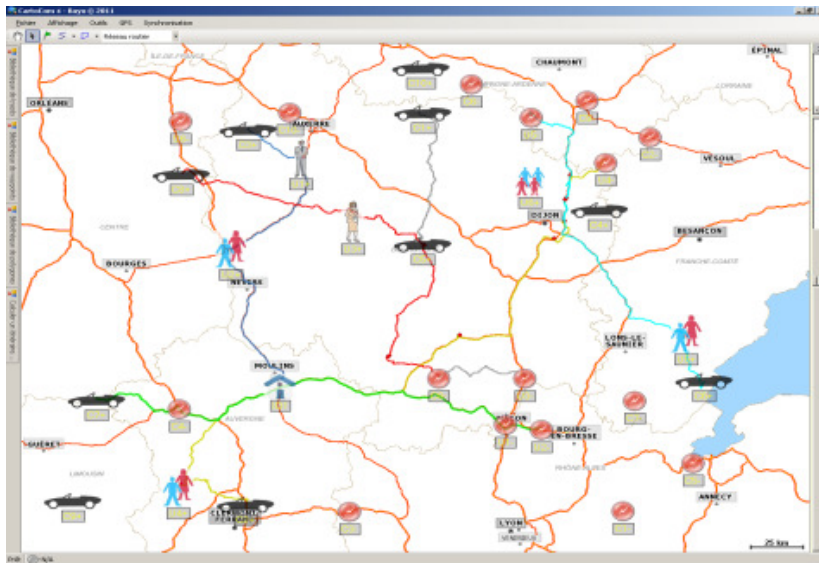


**FIGURE 16:** Itineraries details within solutions provided to users according to the assigned vehicles

Data:  $D_i$  : a specific demand included within the represented zone  $Z_p$  incumbent on  $OA_p$ ;  
 $O(t)$ : set of Offers; time system  $t$ ;  $\omega_{1_p}, \omega_{2_p}$   
 Results:  $S_i$ : the global optimized solution performed for the considered request  $D_i$   
 Initialization: Solution  $S_i \leftarrow \emptyset$  ;

1. **For Each** Offer  $O_{V_j}$  such that  $O_{V_j} \in O(t)$  **do**
2. **If**  $D_i^+ \in IT_{V_j}(t)$  **then**
3. **If**  $D_i^- \in IT_{V_j}(t)$  **then**
4. Calculate  $(W_c, T_c, GD, De, A, Fitness)$
5. **If** Verify Constraints  $(D_i, Pl_{V_j}, De, A) = \text{True}$  **then**
6.  $PS \leftarrow PS \cup (D_i^+, D_i^-, V_j, Pl_{V_j}, GD, De, A, Fitness)$
7. **End if**
8. **End if**
9. **End if**
10. **End for**
11.  $S_i \leftarrow$  Choose  $PS_o$  from  $PS$  with minimum Fitness
12. **Return**  $S_i$

**ALGORITHM 2:** Optimized Global Itinerary (OGI).

**Applying ODAV:**

Here are some results of how the adopted optimizing algorithms are applied over the involved entities (OA) according to the previously given example. Different values of the TAT are represented in Table 4:

Departure Time	Weather	Type of the Road	Traveling Average Time (per 100 km)
Normal Period	Rain	Highway	Speed=100km/h TAT=75 min
Normal Period	Rain	Secondary Road	Speed=70km/h TAT=120 min
Rush Hour	Rain	Highway	TAT=100 min
Rush Hour	Rain	Secondary Road	TAT=150 min
Normal Period	Normal	Highway	TAT=67 min
Normal Period	Normal	Secondary Road	TAT=86 min
...	...	...	...

**TABLE 4:** Given information about the Traveling Average Time (TAT)

According to the subdivision process previously performed on the given example, four Optimizing Agents are firstly launched at the same time dealing with users' requests located within the determined Primary Zones. Then, if partial requests are established with intermediate origins situated in Intermediate Zones, the corresponding agents begin their process at the first request received.

Some computational details are shown through Figures 17, 18, and 19 showing computing operations performed respectively by OA<sub>3</sub>, OA<sub>4</sub> and OA<sub>2</sub>.

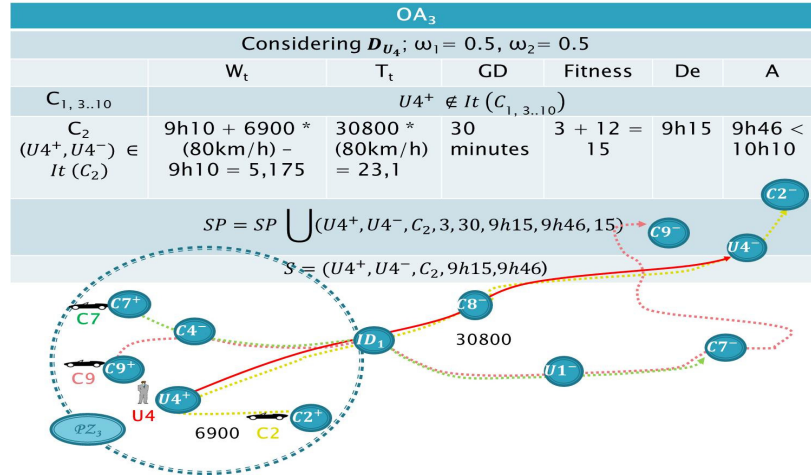


**FIGURE 17:** Searching for optimized vehicle assignment matching U<sub>4</sub>'s request appropriately to the specified parameters

Figure 17 illustrates the operational process performed by OA<sub>3</sub> searching for an optimal journey responding to the only request involved within the zone it is responsible for (PZ<sub>3</sub>). It shows a basic scenario where only a car (C<sub>2</sub>) may satisfy the asked trip and so presents a feasible but also complete solution. Thus, no optimizing choice is done in this case; C<sub>2</sub> also corresponds to U<sub>4</sub>'s expectations with regards to the time of Departure at the earliest and Arrival time at the latest.



the communication support in the sense that only concerned agents with the extracted possibilities interact and then avoid extra flows.

#### 4. CONCLUSION & FUTURE WORK

With the rise of communication technologies, it becomes relatively easier to deal with problems requiring short process delays. A negligible solving time is of prior order when having to instantly carry out responses for real time queries. Dynamic carpooling is set in this problems category. Therefore, this problem is given priority in this paper. Indeed, to support sustainable mobility mainly based on carpooling, we focus on processing dynamic users' requests in an optimized way. Thus, a new approach called Distributed Optimized approach based on the Multi-Agent concept for Real Time Carpooling service (DOMARTIC) is proposed. In this approach, we introduce a distributed technical architecture to optimize parallel users' requests' processing considering the principle of Multi-Agent systems. In conjunction with the proposed geographical network decomposition, the multi-agent concept highlights the distributed architecture and helps decomposing complex initial tasks to better perform optimized cars' assignment (efficiently and promptly).

Thanks to the proposed graph modeling and the multi-agent concept, the original problem is then decomposed into multiple less complex tasks helping to perform decentralized parallel process over the established areas. This importantly reduces optimization problem's complexity and so helped to set up a process generating optimized responses within a reasonable runtime.

#### 5. REFERENCES

- [1] T. Fraichard. "Cybercar: l'alternative à la voiture particulière". Navigation (Paris), 53(209): 53-74, 2005. URL : <http://emotion.inrialpes.fr/bibemotion/2005/Fra05>.
- [2] R. Clavel. "Le covoiturage en France et en Europe, Etat des Lieux et Perspectives". 88, 2007. CERTU, France.
- [3] A. Rocci. "Les évolutions du rapport à l'automobile". Journée Technique ATEC-ITS, regards croisés sur l'offre de véhicules en libre service, 2008.
- [4] M. Jean. "Car sharing, taxi, etc.: To share the car use: in france too ?" T.E.C. ISSN 0397-6513, 158(12 ref.): 22-29, 2000
- [5] K.W. Steininger, C. Vogl, and R. Zettl. "Car-sharing organizations : The size of the market segment and revealed change in mobility behavior". Transport Policy, 3(4): 177-185, 1996. URL: <http://ideas.repec.org/a/eee/trapol>
- [6] C. Morency, M. Trépanier, B. Agard, B. Martin, and J. Quashie. "Car sharing system: what transaction datasets reveal on users' behaviors". Intelligent Transportation Systems Conference, 1(4244-1396): 284-289, 2007.
- [7] R. Clavel and P. Legrand. "Le covoiturage dynamique, Etude préalable avant expérimentation". 92. CERTU, 2009. URL : <http://www.certu.fr>.
- [8] H. Zgaya. "Conception et optimisation distribuée d'un système d'information d'aide à la mobilité urbaine : une approche multi-agent pour la recherche et la composition des services liés au transport". PHD Thesis, tel-00160802, version 1, Ecole Centrale, Lille, July 2007.
- [9] S. Anily. "Comments on: Static pickup and delivery problems: a classification scheme and survey". Sociedad de Estadística e Investigación Operativa 2007 15: 32-34. Published online: 18 April 2007. URL: <http://www.springerlink.com/content/908w031877687407/fulltext.pdf>.

- [10] G. Berbeglia, J.F. Cordeau and J. Laporte. "*Dynamic Pickup and delivery problems*". European Journal of Operational Research, volume 202, issue 1, pages: 8-15, 2010.
- [11] M. Iori and J.J. Salazar González and D. Vigo, "*An Exact Approach for the Vehicle Routing Problem with Two-Dimensional Loading Constraints*", Transportation Science 41(2): 253-264, 2007.
- [12] MM.Hizem. "*Recherche de chemins dans un graphe à pondération dynamique : application à l'optimisation d'itinéraires dans les réseaux routiers*". PHD Thesis, tel- 00344958, version 1, Ecole Centrale, Lille, 2008.
- [13] M.A. Kamoun. "*Conception d'un système d'information pour l'aide au déplacement multimodal : une approche multi-agents pour la recherche et la composition des itinéraires en ligne*". PHD Thesis, tel-00142340, version2, Ecole Centrale, Lille, 2007.
- [14] M. Sghaier, H. Zgaya, S. Hammadi, C. Tahon. "*ORTiC : A novel Approach towards Optimized Real Time CarPooling with an advanced Network Representation Model on siblings*". In Proceedings of the 12th LSS symposium, Large Scale Systems : Theory and Applications, Lille, France, 2010.
- [15] W. Jiao, and Z. Shi. "*A dynamic architecture for multi-agent systems*". In Proceedings of the 31st International Conference on Technology of Object-Oriented Language and Systems, 253-260, 1999.
- [16] F. Sottini, S. Abdel-Naby and P. Giorgini. "*Andiamo: A Multiagent System to Provide a Mobile-based Rideshare Service*". University of Trento, DIT. Technical Report 06 -097, 2006.
- [17] G., M., B., B., A., H. "*Applications of multi agent systems in traffic and transportation*". In IEEE Transactions on Software Engineering. 144(1):51-60, 1997.
- [18] A.B. Kothari. "*Genghis - a multiagent carpooling system*". B.Sc. Dissertation work, submitted to the University of Bath, May 11, 2004.
- [19] C. Carabelea, M. Berger. "*Agent negotiation in ad-hoc networks*". In Proceedings of the Ambient Intelligence Workshop at AAMAS'05 Conference, Utrecht, The Netherlands. 5–16, 2005.
- [20] B. Volha, G. Paolo and F. Stefano. "*Toothagent: a multi-agent system for virtual communities support*". In Technical Report DIT-05-064, Informatica e Telecomunicazioni, University of Trento (2005).

## INSTRUCTIONS TO CONTRIBUTORS

The *International Journal of Engineering (IJE)* is devoted in assimilating publications that document development and research results within the broad spectrum of subfields in the engineering sciences. The journal intends to disseminate knowledge in the various disciplines of the engineering field from theoretical, practical and analytical research to physical implications and theoretical or quantitative discussion intended for both academic and industrial progress.

Our intended audiences comprises of scientists, researchers, mathematicians, practicing engineers, among others working in Engineering and welcome them to exchange and share their expertise in their particular disciplines. We also encourage articles, interdisciplinary in nature. The realm of International Journal of Engineering (IJE) extends, but not limited, to the following:

To build its International reputation, we are disseminating the publication information through Google Books, Google Scholar, Directory of Open Access Journals (DOAJ), Open J Gate, ScientificCommons, Docstoc and many more. Our International Editors are working on establishing ISI listing and a good impact factor for IJE.

The initial efforts helped to shape the editorial policy and to sharpen the focus of the journal. Starting with volume 5, 2011, IJE appears in more focused issues. Besides normal publications, IJE intend to organized special issues on more focused topics. Each special issue will have a designated editor (editors) – either member of the editorial board or another recognized specialist in the respective field.

We are open to contributions, proposals for any topic as well as for editors and reviewers. We understand that it is through the effort of volunteers that CSC Journals continues to grow and flourish.

### IJE LIST OF TOPICS

The realm of International Journal of Engineering (IJE) extends, but not limited, to the following:

- Aerospace Engineering
- Biomedical Engineering
- Civil & Structural Engineering
- Control Systems Engineering
- Electrical Engineering
- Engineering Mathematics
- Environmental Engineering
- Geotechnical Engineering
- Manufacturing Engineering
- Mechanical Engineering
- Nuclear Engineering
- Petroleum Engineering
- Telecommunications Engineering
- Agricultural Engineering
- Chemical Engineering
- Computer Engineering
- Education Engineering
- Electronic Engineering
- Engineering Science
- Fluid Engineering
- Industrial Engineering
- Materials & Technology Engineering
- Mineral & Mining Engineering
- Optical Engineering
- Robotics & Automation Engineering

### CALL FOR PAPERS

**Volume:** 5 - **Issue:** 4 - July 2011

**i. Paper Submission:** July 31, 2011

**ii. Author Notification:** September 01, 2011

**iii. Issue Publication:** September / October 2011

## **CONTACT INFORMATION**

### **Computer Science Journals Sdn Bhd**

M-3-19, Plaza Damas Sri Hartamas  
50480, Kuala Lumpur MALAYSIA

Phone: 006 03 6207 1607  
006 03 2782 6991

Fax: 006 03 6207 1697

Email: [cscpress@cscjournals.org](mailto:cscpress@cscjournals.org)

CSC PUBLISHERS © 2011  
COMPUTER SCIENCE JOURNALS SDN BHD  
M-3-19, PLAZA DAMAS  
SRI HARTAMAS  
50480, KUALA LUMPUR  
MALAYSIA

PHONE: 006 03 6207 1607  
006 03 2782 6991

FAX: 006 03 6207 1697  
EMAIL: [cscpress@cscjournals.org](mailto:cscpress@cscjournals.org)

CSC PUBLISHERS © 2011  
COMPUTER SCIENCE JOURNALS SDN BHD  
M-3-19, PLAZA DAMAS  
SRI HARTAMAS  
50480, KUALA LUMPUR  
MALAYSIA

PHONE: 006 03 6207 1607  
006 03 2782 6991

FAX: 006 03 6207 1697  
EMAIL: [cscpress@cscjournals.org](mailto:cscpress@cscjournals.org)